GEOLOGICAL SURVEY OF CANADA

OPEN FILE 2748

Factors controlling postcumulus compositional changes of chrome-spinels in the Crystal Lake Intrusion, Thunder Bay, Ontario

E.H. Cogulu

1993

Natural Resources Canada Ressources naturelles Canada

Canada

Canada

Contribution to Canada-Ontario Subsidiary Agreement on Northern Ontario Development (1991-1995), a subsidiary agreement under the Economic and Regional Development Agreement. Project funded by the Geological Survey of Canada.

Contribution à l'Entente auxiliaire Canada-Ontario de développement du nord de l'Ontario (1991-1995), entente auxiliaire négociée en vertu de l'Entente de développement économique et régional. Ce projet a été financé par la Commission géologique du Canada.

FACTORS CONTROLLING POSTCUMULUS COMPOSITIONAL CHANGES OF CHROME-SPINELS IN THE CRYSTAL LAKE INTRUSION,THUNDER BAY, ONTARIO

ERSEN H. COGULU

Report submitted under the terms
of DSS contract no. 34SZ.23233-7-760
Canada-Ontario Mineral Development Agreement

ABSTRACT

The Crystal Lake intrusion is located 47 km southwest Thunder Bay, Ontario. Chrome-spinel occurs in the cyclically layered zone and forms discontinuous layers that exhibit deformation similar to the types observed in soft sediments: load cast, fluid escape, and drop and sag structures. Two adcumulate and four orthocumulate compositional groups of spinel are distinguished. Each spinel group has definite compositional ranges and textural characteristics. Adcumulate spinels are high in Al, Mg and Cr and exhibit a restricted compositional range. Orthocumulate spinels have a larger range of compositional variations and are rich in Fe and Ti and have high Fe^{3+}/Fe^{2+} ratios. Two main and two auxiliary variation trends are recognized. Cr-trends are characterized by increasing Cr/Al ratios and relatively constant Fe^{3+}/Fe^{2+} ratios. Trends characterized by significant increases in Fe^{3+} and Ti have higher Fe^{3+}/Fe^{2+} ratios. Intercumulus chrome spinels and those associated with polarity textured sulphides have the highest Fe and Ti contents. Those included in biotites are depleted in Al and Mg.

Chrome-spinels are considered to represent early cumulus minerals in gabbros of the Crystal Lake intrusion. The diversity of their compositions appears to result from the combination of two mechanisms. (1) The chrome-spinels reequilibrated continuously with the evolving liquid with which they were in contact as crystallization proceeded; and (2) the reequilibration of individual chrome-spinel grains was halted at different stages of liquid evolution when they were trapped as chadacrysts in the successively crystallizing oikocrystic silicate minerals: plagioclase, olivine, augite and biotite. whether at the base or at the top of an adcumulate layer.

I INTRODUCTION

The Crystal Lake intrusion is located southwest of Thunder Bay, Ontario, a few miles from the USA-Canada border (Fig.1). Cu-Ni sulphide mineralization in the intrusion has been the focus of exploration, and drilling has established a low-grade zone called the Great Lakes Nickel Deposit. The first published description of the chrome spinel mineralization is given by MacRae and Reeve (1968). The group of chrome spinel layers lies above the Cu-Ni sulphide zone, and was used as a marker horizon during exploration to identify the upper limit of the sulphide deposit. Mainwaring and Watkinson (1981) recognized chrome spinel veins and disseminations in a chaotic zone lying below persistent chrome spinel-rich layers. The fact that the chrome spinel-rich layers occur in rhythmic repetitions within a distinct cyclic zone and are also anomalous in platinum group elements (PGE) was first recognized by Cogulu (1984, 1985).

There are two generations of spinel in the Crystal lake gabbros. The earlier generation forms equant, euhedral to irregular or rounded crystals as inclusions in cumulus and intercumulus minerals in the cyclic zone. The younger generation of spinels forms platy dendrites, arborescences or worm-like crystals of a few microns in olivine and augite of orthocumulates. This paper deals mainly with the earlier spinel generation.

The chrome spinels exhibit a large and continuous spectrum of compositions within the ranges 12-30 wt% Cr_2O_3, 4-30 wt% Al_2O_3, 1-12 wt% MgO, 21-41 wt% FeO, and 10-27 wt% Fe_2O_3. They are also rich in TiO_2 which ranges from 2 to 13 wt%.

Compositional variations of spinels have been documented by a number of investigators (Irvine, 1965, 1967; Evans and Moore, 1968; Cameron, 1975, 1977; Eales and Snowden, 1979; Eales and Reynolds, 1983; Henderson and Suddaby, 1971; Henderson, 1975; Ridley, 1977; Wilson, 1982; Roeder and Campbell, 1985). The chemical diversity of spinel is in part the result of variations in physicochemical conditions of magma during primary crystallization. Further chemical changes occur during the post cumulus stage. Roeder and Campbell (1985) described postcumulus reactions of chrome spinels in the Jimberlana intrusion. They related spinel compositions to rock textures, and placed special emphasis on reactions between chromite and intercumulus

liquid. They concluded that chromite compositions reflect the cumulate types and the nature of the surrounding silicate minerals.

Evidence in the Crystal Lake intrusion suggests that compositions of spinels depend mostly upon their opportunity to react with intercumulus liquids. Other factors may also influence their reequilibration. Special attention has been given to cumulate types, compositions and textural varieties of the host minerals, and the time of trapping of chrome spinels by silicate phases. Spinel compositions are also related to location within the hosting mineral. Chemical changes from the base to the top of a given adcumulate layer have also been studied. Whole rock analyses indicate that the more refractory platinum group elements (Os, Ir, Ru) are strongly correlated with chrome spinel (Eckstrand and Cogulu, in preparation).

The nomenclature used in this paper relating to cumulate rocks follows that of Wager et al. (1968) and Irvine (1982).

II SAMPLING AND ANALYTICAL METHODS

150 polished thin sections were prepared, mainly from surface samples. About 600 chrome spinel grains were analysed on two different electron microprobes: 1) a Material Analyses Company electron microprobe equipped with a Kevex energy dispersive spectrometer at the Geological Survey of Canada, Ottawa, under operating conditions of 20 KV accelaration voltage, specimen current of 10 nA, and a counting time of 100 seconds; and 2) a Cambridge Mark V electron microprobe with an ORTEC energy dispersive system at Dalhousie University, Department of Geology, Halifax, under operating conditions of 15 KV acceleration potential and a beam current of 5 nA. The software package used was EDATA 2 (Smith at al. 1980, University of Alberta). The standards were geological samples.

III REGIONAL GEOLOGY

The study area is underlain in large part by the Aphebian sedimentary Rove Formation. It represents a northern portion of an intracratonic basin. These strata were invaded along the Keweenawan Rift Zone by volcanic and intrusive rocks of Helikian age. The latter include the Crystal Lake intrusion and the Duluth Complex in Minnesota, both associated with this intracontinental rifting at about 1,1 Ga (Goldich et al., 1961; Faure et al., 1969; Geul, 1970; Silver and Green, 1972; Sims et al., 1981; Weiblen, 1982; Franklin et al., 1982).

The Crystal Lake intrusion is a layered intrusion of gabbroic composition. It outcrops as a Y-shaped body (Fig.1). Its northern arm which contains the Great Lakes Nickel deposit and chrome spinel mineralization extends for about 5.5 km in a west-northwest direction. Drilling and field studies indicate that the intrusion contains trough-shaped layering which plunges 15-20° eastward. The following four main zones are distinguished (Geul, 1970; Cogulu, 1985: Fig.2): 1) upper zone: massive to weakly layered medium grained gabbro. 2) cyclic zone: four magmatic cycles constitute a distinct layered sequence. Each cycle consists of an upper anorthositic gabbro and a lower chrome spinel-bearing troctolite and olivine gabbro. 3) lower unlayered zone: massive gabbro displaying highly variable textures ranging from fine-grained to pegmatitic, and containing randomly scattered cognate and sedimentary xenoliths. 4) basal zone: fine grained gabbro with abundant sedimentary xenoliths. Footwall sediments at the contact zone are tranformed into hornfels and cut by numerous anastomasing felsic veins which probably represent the product of partial melting (Mainwaring and Watkinson, 1981).

IV CHROME SPINEL OCCURRENCE

Chrome spinel occurs as layers at the bases of four repeated cycles in the cyclic zone, and are characterized by various types of deformation. Modal abundance of chrome spinel in the layers ranges from a few percent to 36%. Thickness of the layers ranges from a few cm to 20-30 cm.

The types of deformation of the layers include slumps, load casts, fluid escape structures, and drop and sag structures (Fig.3). Similar structures were described by Scoates (1983) and Scoates et al. (1986) in the Bird River Sill,

Manitoba, and by Lee (1981) in the Bushveld Complex. These authors attribute the deformation structures to magmatic processes analagous to those which produce soft sediment deformation in sedimentary rocks (Stewart, 1963). The nature of deformation differs, but the intensity increases in a general way from the uppermost to the lowermost of the four cyclic units. In cycle 1, fluid escape structures, load casts, disrupted trough banding, and large sags are observed. Three slumps are prominent in cycle 2. Cycle 3 exhibits mainly load casts and drop and sag structures. Cycle 4 is characterised by discontinous layers and trough banding which are not disrupted.

There are three textural forms of spinel: euhedral to subhedral, rounded, and sintered to irregular. The rounded crystals are in general small, and occur poikilitically within silicate grains, while the irregular ones are large, and form interstitial grains.

About 150 spinel analyses are plotted on the Al-Cr-Fe^{3+} diagram (Fig. 4A), and show a large and continuous range of composition. These are subdivided into six spinel groups (labelled I to VI) based on textural and compositional characteristics. Each group has specific ranges of Al:Cr:Fe^{3+} ratios and hosting rock type or host minerals. The boundaries shown as dashed lines on Fig.4A are approximate as the groups overlap each other. The observed compositional ranges of the groups are given in Table 1.

Spinels of groups I and II are adcumulates that occur in undisrupted and disrupted layers, respectively. Group III represents spinels in poikilitic olivines that contain plagioclase relicts. Group IV spinels occur as inclusions in intercumulus silicates (other than biotite). Group V includes interstitial chrome spinels and those associated with polarity textured sulphides. Finally, group VI spinels occur only as inclusions in biotites.

V PETROGRAPHY OF THE CHROME-SPINEL BEARING GABBROS

The following is a summary of petrographic features, a more detailed account of which is given elsewhere (Cogulu, 1990). Chrome spinel bearing gabbros occur as both orthocumulates and adcumulates (Table 2), the former generally overlying the latter.

V-1 ADCUMULATE ROCKS

Adcumulate rocks are troctolite and augite troctolite in composition. Chrome spinel and olivine are the main cumulus minerals, while plagioclase, biotite and sulphides are intercumulus. Spinel in adcumulates makes up between 20 to 36% of the rock.

Chrome spinel forms chadacryst inclusions dispersed through poikilitic silicates, or as grains located at the margins of cumulus olivines (Photos 1 to 4). Their grain size ranges from about 6 to 75 microns. Spinels included within biotite are larger and may attain 200 microns.

Plagioclase is the most abundant mineral, constituting 45-60% of the rock. It forms tabular crystals up to 2 cm whose An content varies between 78% and 70%. The difference in An content in adjoining plagioclase grains does not exceed 1-3%. In the disrupted adcumulates plagioclase laths may exhibit strong zoning.

Olivine constitutes about 17% of the rock, and occurs in two textural forms: euhedral to subhedral, and irregular. Grain size ranges from 2 to 4mm. Its Fo content ranges from 81 to 77%, and appears related to the presence of spinel inclusions and the degree of disruption of the host layer. Olivines with spinel inclusions are richer in Fo. If spinels occur in the marginal zone, then the olivine is zoned and the marginal zone is Fo rich. In the disrupted adcumulate layers, Fo content of olivine is lower by about 10%.

Biotite is present in accessory amounts of 1-2%. It forms irregular interstitial grains up to 2 mm. Apatite occurs locally in biotite as small prisms. Sulphides form intersilicate grains or are included within biotite.

Ilmenite forms exsolved prisms oriented parallel to crystallographic directions within chrome spinel euhedra (Fig.11).

V-2 ORTHOCUMULATES

Orthocumulate rocks have olivine gabbro composition and locally may be ortho- or mesocumulates. The cumulus minerals are plagioclase, olivine, and chrome spinel, and intercumulus minerals are plagioclase, olivine, augite, orthopyroxene, biotite, apatite, and sulphides.

Chrome spinel may constitute up to 8% of the rock. The grain size generally ranges from 13 to 300 microns, but locally may be more than 2 mm. Spinels within the cores of plagioclase are smaller. Those in the overgrowth zone of cumulus plagioclase and in the intercumulus silicates are larger.

Plagioclase constitutes 60-65% of the rock. It forms tabular to irregular crystals having normal zoning. Anorthite content ranges from 84% to 50%. Plagioclase is often partially resorbed by poikilitic olivine (Figs.5, 6). In contrast its contacts with augite are always straight. The spinel inclusions in the overgrowth zone are in general sintered or irregular and larger than those in the cumulus core (Figs. 3, 4, 7 and 8).

Olivine constitutes about 15% of the rock, and exhibits various textural forms. Olivine euhedra occur locally in fine grained rocks and slumped layers. However in most cases it forms large oikocrysts. Orthocumulate olivines are poikilitic, or interstitial with shapes ranging from polygonal with triple junctions to irregular (Figs. 2, 3, 5 and 6).

Other characteristic features of olivine are the following: 1) its boundaries in contact with feldpar are always irregular and display re-entrants containing spinels; 2) it commonly resorbs plagioclase which remains as relicts and thin envelopes surrounding spinel inclusions (Photos 5 and 6); 3) it contains an inhomogenous population of spinels presenting diverse shapes, sizes and compositions (group III); 4) its Fo content ranges from 73 to 58 mol % Fo, those containing spinels having higher Fo content than those which do not; and 5) interstitial olivine is more fayalitic and may contain large spinels richer in Fe and Ti. These observations suggest that the observed olivines are not cumulus and do not present their initial textures and compositions.

Chalokwu (1985), and Chalokwu and Grant (1987) showed that orthocumulate olivine in the Partridge River intrusion, Duluth Complex, reequilibrated with trapped liquid and became more fayalitic. Textural and compositional evidence together with the great diversity of spinel inclusions (see below) suggest that similar reequilibration of olivine occurred in the Crystal Lake gabbros.

Augite is always interstitial and forms large oikocrysts. It makes up about 10% of the rock. Spinels included within augite are in general larger than those in plagioclase (Photos 7 and 8). Locally augite may contain droplet-shaped sulphide inclusions and may form a cap over the top of polarity textured sulphide blebs (Fig.9).

Biotite occurs as an accessory mineral in almost all samples and has a wide range of composition. It is enriched in MgO when epitactic on olivine, and depleted in MgO when interstitial or epitactic to augite.

Apatite is often associated with biotite and sulphides. Sulphides are generally interstitial to the silicate framework but they may also occur as polarity textured blebs (Cogulu, 1988b). Spinels associated with these blebs are always larger and have the highest contents of Fe and Ti.

Ilmenite occurs as skeletal to irregular crystals, or as exsolved lamellae in interstitial chrome spinels (Fig.10).

VI GEOCHEMISTRY

Systematic electron microprobe analyses were carried out on spinels of all textural types. The compositions of spinel chadacrysts as well as the adjacent hosting silicate from the core to the margin of the host mineral were analysed. Chemical variations across an undisrupted spinel layer as well as in the underlying and overlying rocks were also determined. The analytical data are presented in Tables 3 to 19, and discussed below.

VI-1 Composition of spinel in adcumulate and orthocumulate rocks

Al-Cr-Fe^{3+} diagrams of representative orthocumulate and adcumulate spinels are given in Figs. 5 and 6. They demonstrate that a) chrome spinels exhibit systematic and distinctive compositional variations in adcumulate and orthocumulate rocks; b) spinels in adcumulates have a narrow compositional range while those in orthocumulates exhibit a large range; c) spinels in adcumulates are richer in Mg, Al and Cr, and poorer in Fe^{3+} and Ti, whereas those in orthocumulates have a broad range of compositions from Al- and Mg-rich to Fe^{3+}- and Ti-rich solid-solutions.

The overall compositional variation of chrome spinel in the Crystal Lake intrusion involve four distinct variation trends, shown in Fig.4B: Cr trend 1, Cr trend 2, Fe^{3+}+Ti trend 1, and Fe^{3+}+Ti trend 2. Adcumulate spinel variations follow Cr trend 1 (Fig.5). Orthocumulate spinel variations are more complex and may follow any of the four variation trends (Fig.6).

Comparative binary and ternary diagrams (Figs.7 and 8) illustrate the main compositional trends. Cr trend 1 is characterized by increase of Cr/Al with decreasing Al and Mg, while Fe^{3+}/Fe^{2+} ratios are relatively constant. Fe^{2+} substitutes for Mg, and Fe^{2+}+Ti for 2Al. Cr trend 2 (Fig.4) has similar characteristics but its Fe^{3+}/Fe^{2+} ratios are higher. Fe^{3+}+Ti trend 1 is characterized by significant increases of Fe^{3+} and Ti as Al and Mg decrease. Fe^{3+}/Fe^{2+} ratios are higher than those of the Cr trends. Fe^{3+}+Ti trend 2 has similar characteristics, but is more depleted in Al and Mg.

VI-2 The influence of the host silicate on the compositions of spinels.

VI-2A. In an adcumulate rock, compositions of spinel chadacrysts in three coexisting host silicates, plagioclase, olivine and biotite, fall in spinel group I, described above (Fig. 9). While textural characteristics indicate that olivine may be earlier than, or contemporaneous with plagioclase, and that biotite is interstitial to them, spinel compositions are the same in all three minerals. Similarly, Roeder and Campbell (1985) found that spinel compositions in adcumulates of the Jimberlana intrusion are not dependent on the host minerals.

VI-2B. Conversely in orthocumulates, when crystallization of the host mineral proceeds to the point where the chrome spinel crystal is completely enclosed, further reaction of the spinel with the magmatic liquid is prevented. Spinel compositions depend on the nature and crystallization order of the host silicates. In these rocks minerals crystallized at different times over a large temperature interval. Plagioclase was the first silicate to nucleate after spinel crystallization. Olivine crystallized later and resorbed some of the plagioclase. Augite and biotite crystallized still later. Compositions of spinel hosted in plagioclase, olivine, augite and biotite from several orthocumulate samples are presented in Figs. 10 to 13. The systematically differing compositions of spinel are considered to result from continuous reequilibration of the spinels while in contact with the evolving liquid. When the spinel crystals are removed from contact with the liquid by enclosure in the growing silicate oikocrysts, further change in composition is prevented.

Spinel chadacrysts in plagioclase oikocrysts exhibit the largest spectrum of compositions, ranging from Mg- and Al-rich all the way to Fe^{3+}- and Ti-rich. Both the Cr and Fe^{3+}+Ti composition trends are commonly present in a single plagioclase lath (Fig. 10A). Spinel groups I, II, IV and V may all occur in plagioclase.

Spinels included in olivine also present a large compositional range. The various textural forms of olivine exhibit different variation trends. Spinels in poikilitic olivine which resorb plagioclase exhibit Cr-trend 2 which is slightly shifted toward the Fe^{3+} apex of the triangle (Figs. 4 and 11A). Spinel in polygonal olivines plot at the iron rich end of Cr-trend 2 (Fig.11 B). Finally, spinels in poikilitic to interstitial olivines plot on the Fe^{3+}+Ti trend 1 line (Fig. 11B).

Resorption of plagioclase by olivine is a consequence of its reequilibration with iron rich intercumulus liquid. This means that spinels originally trapped by plagioclase might later be enclosed by reequilibrated olivine. Recrystallization of interstitial olivine occurred still later.

Augite is always interstitial to plagioclase, and spinels included in augite are richer in Fe^{3+} and Ti, and poorer in Cr than those in plagioclase. Two coexisting plagioclase-augite pairs were chosen and the compositions of the included spinels are plotted in the ternary diagrams of Fig.12A and B, and are given in Tables 8 and 15. In Fig 12A the plagioclase has two overgrowth zones (Photos 3 and 4). The Cr2O3 contents of spinels within augite are lower than those in plagioclase but the $Fe2O_3$ and TiO_2 contents are higher. In Fig.12B plagioclase displays only one overgrowth zone, but the chemical trend of the spinels is similar. This evidence suggests that spinels in augite were trapped later than those in plagioclase, and chromium was transferred to pyroxene from chrome-spinel inclusions.

Biotite is interstitial to other cumulus silicates, and its spinel inclusions are always depleted in Al and Mg. As described above, spinels of group VI occur only in biotite, and their compositions follow $Fe^{3+}Ti$ trend 2 (Figs. 4 and 13; Tables 18 and 19). Spinels in biotite are the poorest in Mg and Al. Ti contents are higher and similar to those found in spinels in augite. The Mg and Al depletions are interpreted as the result of exchange with host biotite.

VI-3 The dependence of composition of spinel chadacrysts on their position within zoned oikocrysts.

Spinel chadacrysts may be located anywhere from the central core to the outermost overgrowth zone of the host oikocryst. Changes in composition of spinel from core to overgrowth zone are interpreted as evidence of difference in the time of trapping. Furthermore these variations reflect the nature and compositional evolution of the magmatic environment, which may be either an open or closed system. If the system is open, exchange with the main magma continues and adcumulate growth occurs. If it is closed the magmatic liquid is trapped, and orthocumulate growth takes over.

VI-3A Spinels in plagioclase oikocrysts.

Systematic analyses across individual plagioclases have revealed that spinels exhibit a systematic compositional change from core to margin of the host feldspar. The core does not always lie at the geometrical centre of the crystal, but it has the highest An content and the enclosed spinels are the smallest. Observations under reflected light demonstrate that reflectivity and color of spinels change as a function of their compositional change from core to margin of the host plagioclase. Typical profiles of plagioclase and spinel compositions across a single plagioclase oikocryst are given in Fig. 14. An content of the plagioclase diminishes gradually from the homogeneous core toward the margin. Spinel composition shows similar gradual change (Fig. 9-A). Spinels in the plagioclase core are rich in MgO and Al_2O_3, but become more Cr_2O_3-rich toward the margin, typical of Cr trend 1.

The Al-Cr-Fe^{3+} diagram of Fig. 5B shows spinel compositions in a disrupted adcumulate layer. Plagioclases in these rocks are zoned and spinels in overgrowth zones have compositions of group II, while those in the plagioclase core are of group I.

In orthocumulate rocks, the plagioclase may be both cumulus and intercumulus, and this textural difference influences the compositions of the included spinels. Orthocumulate plagioclase may include three groups of spinels in a single crystal (Groups I, II and IV, Fig. 10A). Compositional variations in spinels and host plagioclase (Photos 3 and 4) from plagioclase core to margin in an orthocumulate rock are gradational (Fig.15). Spinels lying at the plagioclase core have the same high values of MgO and Al_2O_3 as those in the adcumulates of the group I, but those in the plagioclase overgrowth zone are richer in Fe^{3+} and Ti. Two subzones, each enclosing a different group of spinel are distinguished. The inner subzone contains spinels of group II with higher Cr_2O_3, while the outer (or marginal) zone spinels are enriched in Fe_2O_3 and TiO_2 (group IV). These observations appear tokll indicate that during the growth of the plagioclase the nature of the magmatic system changed: the core and inner overgrowth zone crystallized in an open system which gave rise to adcumulate growth. Later the system was closed when the marginal zone crystallized. The spinels included in the latter reflect chemical changes in trapped intercumulus liquid.

VI-3B Spinels in olivine oikocrysts

In adcumulates the olivine may crystallize prior to, and at the same time as plagioclase. Spinels may be included in only the marginal zone of the olivine or be dispersed throughout the host silicate (Photos 1 and 2). Fig. 16 shows olivine and spinel compositional variations from the core to the margin of an olivine grain. The olivine core has no spinel and a low Fo content relative to that of the spinel-bearing margin. The spinels show increasing Cr_2O_3 and decreasing Al_2O_3 toward the grain boundary. Fig. 9B shows the compositional variation of trivalent elements in the same grain.

In orthocumulates, olivine exhibits several textural forms which contain different spinel groups (Fig. 11 A, B). The compositional variations of a poikilitic olivine and included spinels (group III) are plotted in Fig. 17. Compositional gradients exist, but the regularity of variations is perturbed by large spinels and those in plagioclase relicts. Fig. 11A shows Al-Cr-Fe^{3+} ratio variations in the same spinels. These data together with those of Fig. 18 indicate the following: 1)poikilitic olivines contain an inhomogeneous population of spinels; 2) the latter have high Fe^{3+}/Fe^{2+} ratios, and their chemical variations follow Cr-trend 2; 3) spinels in the host olivine core are higher in Al and Mg than those in the marginal zone, but intermediate spinels may show irregular fluctuations. All these observations and data are consistent with the reequilibration of the orthocumulate olivine with intercumulus liquid. Spinels of group III were originally included in primary silicates that were later resorbed by olivine, at which time the exposed spinels reequilibrated with the olivine.

Finally, compositions of spinels in interstitial olivine are consistent with late reequilibration. Spinels in these silicates (group IV) lie on Fe^{3+}+Ti trend 1 (Fig. 11B). They are richer in Fe and Ti than those of group III.

VI-3C Intercumulus spinels

Intercumulus spinels generally form large and irregular crystals up to a few mm in size. They often contain ilmenite exsolution lamellae. Large spinel crystals are also associated with polarity textured sulphides, and may occur as inclusions within sulphide, or in silicate overgrowth zones (Photos 9 and 10). These large crystals constitute group V spinels, which are the richest in Fe and Ti (Tables 16 and 17, Fig. 19). Because they were not trapped by a silicate until

late during magma crystallization, they had the opportunity to react continuously with intercumulus liquid down to a relatively low temperature. As a result these spinels became enriched in Fe^{3+} and Ti and grew to comparatively large size.

VI-4 Compositions of silicates and spinels in a chrome spinel layer.

Spinel layer No 3 overlying the magmatic trough of cycle 4 has been studied in detail. This layer extends laterally over a few meters and its thickness ranges from 1 to 15 cm. The underlying gabbro is a plagioclase-olivine-spinel orthocumulate, while the overlying rock is pegmatite.

Silicates and included spinels at the base, middle and upper portions of the layer were analysed systematically from core to margin of the host mineral. The analytical data are given in Tables 3 to 7. Spinel Al:Cr:Fe^{3+} ratios are not affected by the nature of the host minerals in that layer (Fig.9). Silicates located at the bottom of the layer were crystallized earlier than upper ones. Compositions of spinels and host silicates from the base to the top of the layer are compared in Fig.20, and indicate the following: 1) basal spinels whether they are surrounded by plagioclase or olivine are richer in Mg and Al; 2) spinel compositons change gradually from the bottom to the top of the layer, in the same manner as they change from the core to the margin in individual silicate grains; 3) upper spinels are higher in Cr and depleted in Al and Mg.

VI-5 Comparison of an adcumulate layer with adjacent orthocumulates.

Comparison of the compositions of spinels and silicates in orthocumulate and adcumulate rocks are shown in Fig.21, which gives rise to the following observations: 1) there are dramatic differences in the compositions of silicates and spinels between adcumulates and orthocumulates; 2) the orthocumulate olivines are more fayalitic and contain partially resorbed plagioclase relicts; these are the result of their reequilibration with iron rich intercumulus liquid; 3) the adcumulate olivines may have up to 10% higher Fo content than orthocumulate olivines; 4) the compositional variability of silicates and spinels is more restricted in adcumulates than in orthocumulates; 5) orthocumulate plagioclase may have patchy zoning while that in an adcumulate layer is always normally zoned.

2

VII DISCUSSION AND INTERPRETATION

Hypotheses which explain variations in chromite composition may be grouped into two categories: 1) chromite compositional variations are consequences of variations in physico-chemical conditions of the parent magma. Changes in magma composition, pressure and temperatures of crystallization, and oxygen fugacity may change chromite composition during the cumulus stage (Osborn, 1969; Ulmer, 1969; Cameron, 1975, 1977; Wilson, 1982). The hypothesis proposed by Mainwaring and Watkinson (1981) on the origin of chromian spinel in the Crystal Lake intrusion falls in this category. According to these authors the magma was contaminated during emplacement by assimilation of country rocks, and this induced the crystallization of Cr-spinels. The variable compositions of the spinels in the chaotic zone is the "result of reaction of early cumulus spinels with contaminated gabbroic liquids. The more restricted compositions of Cr-spinels in the stratiform upper zone may be due to more quiescent crystallization conditions." 2) According to hypotheses in the second category, chromite compositions are modified later by reaction with enclosing silicate or intercumulus liquid during the post cumulus stage (Irvine, 1965, 1967; Henderson, 1975; Ridley, 1977; Roeder and Campbell, 1985).

The chrome-spinels of the Crystal Lake intrusion are almost all early cumulus as indicated by their extraordinarily homogenenous distribution in non disrupted layers. The cyclic nature of their occurrence suggests that their crystallization is related to repetitive magma influx and mixing of the new, more primitive magma with the preexisting, more evolved magma (Irvine, 1975, 1977; Duke, 1983). The changes in physico-chemical conditions of magma undoubtedly affect their compositions. In fact, the chrome-spinels in cumulus silicate cores do not represent liquidus compositions. The small and rounded crystals are richer in Al and Mg than adjacent euhedral ones. This indicates that some changes happened during the cumulus stage, but these variations are small and remain within the compositional range of spinel group I. The main chemical changes are related to factors which are described in the previous section, and are due to subsequent modifications during the post cumulus stage. The question which then arises is whether these modifications are results of solid state diffusion between spinel and the host silicate, or reaction between spinel and intercumulus liquid. In adcumulates, the composition of the host silicate does not affect Al:Cr:Fe^{3+} ratios of spinel inclusions (Fig. 9). In orthocumulates, spinel inclusions in interstitial olivine and augite may have

similar ratios (Figs. 11 and 12). This evidence suggests that cation redistribution between spinels and host mineral has occurred but is probably not significant. Solid state diffusion between spinels and surrounding silicate phases has been described by Evans and Moore (1968). However in the Crystal Lake intrusion the major cation exchanges appear to involve intercumulus liquid. The evidences is abundant: 1) the chemical changes are systematic and regular; 2) spinels exhibit gradual enrichment in Fe^{3+} and Ti, and depletion in Al and Mg; 3) the chemical changes correlate well with magma fractionation; 4) the variations are related to rock textures, fractional crystallization order of the host silicates, and location of spinel within the host mineral.

Roeder and Campbell (1985) found that in the Jimberlana intrusion adcumulate chromites are high in Mg, Al and Cr, and show a restricted range of composition; but the orthocumulate chromites are much higher in Fe and Ti, have a higher Fe^{3+}/Fe^{2+} ratio, and show a much larger range of composition. In the Crystal Lake intrusion the adcumulate chrome-spinels also have high Al, Cr and Mg contents and their compositions exhibit a restricted range (Fig.5A). Orthocumulate spinels have a wide spectrum of compositions, ranging from those found in adcumulates to Fe^{3+}- and Ti-rich spinels (Fig. 6A and B).

Henderson (1975) found two reaction trends in chrome-spinels of the Rhum layered intrusion. The Al-trend involves an enrichment in Mg and Al at the expense of Cr. Along the Fe-trend spinels are enriched in Fe^{3+}. The Crystal Lake spinels exhibit four distinct variations trends which are grouped in two main trends: Cr-trend and Fe^{3+}+Ti-trend. (Fig. 4B).

The Cr-trends are characterized by an increase in the Cr/Al ratio. Cr-trend 2 has higher Fe^{3+}/Fe^{2+} ratios and is richer in Ti than Cr-trend 1. Fe^{3+}+Ti-trends involve increases in Fe^{3+} and Ti, resulting in higher Fe^{3+}/Fe^{2+} ratios than those of the Cr-trends. Fe^{3+}+Ti-trend 2 is characterized by the lowest Al and Mg contents.

Each variation trend is associated with specific rock textures or host silicates. Cr-trend 1 is observed in adcumulate rocks. Cr-trend 2 is exhibited by spinels in poikilitic olivine containing partially resorbed plagioclase relicts. Fe^{3+}+Ti-trend 1 is shown by spinels included in interstitial silicate oikocrysts and by those lying between silicate grains. Finally, variations in composition of spinel in biotites occur along the Fe^{3+}+Ti-trend 2 line.

Peritectic reactions of chromite and magmatic liquid with the crystallization of olivine, pyroxene and plagioclase have been described by many authors (Irvine, 1965, 1967; Hill and Roeder, 1974; Henderson, 1975; Roeder and Campbell, 1985). During these reactions, Al, Cr and Mg of the chromite are transferred into surrounding liquid or silicates. Similar exchanges would also have occurred in the Crystal Lake intrusion.

The increase in Cr/Al in adcumulate spinels may be explained by Al transfer from spinel to crystallizing host plagioclase (Fig.14 and 15), while the increase of Fo content in olivine containing spinel inclusions may be explained by Mg transfer from spinels (Fig.16). Another example of significant cation exchange is provided by chrome-spinel inclusions within biotites: these spinels are strongly depleted in Mg and Al (Fig.13).

The nature of orthocumulate silicate and its crystallization timing has a strong influence on spinel compositions (Figs.10 to 13). The influence of the host mineral is exerted when it encloses spinel crystals so that they are protected from reaction with intercumulus liquid. The earlier the spinel is trapped, the more closely its composition resembles the original one. According to Roeder and Campbell (1985) crystallization of orthocumulate occurs over a temperature range of about 300 C. Thus the timing of enclosure of spinels may differ greatly depending on host silicates. That difference is one of the main controls on spinel composition, and is well illustrated by variations in spinel compositions from plagioclase core to margin (Fig.10). Spinels within adjacent plagioclase and augite as well as in biotite give other good examples of chemical changes related to differences in host silicate crystallization order.

An contents of the plagioclase overgrowth in disrupted adcumulates are lowered, and olivines became more fayalitic. Parallel with these modifications the chrome spinel inclusions exhibit Al:Cr:Fe^{3+} ratios typical of group II, representing loss of Al and Mg (Fig.5B). These changes may be explained by infiltration metasomatism due to upwardly migrating magmatic liquid as described by Irvine in the Muskox intrusion (1980). Parallel laminations, load casts, fluid escape structures, and drop and sag structures as described by Cogulu (1988a) indicate a dynamic environment during late stages of crytallization. It is significant that spinels in adcumulate plagioclase cores remained in group I, while those in olivines are all in group II (Fig.4 and 5).

This indicates that adcumulate olivine might have reequilibrated with intercumulus liquid during soft sediment-like disruption.

This study provides evidence supporting the reequilibration of orthocumulate olivine with intercumulus liquid. Chalokwu (1985) and Chalokwu and Grant (1987) demonstrated reequilibration of olivine with trapped liquid in the Duluth Complex, Minnesota. Cogulu (1988) described similar textural 2relationships in orthocumulate gabbros of the Crystal Lake intrusion. These spinels were probably included originally in other silicates, and were retrapped by recrystallizing olivine. They form a distinct compositional group and display a specific variation trend (Fig.4 and 11) that originated through reequilibration with the host olivine.

The polygonal texture of subhedral olivines indicates their adcumulus growth, and the composition of their spinel inclusions demonstrate the late recrystallization of the host silicate. Spinels of interstitial olivines are richer in Fe and Ti, and their compositions plot on the Fe^{3+}+Ti-trend line. This is consistent with late recrystallization of interstitial olivine (Fig.11B).

The large intersilicate chrome-spinels are the result of continued reaction and growth of earlier spinels that were not enclosed by silicate grains. The addition of Fe^{3+} and Ti with increasing size of the spinel grain had the effect of diluting the Cr and Al content. The Fe- and Ti-rich spinels in biotites are strongly depleted in Al and Mg (Fig.13); this demonstrates that they also had access to trapped liquid until late during magma crystallization.

VIII CONCLUSIONS

The Crystal Lake spinels have great diversity of compositions, and occur in rocks presenting a wide spectrum of textural variations from adcumulates to orthocumulates and their disrupted equivalents. These variations reflect a complex history of reequilibration.

Chrome-spinels are the earliest cumulus minerals in the cyclic zone, and probably first crystallized as a result of magma mixing on the influx of new magma. The spinels probably had fairly similar compositions during their initial

crystallization, but were subject to reequilibration with evolving magmatic liquid. Cation exchanges with intercumulus liquid were relatively insignificant during the cumulus stage. Postcumulus reactions of spinel were the main mechanism responsible for their compositional variability. Reflecting the crystallization order of silicates, spinels were successively trapped by plagioclase, olivine, augite, and finally biotite.

Spinels are well known as petrologic indicators of the compositions of liquids with which they equilibrated. It is considered that the present compositions of spinels reflect the composition of the intercumulus liquid at the time of trapping. They are believed to have been protected from further reaction with magmatic liquid by the enclosing silicate. Solid state elemental diffusion between spinel and surrounding silicates appears to have been relatively insignificant in the Crystal Lake intrusion.

The main control on compositional variations in spinel is reaction with intercumulus liquid. The nature of reequilibration of spinel is related to the following features: the immediate textural environment (whether between silicates, included in a host mineral, in an adcumulate layer), nature of the host silicate, crystallization order of host silicates, and reequilibration of orthocumulate olivine.

Six spinel groups are distinguished on the basis of definite compositional ranges and textural characteristics. Group I and II are adcumulates, the latter of which occurs in disrupted layers. Group III is observed in reequilibrated orthocumulate olivines. Group IV occurs in interstitial silicates. Group V comprises large intersilicate spinels. Group VI is included in biotites.

Four post-cumulus variation trends are recognised. (1) Cr-trend 1 is observed in adcumulate spinels of groups I and II. It is characterised by increasing Cr/Al while Al and Mg decrease. (2) Cr-trend 2 occurs only in spinels of recrystallized orthocumulate olivine, and has higher Fe^{3+}/Fe^{2+} ratios than those of Cr-trend 1. (3) Fe^{3+}+Ti-trends 1 and 2 are found in orthocumulate spinels. They are characterized by significant increases of Fe^{3+} and Ti with decreasing Al and Mg. (4) Fe^{3+}+Ti-trend 2 is restricted to spinel inclusions of biotites. It is characterized by the lowest Al and Mg.

The Fe^{3+}/Fe^{2+} ratios of the Cr-trends are low and relatively constant. The reactions between intercumulus liquid and the main magma body may have occurred at relatively constant temperatures. The Fe^{3+}/Fe^{2+} ratios of the Fe^{3+}+Ti-trends are higher, and reactions with trapped intercumulus liquid probably occurred at relatively low temperatures.

Spinel compositions reveal that orthocumulate plagioclase probably experienced adcumulate growth during early stages of crystallization. As soon as the intercumulus liquid was trapped, the olivine reequilibrated with it. The compositional diversity of spinels in olivine is the result of resorption of primary host silicates, and reequilibration of their spinels with the recrystallized host olivine.

Large intersilicate chrome-spinels are the result of continued growth of spinels and their reaction with trapped intercumulus liquid until complete solidification.

ACKNOWLEDGEMENTS

The author would like to thank J.M.Duke, R.F.J.Scoates and O.R.Eckstrand of the Geological Survey of Canada for constructive comments and for providing microprobe analytical facilities. Thanks are also due to D.C.Harris, G.Lecheminant and M.Bonardi for assistance with microprobe analyses. W. Petruk of CANMET carried out modal analyses by image analyser, for which the author is grateful. R. M. Laramee is thanked for assistance with computer aspects of printing. Boliden Canada Ltd., and J.McGoran of Fleck Resources Ltd. kindly granted access to the property and drill core at Thunder Bay.

This research was partly supported by the grant A0590 from the Natural Sciences and Engineering Research Council of Canada.

REFERENCES

CAMERON, E.N., 1975, Postcumulus and subsolidus equilibrium of chromite and coexisting silicates in the Eastern Bushveld Complex; Geochimica et Cosmochimica Acta, v.39, p.1021-1033.

CAMERON,E.N.,1977, Chromite in the central sector of the Eastern Bushveld Complex, South Africa; American Mineralogist, v.62, p.1082-1096.

CHALOKWU, C.I., 1985, A geochemical, petrological and compositional study of the Partridge River intrusion, Duluth Complex, Minnesota; Ph.D.thesis, Miami University, Oxford, Ohio, 232 p.

CHALOKWU, C.I. and NORMAN, K.G., 1987, Reequilibration of olivine with trapped liquid in the Duluth Complex, Minnesota; Geology, v.15, p.71-74.

COGULU, E.H., 1984, Magmatic cycles in the Crystal Lake gabbros, Thunder Bay, Ontario; Geological Association of Canada/Mineralogical Association of Canada Annual meeting, Program with Abstracts, p.53.

COGULU, E.H., 1985, Platinum group elements and chromian spinel variations in the Crystal Lake gabbros,Thunder Bay, Ontario; (abstract) Fourth International Platinum Symposium, Canadian Mineralogist, v.23, p.299-300.

COGULU,E.H.,1990, Mineralogical and Petrological studies of the Crystal Lake intrusion. Thunder Bay, Ontario. Open File 2277. Geological Survey of Canada. Ottawa.

COGULU, E.H.,1993, Mineralogy and chemical variations of sulphides in the Great Lakes Nickel deposit, Thunder Bay, Ontario; Geological Survey of Canada, Open File.

DUKE, J.M., 1983, Magmatic segregation deposits of chromite; Geoscience Canada; v.10, no.1, p.133-143.

EALES,H.V., and SNOWDEN,D.V.1979, Chromiferous spinels of the Elephant's Head dike. Mineralum deposita, vol. 14, pp.227-242.

EALES, H.V. and REYNOLDS, I.M., 1983, Factors influencing the composition of chromite and magnetite in some southern African rocks; Geological Society of South Africa, Special Publication, v.7, p.5-20.

ECKSTRAND, O.R. and COGULU, E.H. 1986, Se/S evidence relating to the genesis of sulphides in the Crystal Lake gabbro, Thunder Bay, Ontario. Geological Association of Canada, Annual meeting, Ottawa. Program with abstracts, v.11, p.66.

EVANS, B.W. and MOORE, J.G., 1968, Mineralogy as a function of depth in the prehistoric Makaopuhi tholeiitic lava lake, Hawaii; Contributions to Mineralogy and Petrology, v.17, p.85-115.

GEUL, J.J.C., 1970, Geology of Devon and Pardee Townships and The Stuart Location; Ontario Department of Mines, Geological Report 87, 52 p.

HENDERSON, P., 1975, Reaction trends shown by chrome-spinels of the Rhum layered intrusion; Geochimica et Cosmochimica Acta., v.39, p.1035-1044.

HENDERSON, P. and SUDDABY, P., 1971, The nature and origin of the chrome-spinel of the Rhum layered intrusion; Contributions to Mineralogy and Petrology,, v.33, p.21-31.

HILL, R. and ROEDER, P.L., 1974, The crystallization of spinel from basaltic liquid as a function of oxygen fugacity; Journal of Geology, v.82, p.709-729.

IRVINE, T.N., 1965, Chromian spinel as a petrogenetic indicator. Part 1. Theory; Canadian Journal of Earth Sciences, v.2, p.648-672.

IRVINE, T.N., 1967, Chromian spinel as a petrogenetic indicator. Part 2.; Canadian Journal of Earth Sciences, v.4, p.71-103.

IRVINE, T.N., 1977, Origin of chromitite layers in the Muskox intrusion and other stratiform intrusions: A new interpretation; Geology, v.5, p.273-77.

IRVINE, T.N., 1980, Magmatic infiltration metasomatism, double-diffusive fractional crystallization, and adcumulus growth in the Muskox intrusion and other layered intrusions, in Physics of Magmatic Processes, Hargraves,R.B., ed., Princeton University Press, New Jersey, p.325-383.

IRVINE, T.N., 1982, Terminology for layered intrusions; Journal of Petrology, v.23, p.127-162.

MACRAE, N.D. and REEVE, E.J., 1968, Differentiation sequence of the Great Lakes Nickel intrusion; (abstract) Institute of Lake Superior Geology, Annual Meeting, Wisconsin.

MAINWARING, P.R. and Watkinson, D.H., 1981, Origin of chromian spinel in the Crystal Lake intrusion, Pardee Township, Ontario; Ontario Geological Survey, Miscellaneous Paper 98, p.180-186.

OSBORN, E.F., 1959, Role of oxygen pressure in the crystallization and differentiation of basaltic magma; Americal Journal of Science, v.257, p.609-647.

RIDLEY, W.I, 1977, The crystallization trends of spinels in Tertiary basalts from Rhum and Muck and their petrogenetic significance; Contributions to Mineralogy and Petrology, v.64, p.243-255.

ROEDER, P.L. and CAMPBELL, I.H., 1985, The effect of postcumulus reactions on composition of chrome-spinels from Jimberlana intrusion, Journal of Petrology, v.26, p.763-786.

SCOATES, R.F.J., 1983, A preliminary stratigraphic examination of the ultramafic zone of the Bird River Sill; Manitoba Department of Energy and Mines, Report of Field Activities, p.70-83.

SCOATES, R.F.J., WILLIAMSON, B.L. and DUKE, J.M., 1986, Igneous layering in the ultramafic series, Bird River Sill, in Layered intrusion of southeastern Manitoba and Northwestern Ontario; Geol.Assoc. Canada, Annual Meeting, Field trip guidebook.

SILVER, L.T. and GREEN, J.C., 1972, Time constants for Keweenawan igneous activity; Geological Society of America, Program and Abstracts, v.4, p.665-666.

STEWART, A.D., 1963, On certain slump structures in the Torridonian sandstones of Applecross; Geological Magazine, v.100, p.205-218.

ULMER, G.C., 1969, Experimental investigations of chromite spinels; Economic Geology, Monograph 4, p.114-131.

WILSON, A.H., 1982, The geology of the Great Dyke, Zimbabwe: The ultramafic rocks; Journal of Petrology, v.23, p.240-292.

FIGURES

Fig. 1 Geological map of the Crystal Lake area (modified from Geul, 1970). Star indicates location of surface sampling.

Fig. 2 Stratigraphic column for the western portion of the Crystal Lake intrusion.

Fig. 3 Stratigraphic column of the cyclic zone. The thicknesses of the chrome-spinel occurrences are exaggerated.

Fig. 4 Compositions of Cr-spinel groups I to IV of the cyclic zone. A) Al-Cr-Fe^{3+} diagram, plotted analyses. B) Generalized compositional trends of the four groups. Two of the trends reflect variations mainly in Cr content, and two mainly in Fe^{3+}+Ti content.

Fig. 5 A) Al-Cr-Fe^{3+} diagram of Cr-spinel chadacrysts in plagioclase, olivine and biotite in adcumulate rocks. B) Al-Cr-Fe^{3+} diagram of chrome spinel occurring in a disrupted adcumulate layer. Open rectangles = Cr-spinel in plagioclase; crosses = Cr-spinel in olivine; X's = Cr-spinel in biotite.

Fig. 6 Al-Cr-Fe^{3+} diagrams of Cr-spinels in orthocumulate rocks. A) Sample No: 271. B) Sample No: 268.

Fig. 7 Compositions of adcumulate and orthocumulate Cr-spinel with respect to A) Al-Cr-Fe^{3+}, and B) Fe^{3+}-Fe^{2+}-Mg. Filled rectangles = adcumulate Cr-spinel, crosses = orthocumulate Cr-spinel.

Fig. 8 Compositions of adcumulate and orthocumulate Cr-spinel with respect to A) Fe^{3+}/Fe^{2+} versus $Mg/Mg+Fe^{2+}$; B) Cr/Cr+Al versus $Mg/Mg+Fe^{2+}$; C) Ti/Ti+Cr+Al versus $Mg/Mg+Fe^{2+}$; and D) Al versus Fe^{2+}+Ti. . Filled rectangles = adcumulate Cr-spinel, crosses = orthocumulate Cr-spinel.

Fig. 9 Al-Cr-Fe^{3+} diagrams of adcumulate Cr-spinels in A) a single plagioclase oikocryst; B) a single olivine oikocryst; and C) a single biotite oikocryst. Arrow shows the sense of Cr-spinel compositional changes from core (C) to margin (M) of the host silicate.

Fig. 10. Al-Cr-Fe^{3+}diagrams of Cr-spinels in orthocumulate-textured rocks A) in a single cumulus plagioclase grain, and B) in cumulus plagioclase grains of a single rock sample. I = Cr-spinels in the core of the plagioclase; II = Cr-spinels in the zoned cumulus plagioclase surrounding the core; and III = Cr-spinels in the post cumulus plagioclase overgrowth zone.

Fig. 11 A) Al-Cr-Fe^{3+} diagram of Cr-spinel in poikilitic olivine which contains partially resorbed plagioclase relicts. B) Al-Cr-Fe^{3+} diagram of Cr-spinel in polygonal and poikilitic interstitial olivine. Filled rectangles = Cr-spinel in polygonal olivines. X's = Cr-spinel in poikilitic interstitial olivines. Cr-Trend 1 line is shown in for comparison.

Fig. 12 Al-Cr-Fe^{3+} diagrams of Cr-spinels in adjacent plagioclase (open rectangles) and interstitial augite (X's). A) The plagioclase is a normally zoned cumulus mineral with a post cumulus marginal overgrowth (see Photos 3, 4). B) Post cumulus plagioclase as a marginal overgrowth.

Fig. 13 Al-Cr-Fe^{3+} diagrams of Cr-spinel: A) in biotite of disrupted adcumulates; B) in biotite of orthocumulate. Fe^{3+}+Ti-Trend 1 line is shown for comparison.

Fig. 14 Compositional variations of Cr-spinel chadacrysts and host plagioclase in adcumulate rock. A) Compositional profile of a zoned plagioclase oikocryst; B) profile of compositions of Cr-spinel chadacrysts in a plagioclase host. I and II represent plagioclase core and overgrowth zone respectively.

Fig. 15 Compositional variations of Cr-spinel chadacrysts and host plagioclase in orthocumulate rock. A) Compositional profile of host plagioclase; B) profile of compositions of Cr-spinel chadacrysts in a plagioclase host. I,II,III represent orthocumulate plagioclase core, cumulus overgrowth, and post cumulus marginal overgrowth zones, respectively.

Fig. 16 Compositional variations of Cr-spinel chadacrysts and host olivine in adcumulate rock. A) Compositional profile of host olivine; B) profile of compositions of Cr-spinel inclusions in host olivine.

Fig. 17 Compositional variations of Cr-spinel chadacrysts and host olivine in orthocumulate rock. A) Compositional profile of host olivine; B) profile of compositions of Cr-spinel inclusions in host olivine. Spinels 3 and 4 are surrounded by relict plagioclase (analyses are given in Table 12).

Fig. 18 Comparison of compositions of Cr-spinel chadacrysts in olivine oikocrysts in adcumulate (crosses) and orthocumulate (X's) rocks. A) Cr/Cr+Al versus $Mg/Mg+Fe^{2+}$; B) $Fe^{2+}+Fe^{3+}$ versus Ti. Arrow shows the trend of Cr-spinel compositions from core to margin of the host olivine.

Fig. 19 Al-Cr-Fe^{3+} diagram for A) large interstitial Cr-spinel grains; and for B) Cr-spinel associated with polarity textured sulphide blebs.

Fig. 20 $Mg/Mg+Fe^{2+}$ versus Cr/Cr+Al of Cr-spinels from the base and the top of an undisrupted adcumulate layer. Crosses = in plagioclase at the base of the layer; open rectangles = in plagioclase at the top; filled rectangles = in olivine at the base; X's = olivine at the top; circles = Cr-spinel in biotites.

Fig. 21 Comparison of compositions of Cr-spinel and hosting silicates in the base and the top of the adcumulate layer, and in the adjacent orthocumulate rocks.

PHOTOGRAPHS

Photo 1 Homogeneous distribution of chrome-spinel in adcumulate rock. Transmitted light. Magnification ×8. Sample 255. Cycle 2.

Photo 2 Chrome-spinels in adcumulate rock.Reflected light. Magnification ×10. Sample 14/2. Cycle 4.

Photo 3 Poikilitic olivine resorbing plagioclase. Plagioclase relicts surround chrome-spinel inclusions. Transmitted light.Magnification ×16. Sample 267/1. Cycle 3.

Photo 4 Poikilitic olivines containing chrome spinels and partially resorbed plagioclase relicts. Transmitted light. Magnification ×10. Sample 267. Cycle 3.

Photo 5 Large chrome spinels containing ilmenite exsolution lamellae. Composite sulphide grains comprise chalcopyrite,cubanite,prrhotite and pentlandite. Reflected light. Magnification ×60. Sample 268. Cycle 3.

Photo 6 Adcumulate chrome-spinel containinig acicular ilmenite inclusions. Reflected light. Magnification ×150. Sample 14/2. Cycle 4.

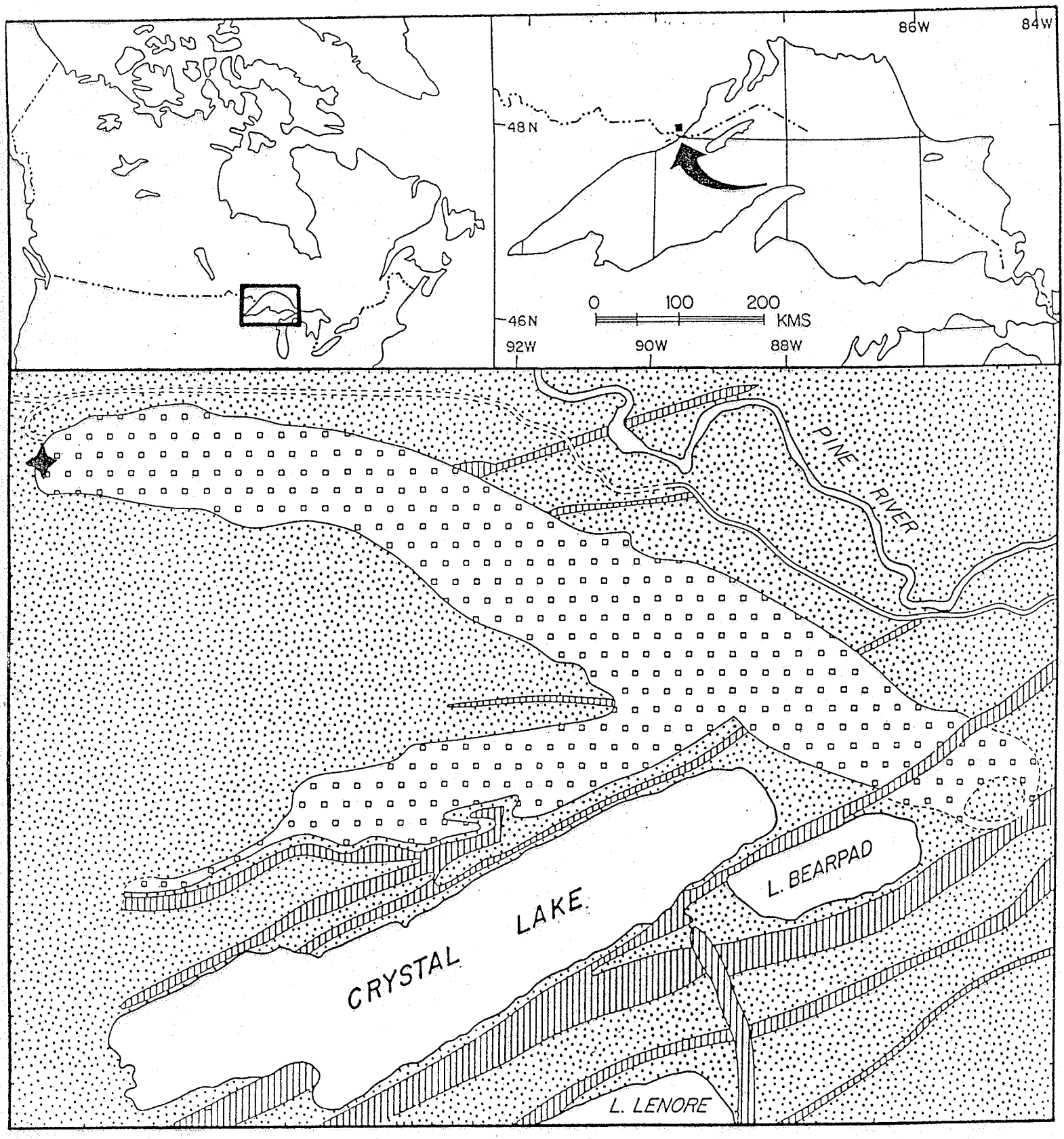
86W
84W
48N
46N
92W
90W
88W
0 100 200
KMS
PINE RIVER
CRYSTAL LAKE
L. BEARPAD
L. LENORE
SEDIMENTARY ROCKS (ROVE FORMATION) AND GLACIAL DEPOSITS
PIGEON RIVER DIABASE DYKES
CRYSTAL LAKE GABBROIC INTRUSION
0 1 2
KILOMETRES

Fig. 1

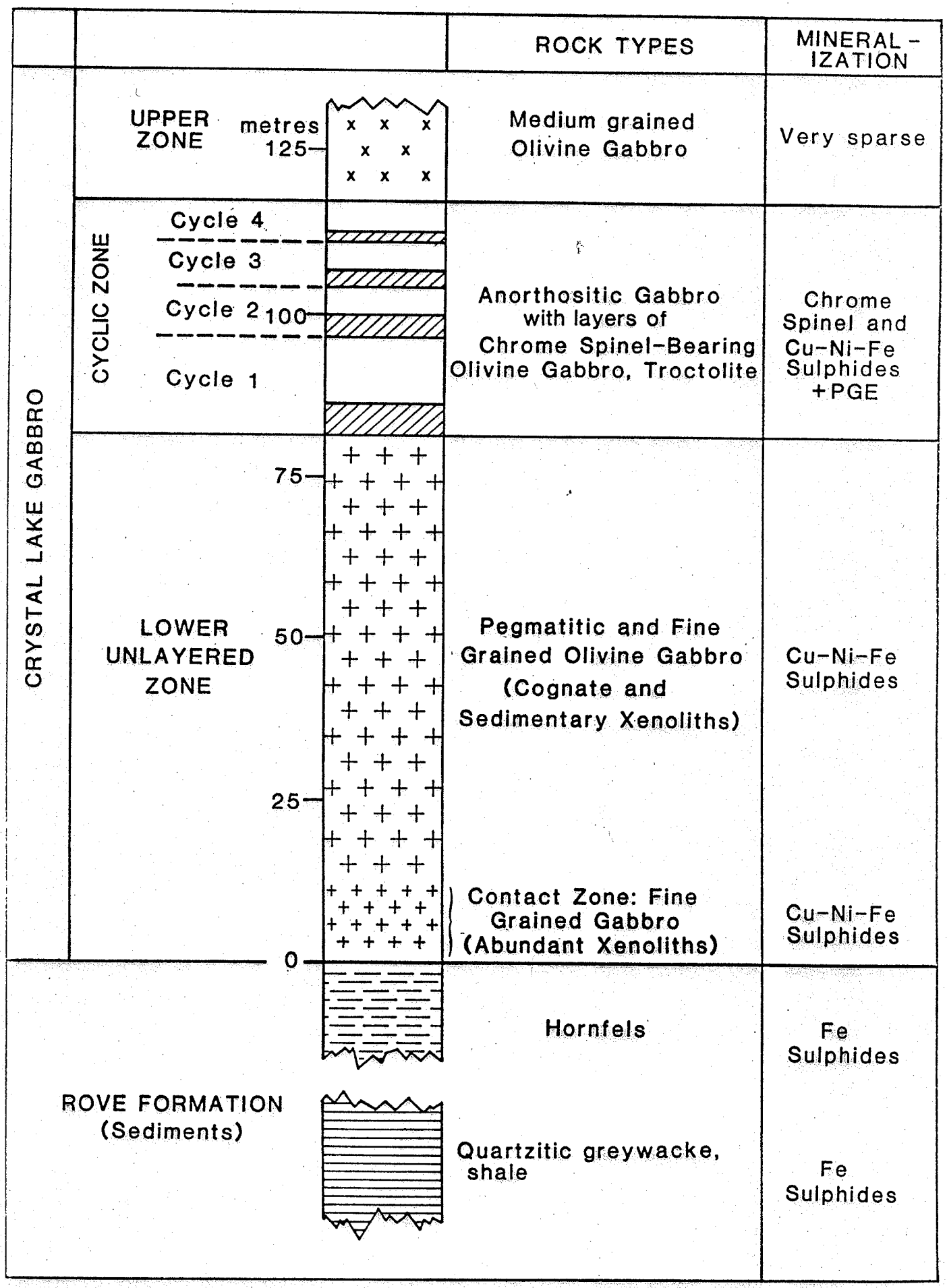
ROCK TYPES
MINERAL-IZATION
CRYSTAL LAKE GABBRO
UPPER ZONE
metres
125
Medium grained Olivine Gabbro
Very sparse
CYCLIC ZONE
Cycle 4
Cycle 3
Cycle 2
100
Cycle 1
Anorthositic Gabbro with layers of Chrome Spinel-Bearing Olivine Gabbro, Troctolite
Chrome Spinel and Cu-Ni-Fe Sulphides +PGE
75
LOWER UNLAYERED ZONE
50
Pegmatitic and Fine Grained Olivine Gabbro (Cognate and Sedimentary Xenoliths)
Cu-Ni-Fe Sulphides
25
Contact Zone: Fine Grained Gabbro (Abundant Xenoliths)
Cu-Ni-Fe Sulphides
0
Hornfels
Fe Sulphides
ROVE FORMATION (Sediments)
Quartzitic greywacke, shale
Fe Sulphides

Fig. 2

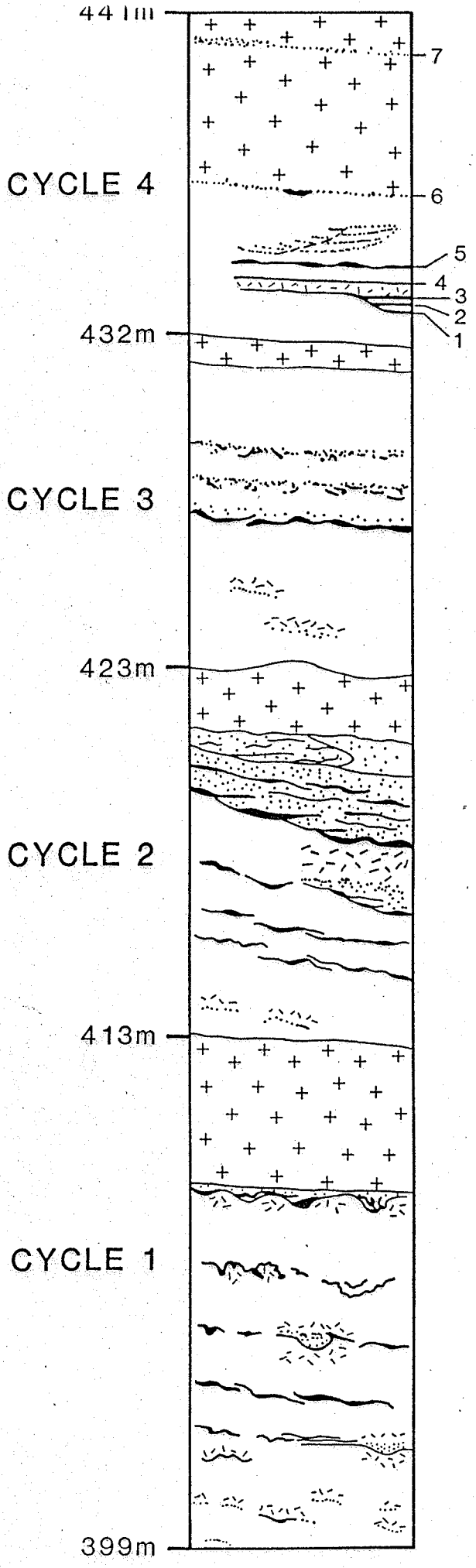

ANORTHOSITIC GABBRO

OLIVINE GABBRO

PEGMATITE

Cr-SPINEL ADCUMULATE

Cr-SPINEL ORTHOCUMULATE

Cr-SPINEL SEAM

CROSS LAMINATION

1m
0 1m

(The thickness of the Cr-spinel occurrences are exaggerated)

Fig. 3

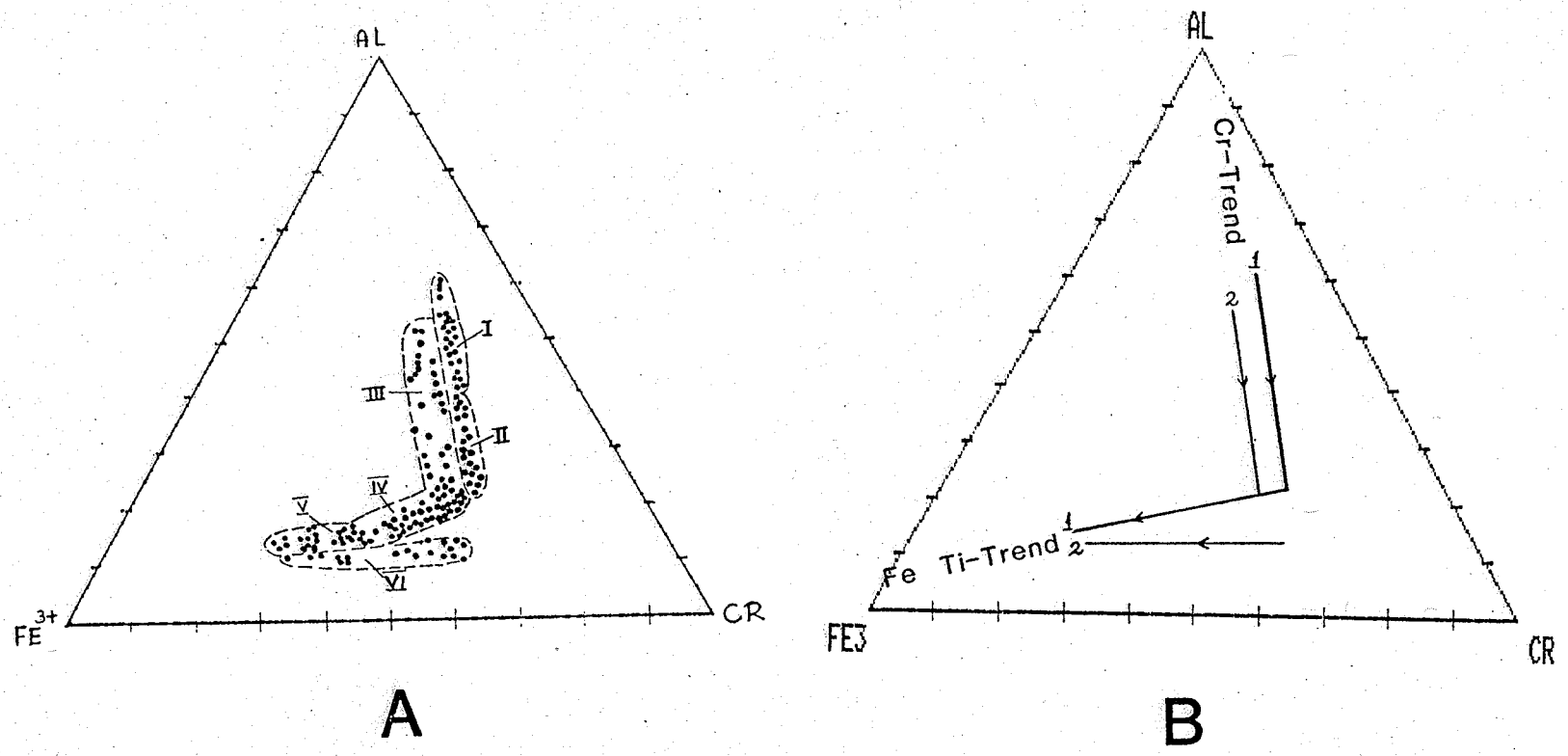

Fig. 4

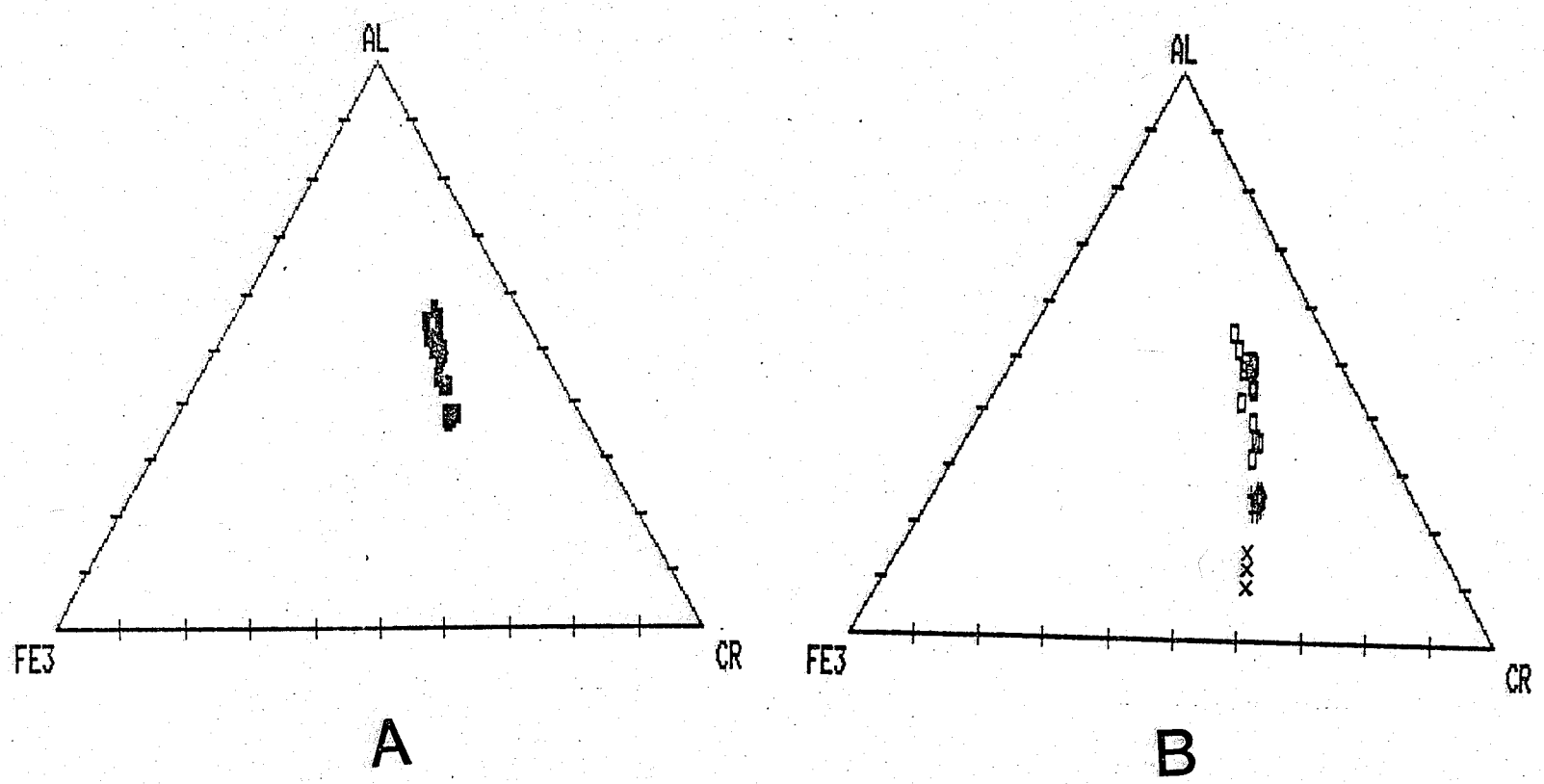

Fig. 5

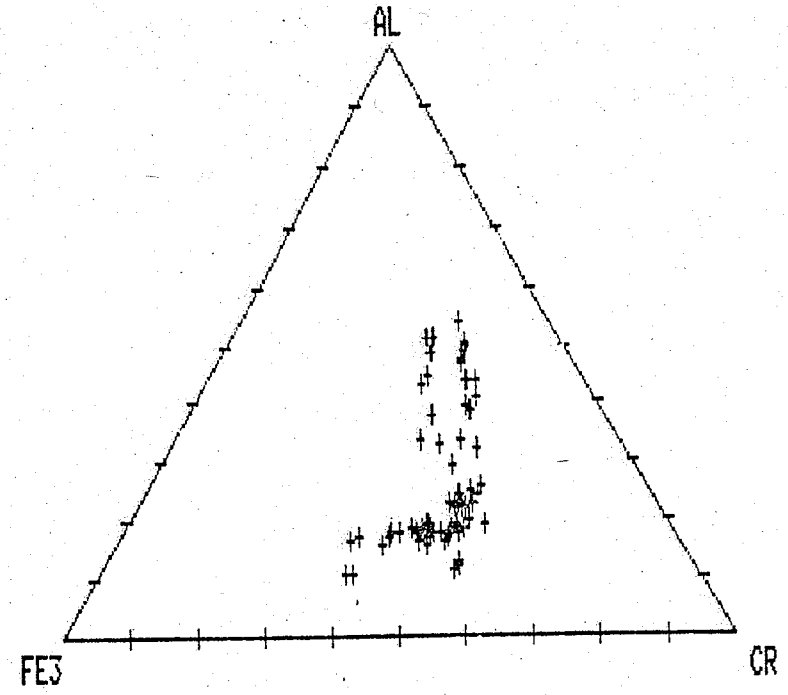

A

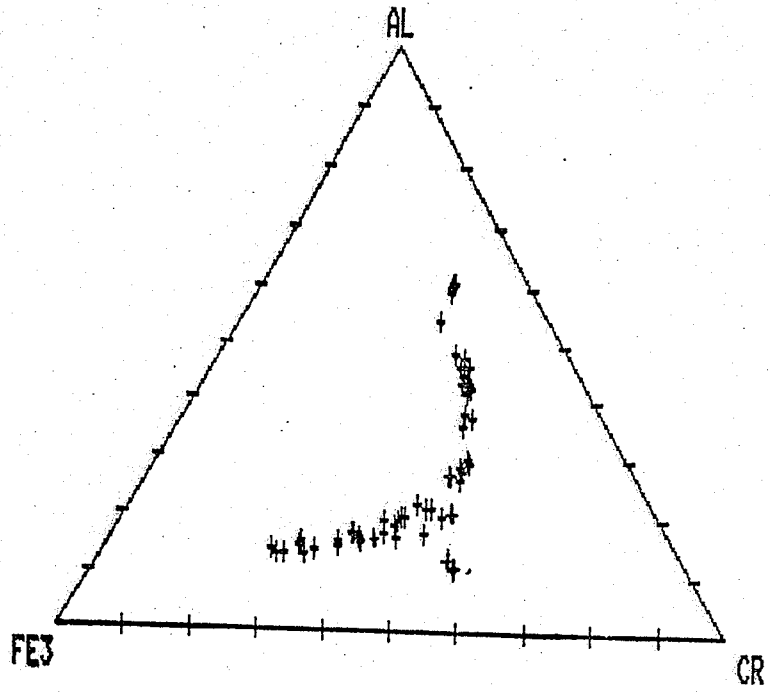

B

Fig. 6

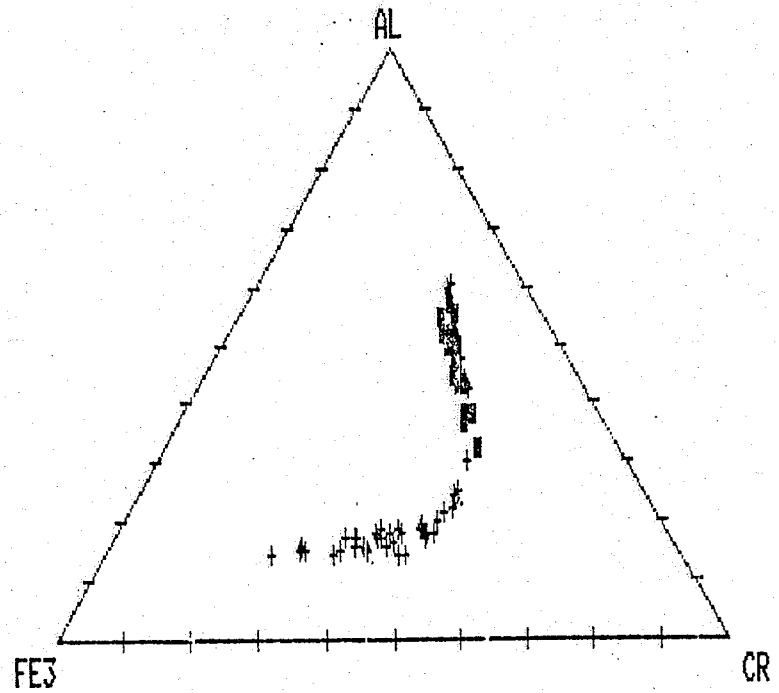

A

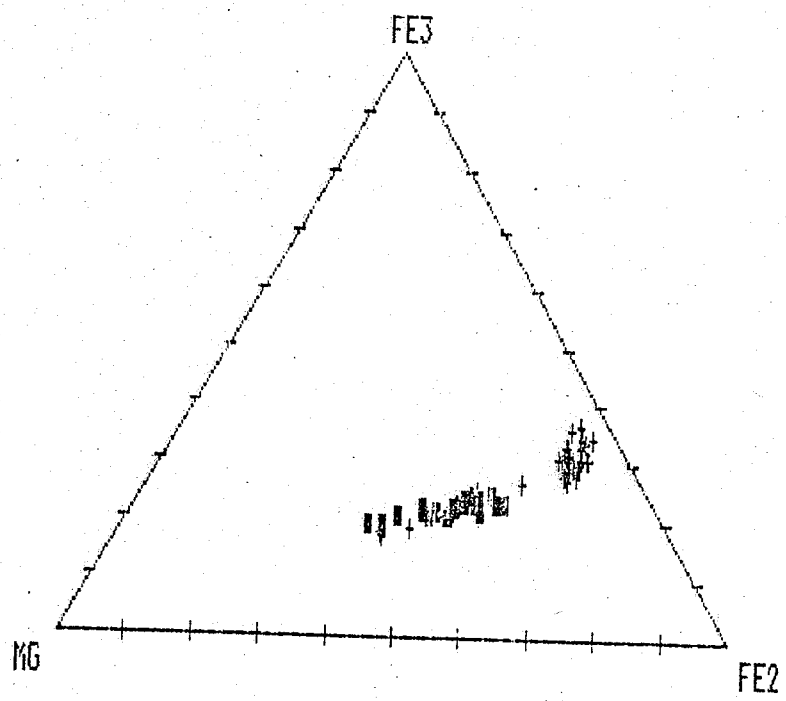

B

Fig. 7

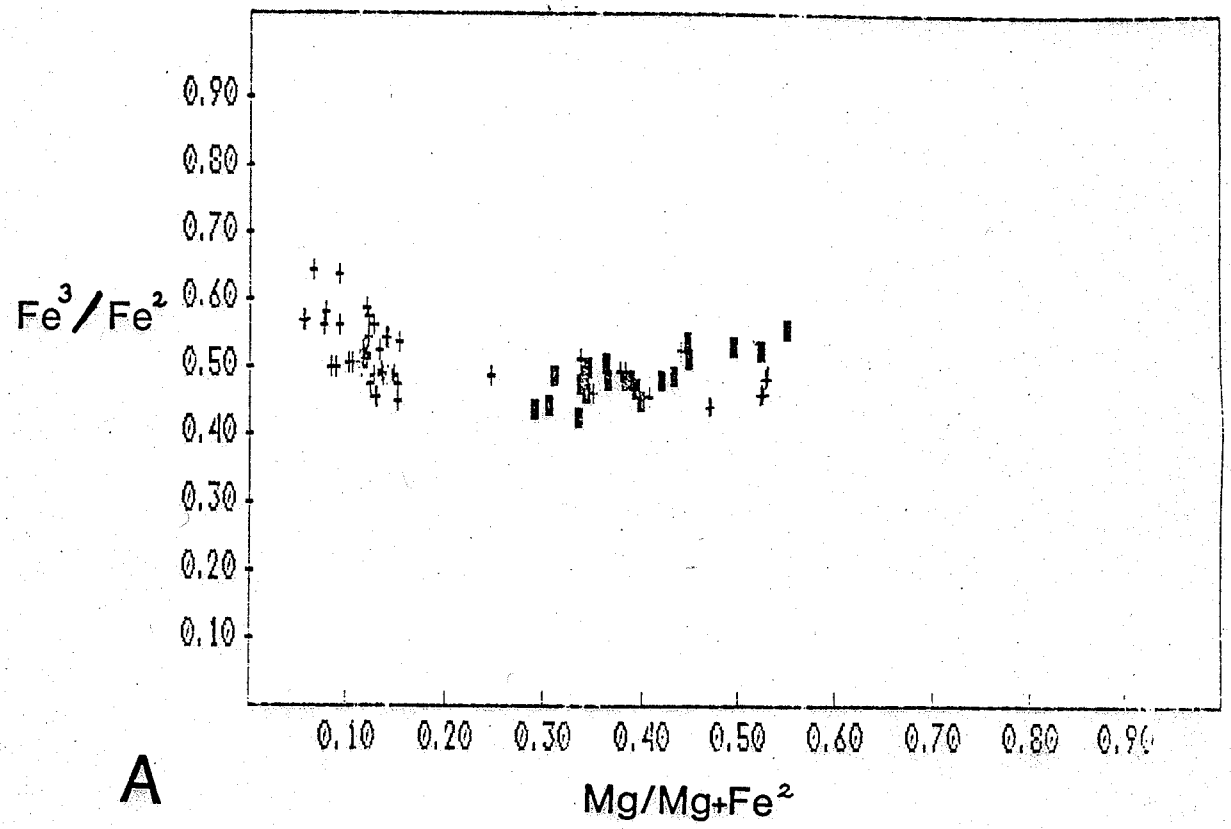

A

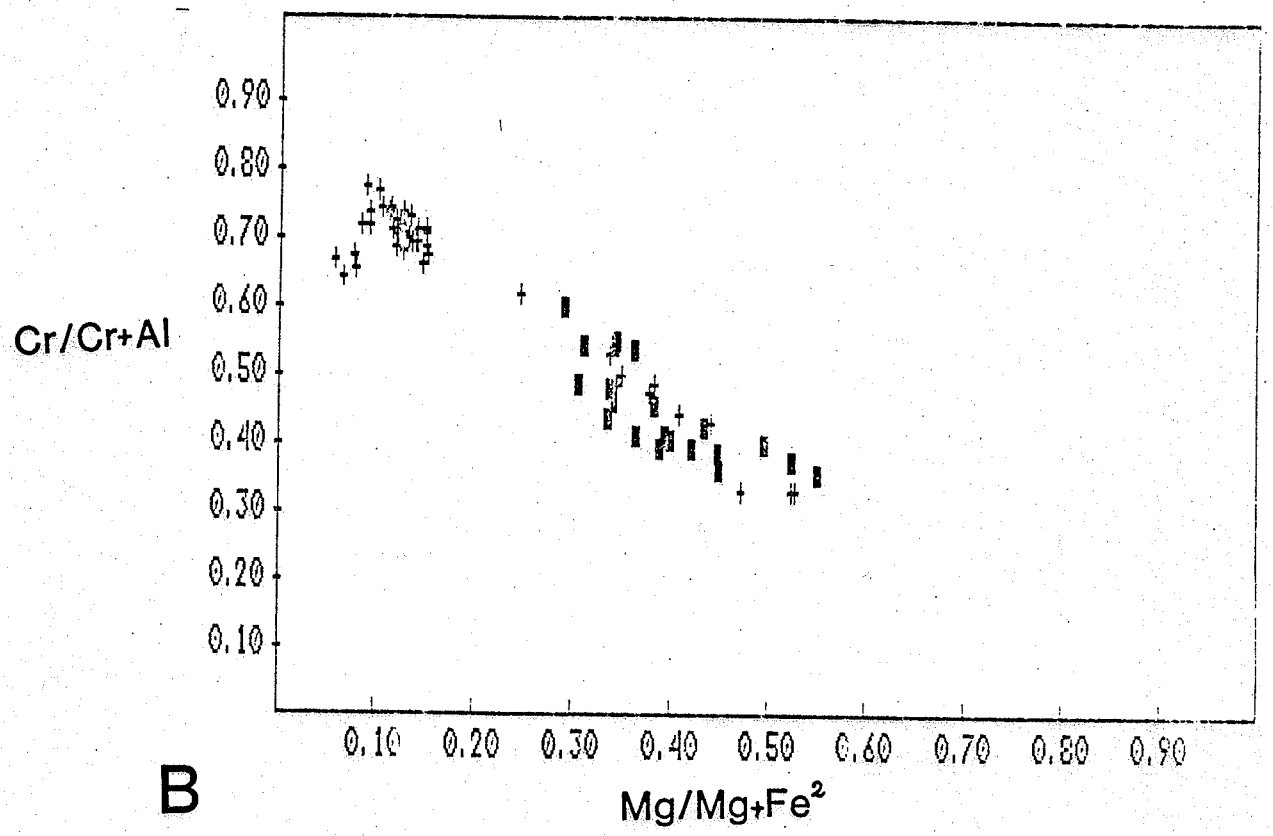

B

Fig.8 A and B

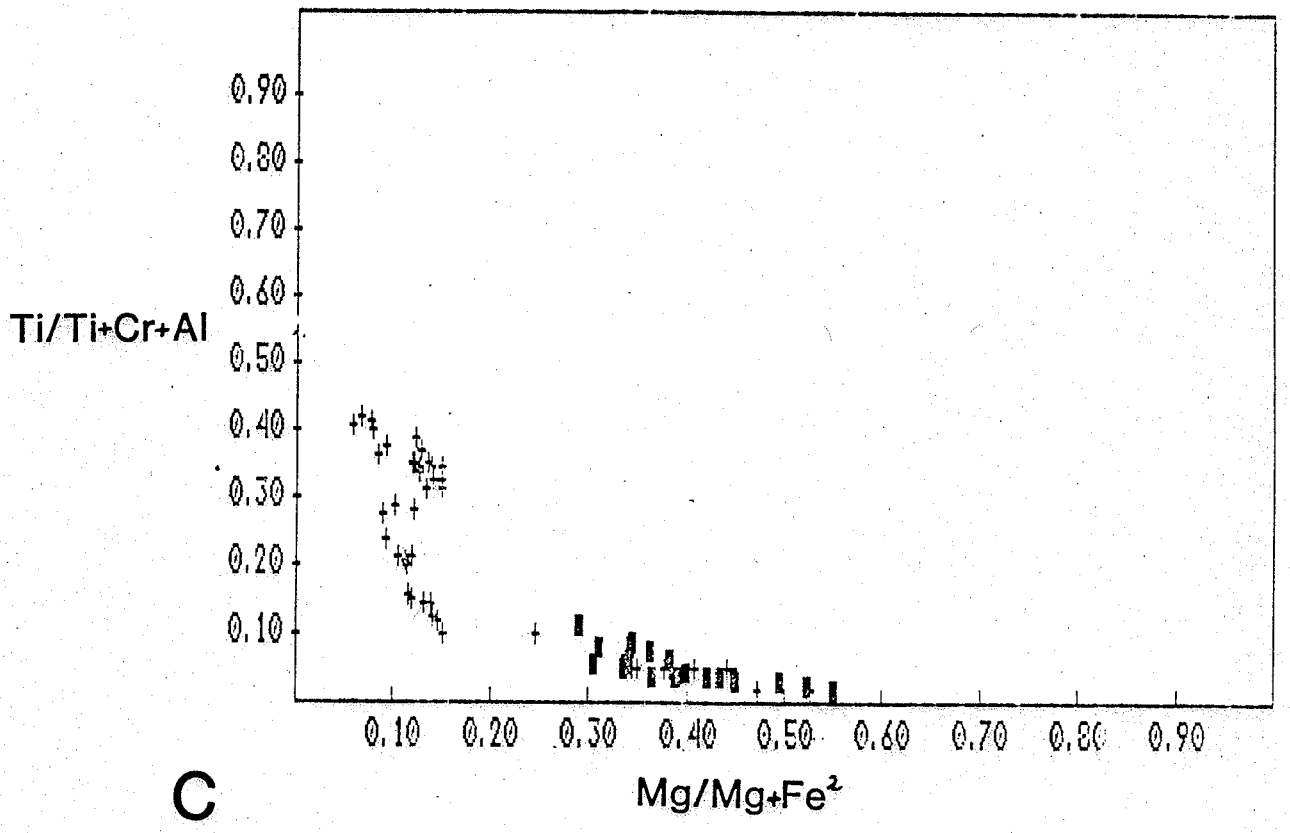

C

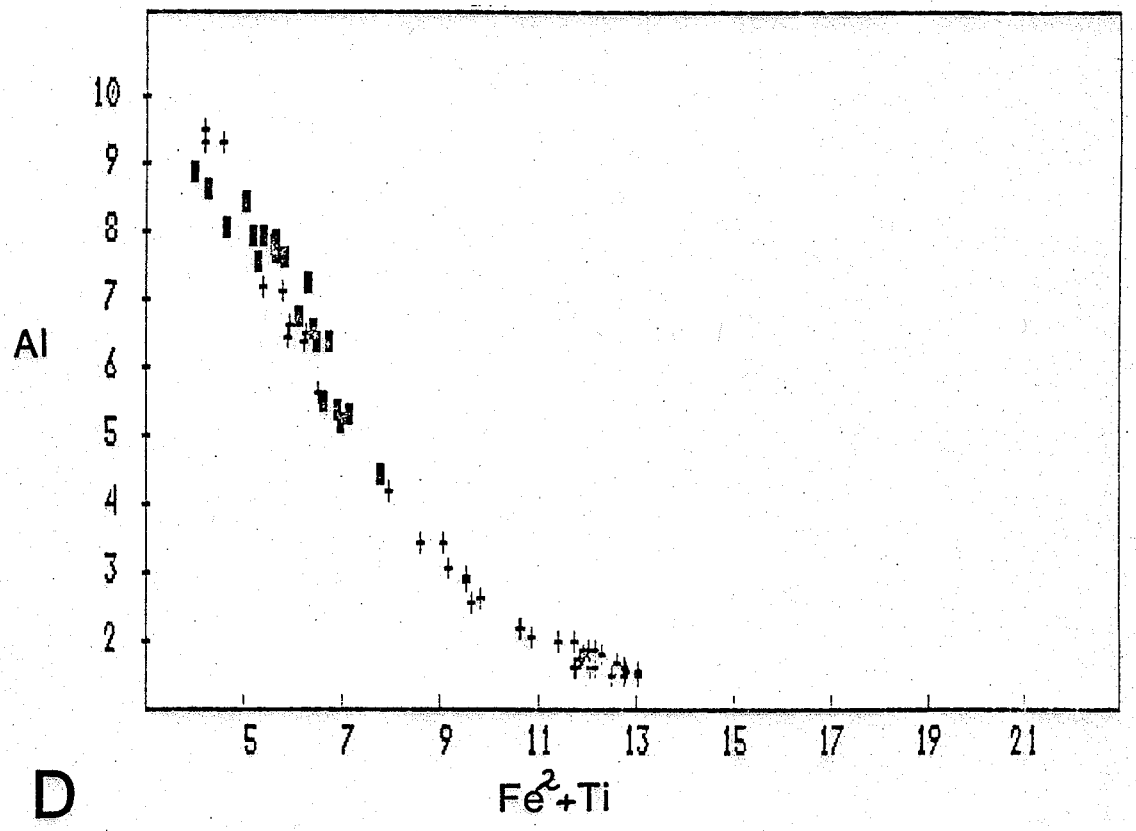

D

Fig.8 C and D

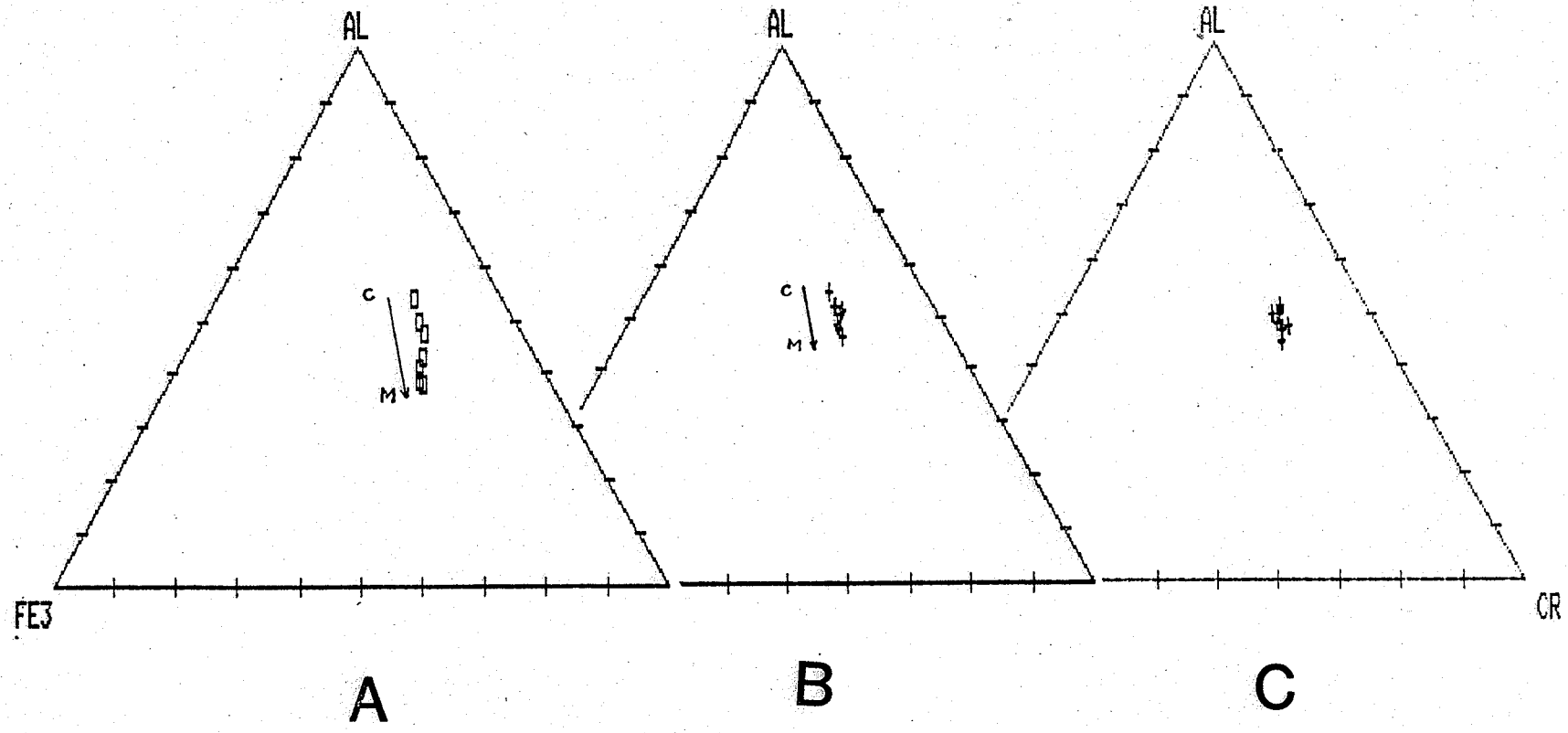

Fig. 9

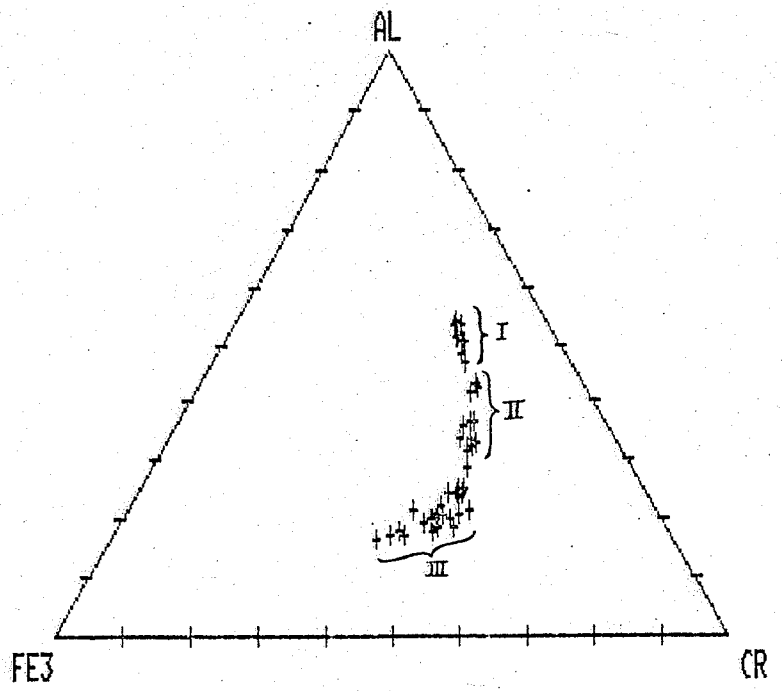

A

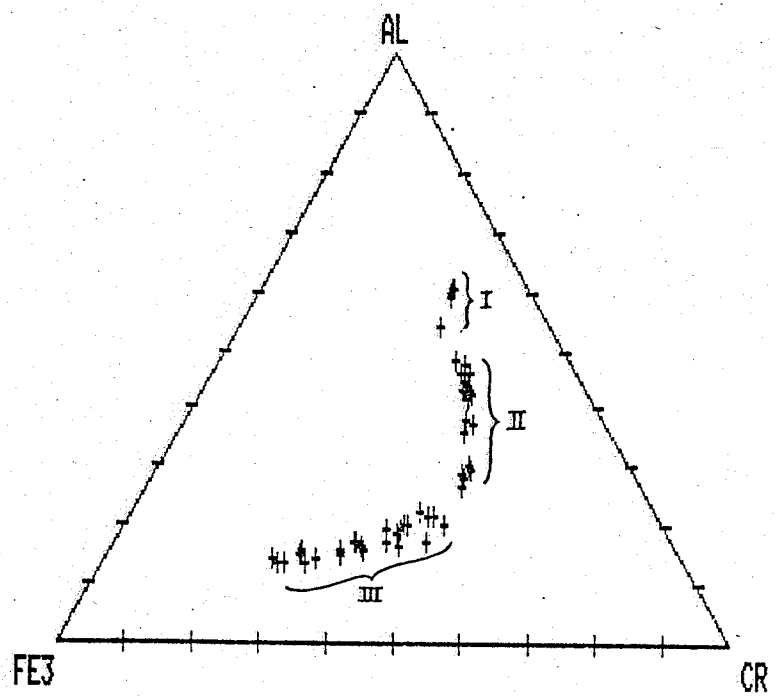

B

Fig. 10

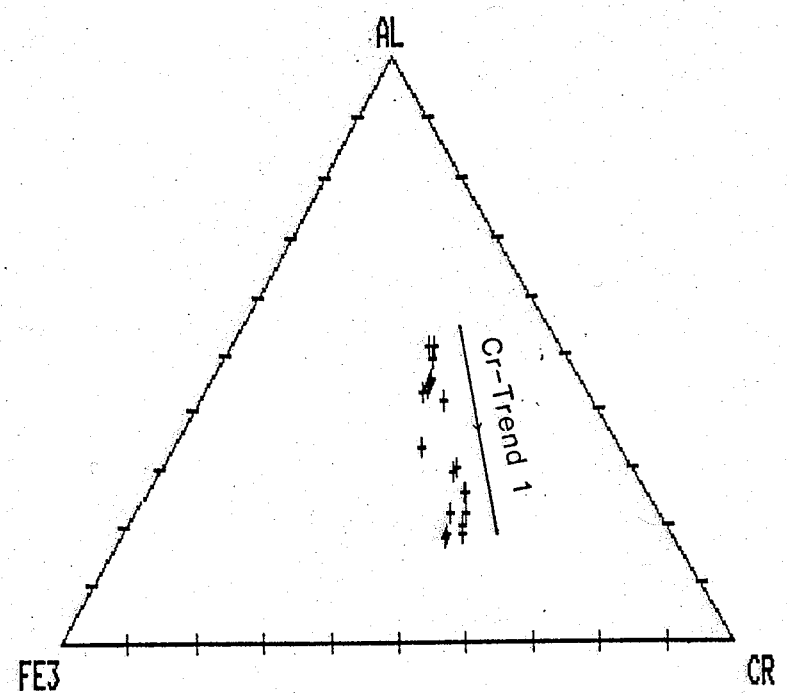

A

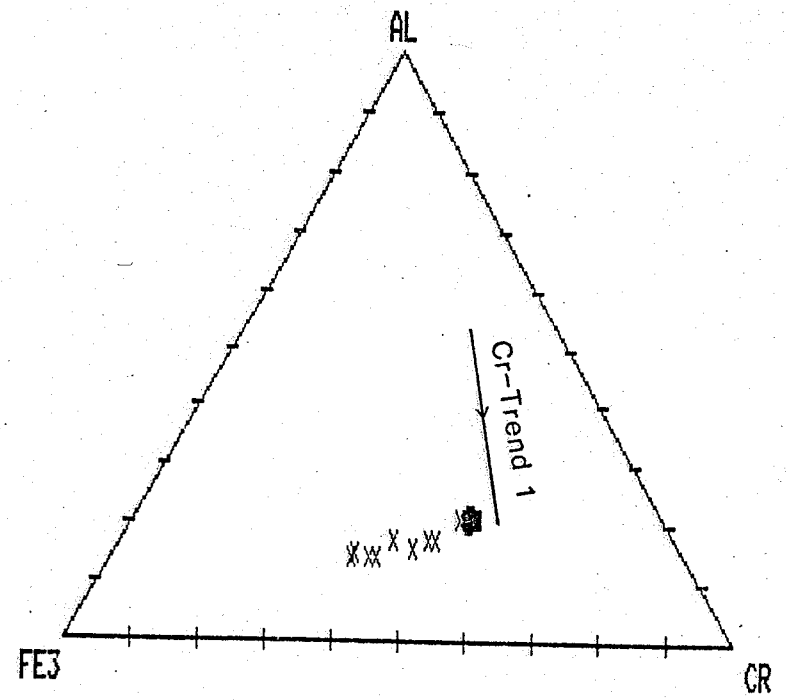

B

Fig. 11

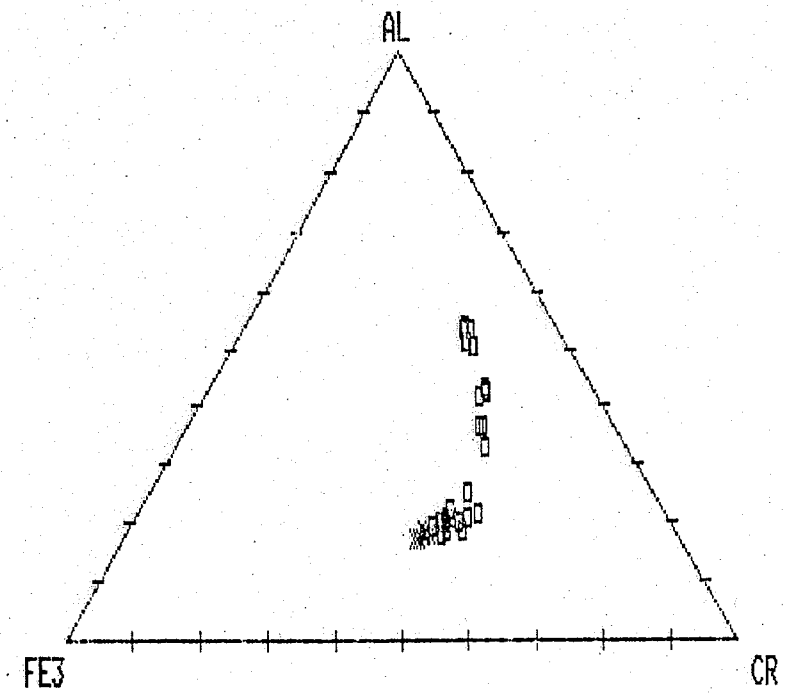

A

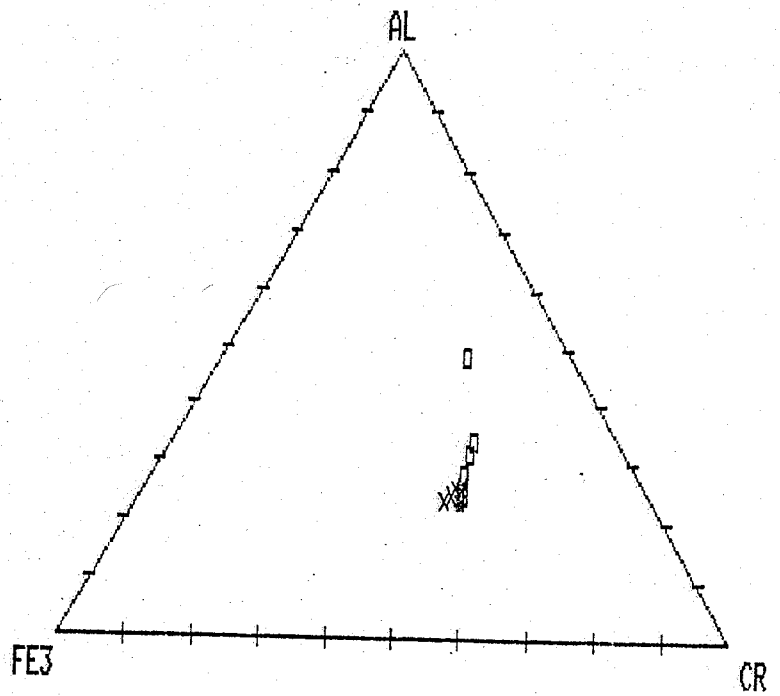

B

Fig. 12

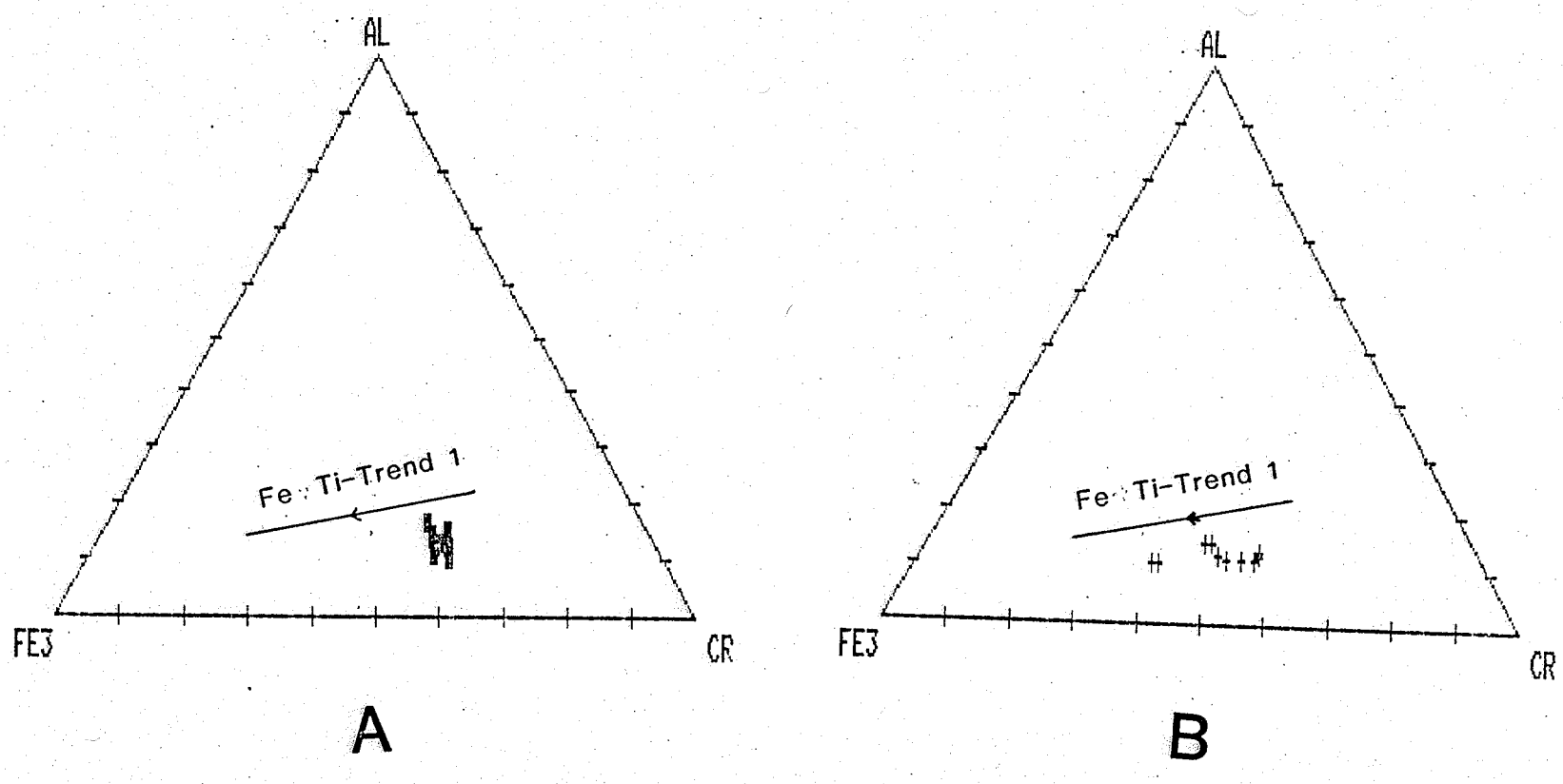

Fig. 13

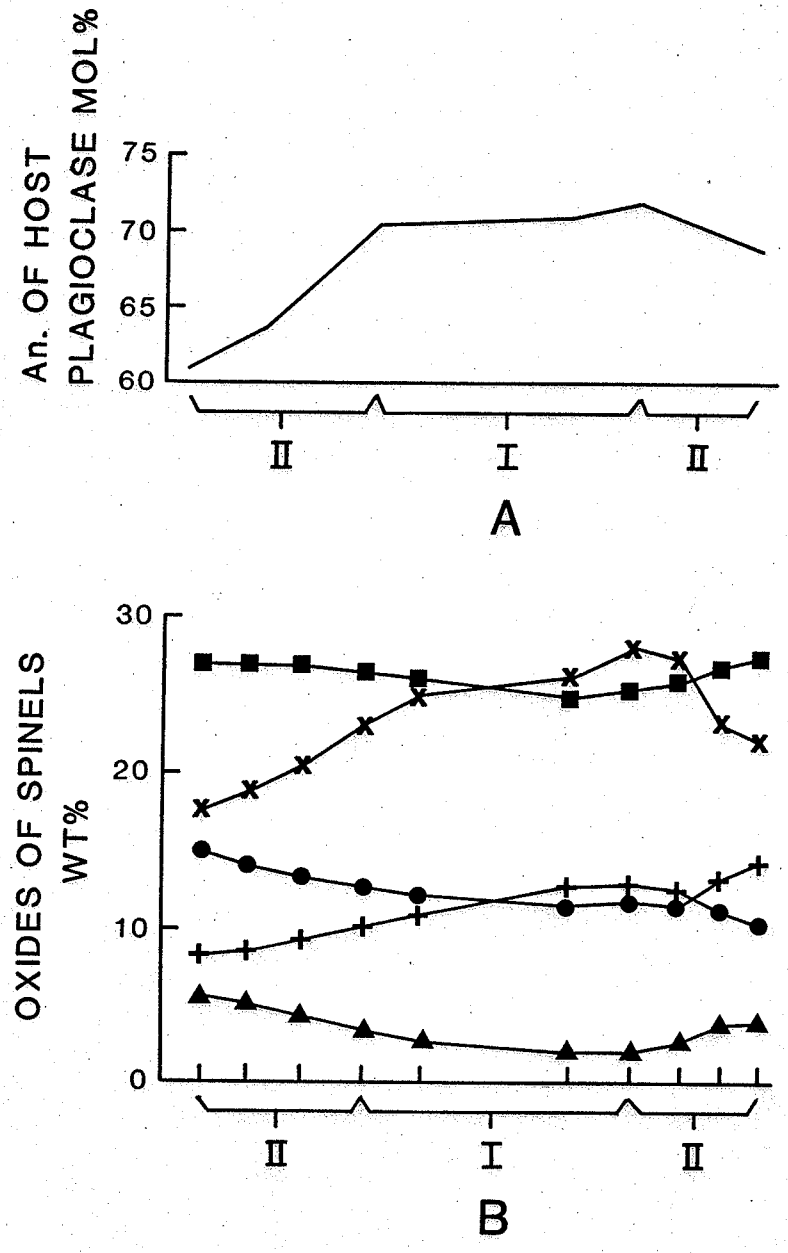
An. OF HOST PLAGIOCLASE MOL%
75
70
65
60
II
I
II
A
OXIDES OF SPINELS WT%
30
20
10
0
Cr_2O_3
Al_2O_3
Fe_2O_3
MgO
TiO_2
II
I
II
B

Fig. 14

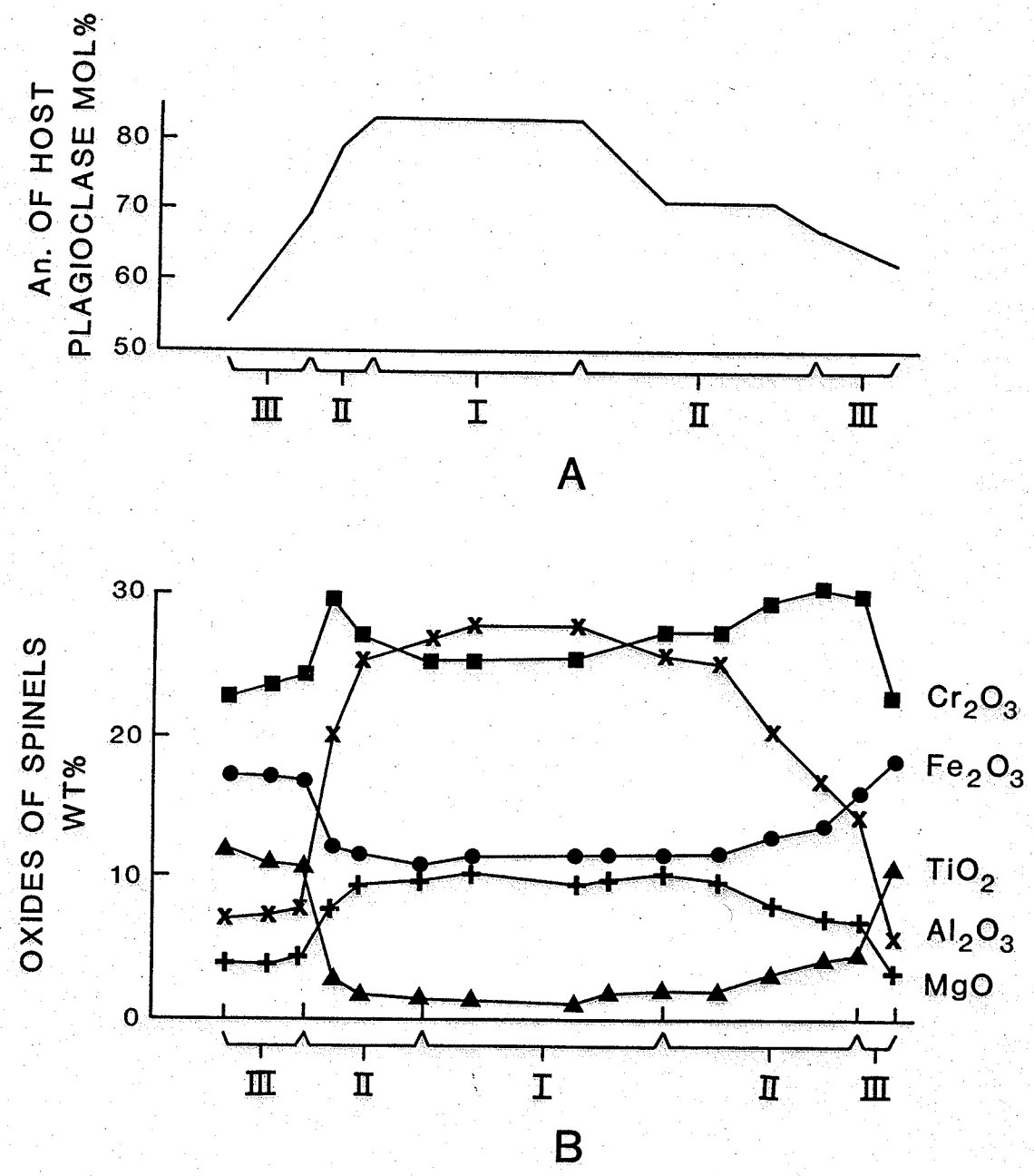
An. OF HOST
PLAGIOCLASE MOL%
80
70
60
50
III
II
I
II
III
A
OXIDES OF SPINELS
WT%
30
20
10
0
Cr_2O_3
Fe_2O_3
TiO_2
Al_2O_3
MgO
III
II
I
II
III
B

Fig. 15

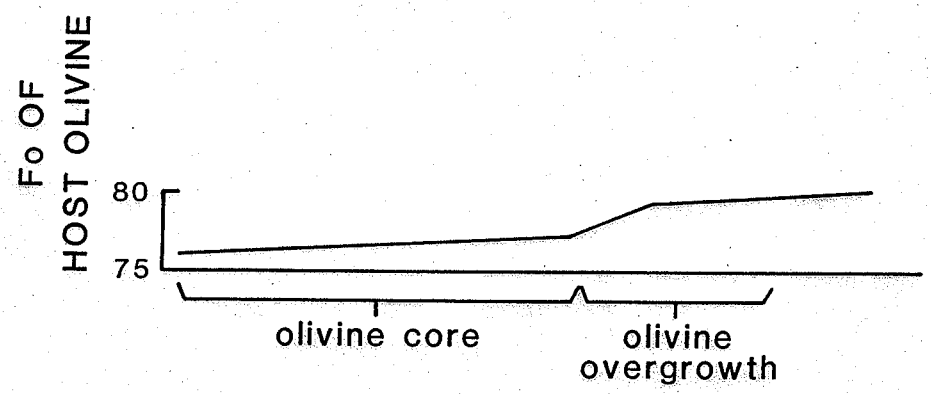
Fo OF
HOST OLIVINE
80
75
olivine core
olivine
overgrowth

A

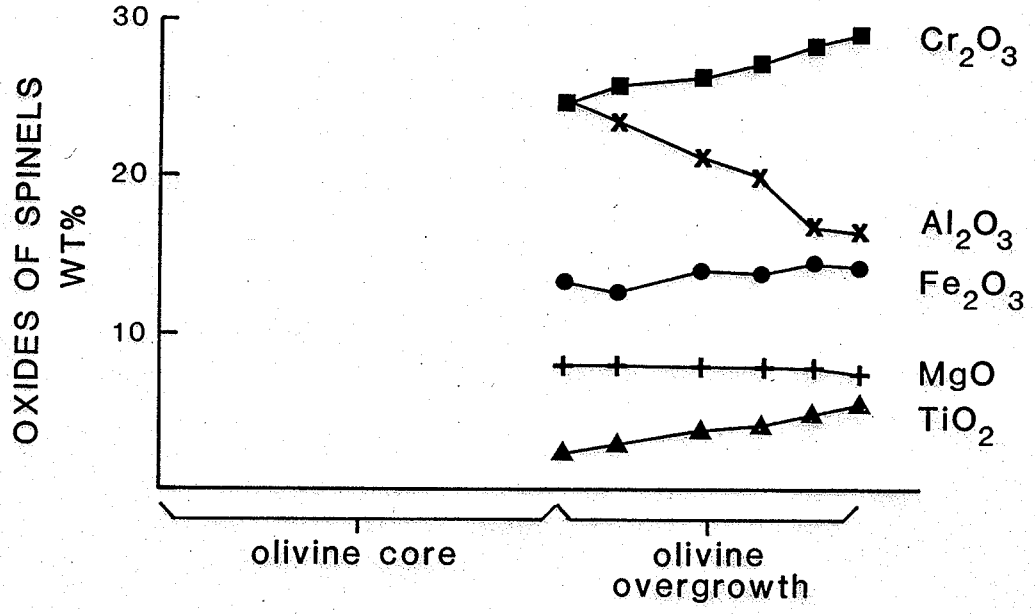
OXIDES OF SPINELS
WT%
30
20
10
Cr_2O_3
Al_2O_3
Fe_2O_3
MgO
TiO_2
olivine core
olivine
overgrowth

B

Fig. 16

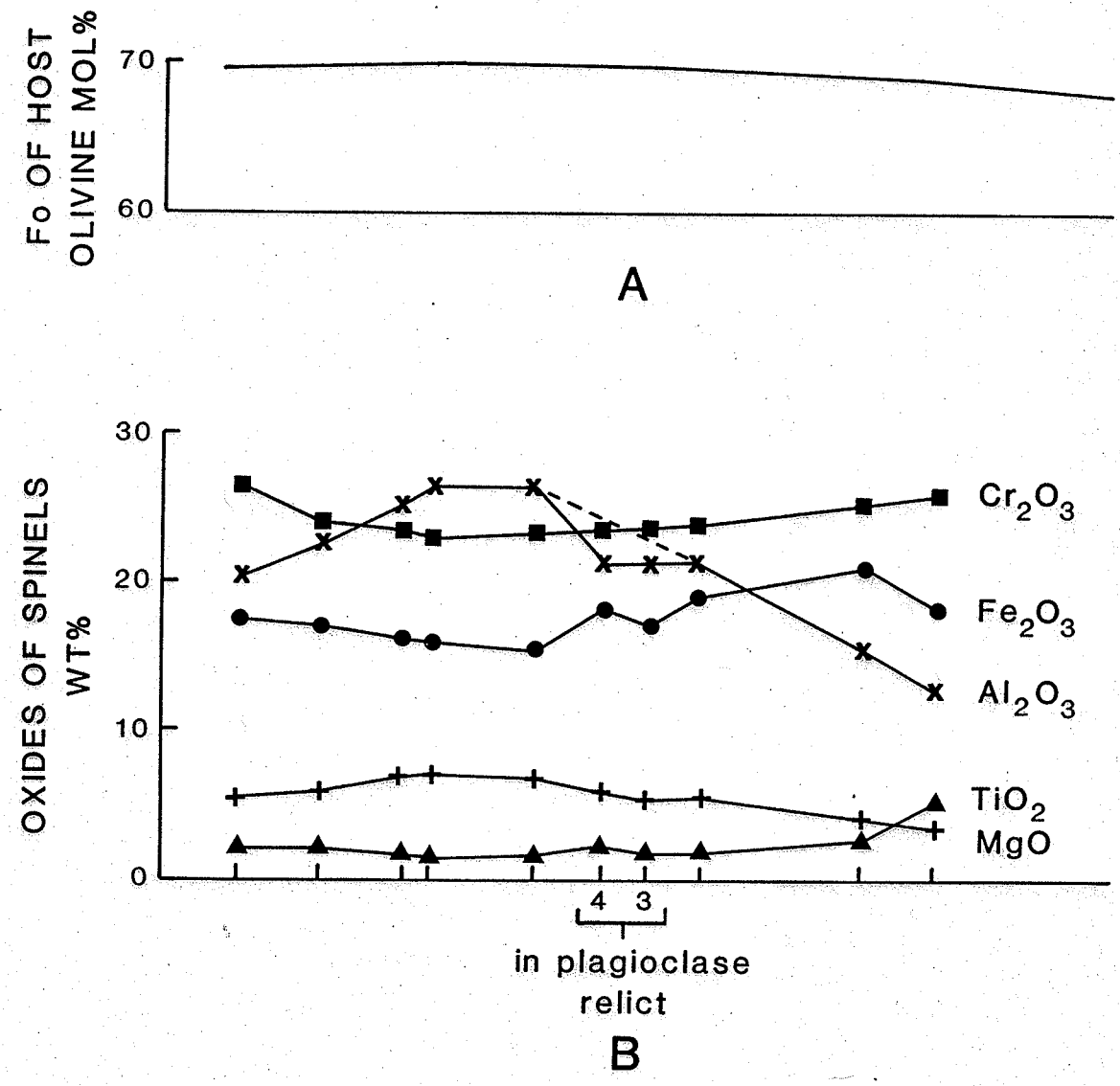
Fo OF HOST
OLIVINE MOL%
70
60
A
OXIDES OF SPINELS
WT%
30
20
10
0
Cr_2O_3
Fe_2O_3
Al_2O_3
TiO_2
MgO
4 3
in plagioclase
relict
B

Fig. 17

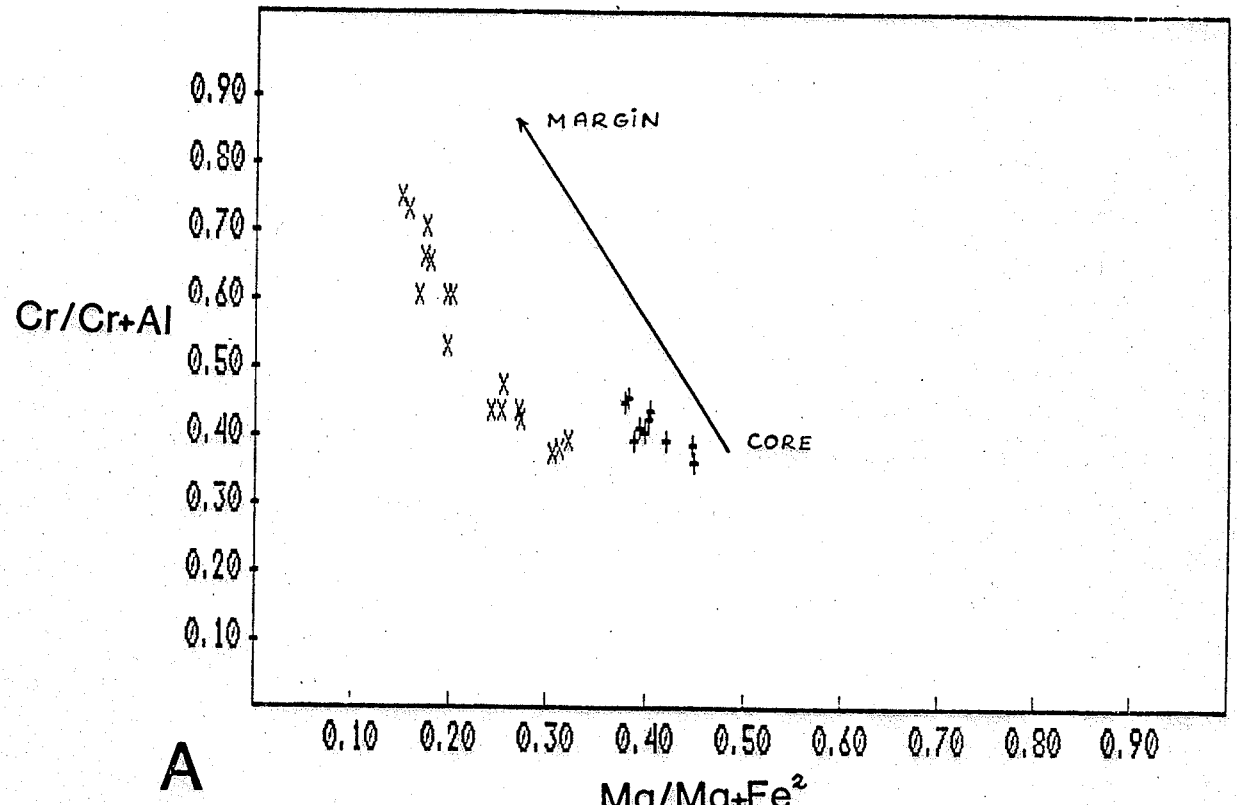

A

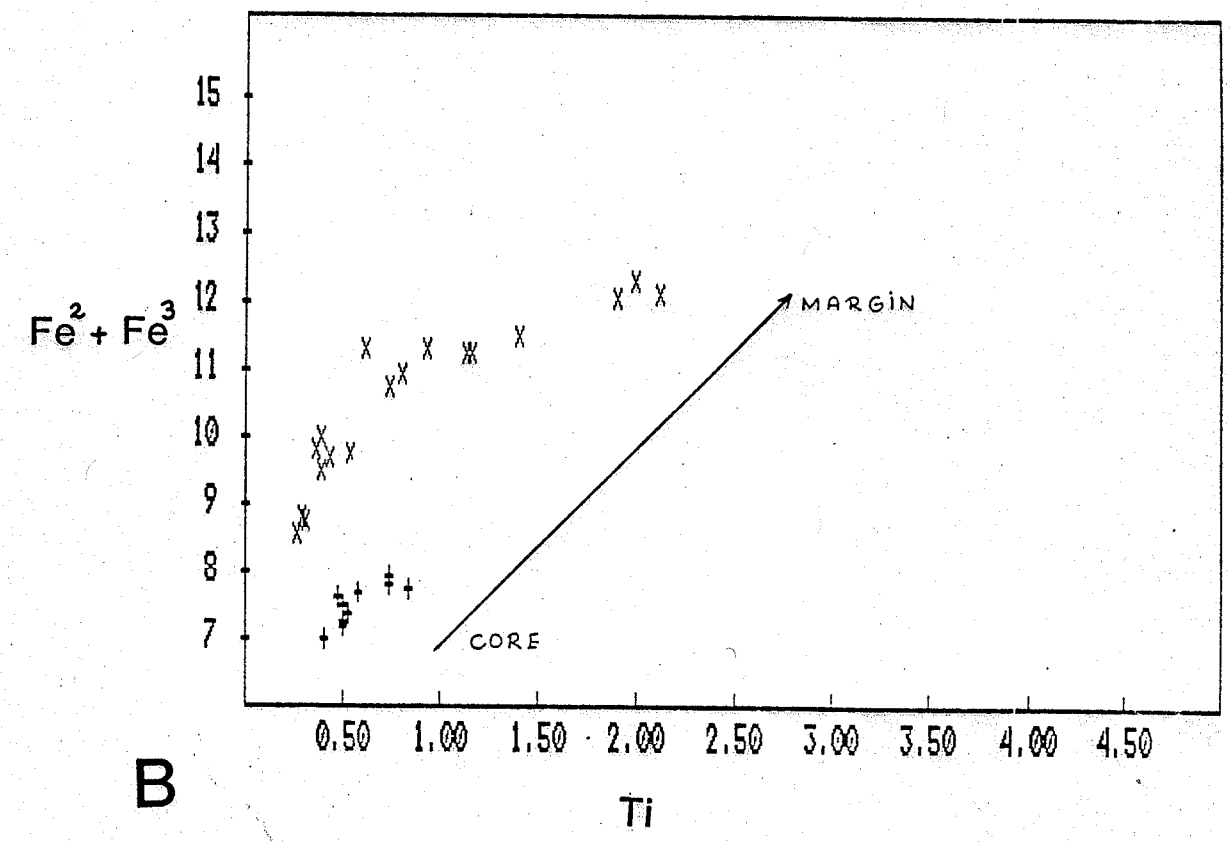

B

Fig.18 A and B

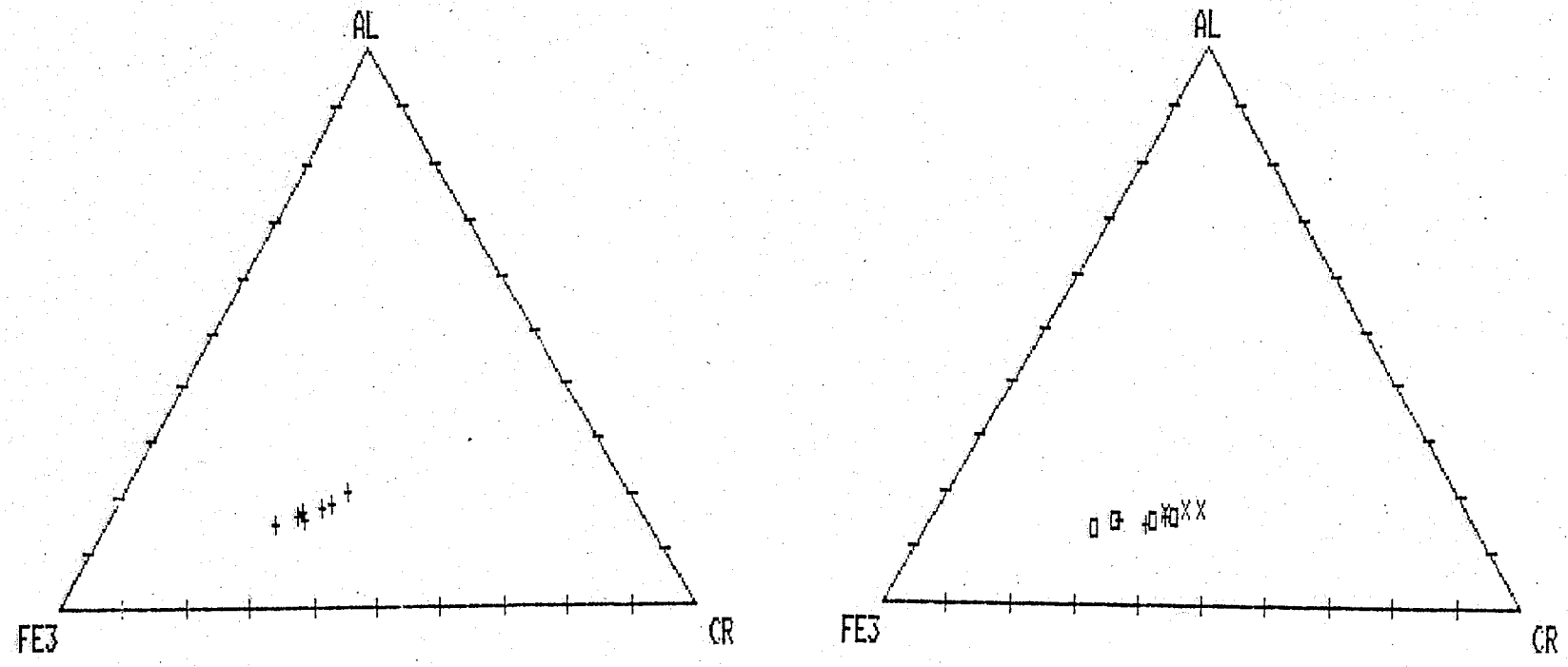

Fig. 19

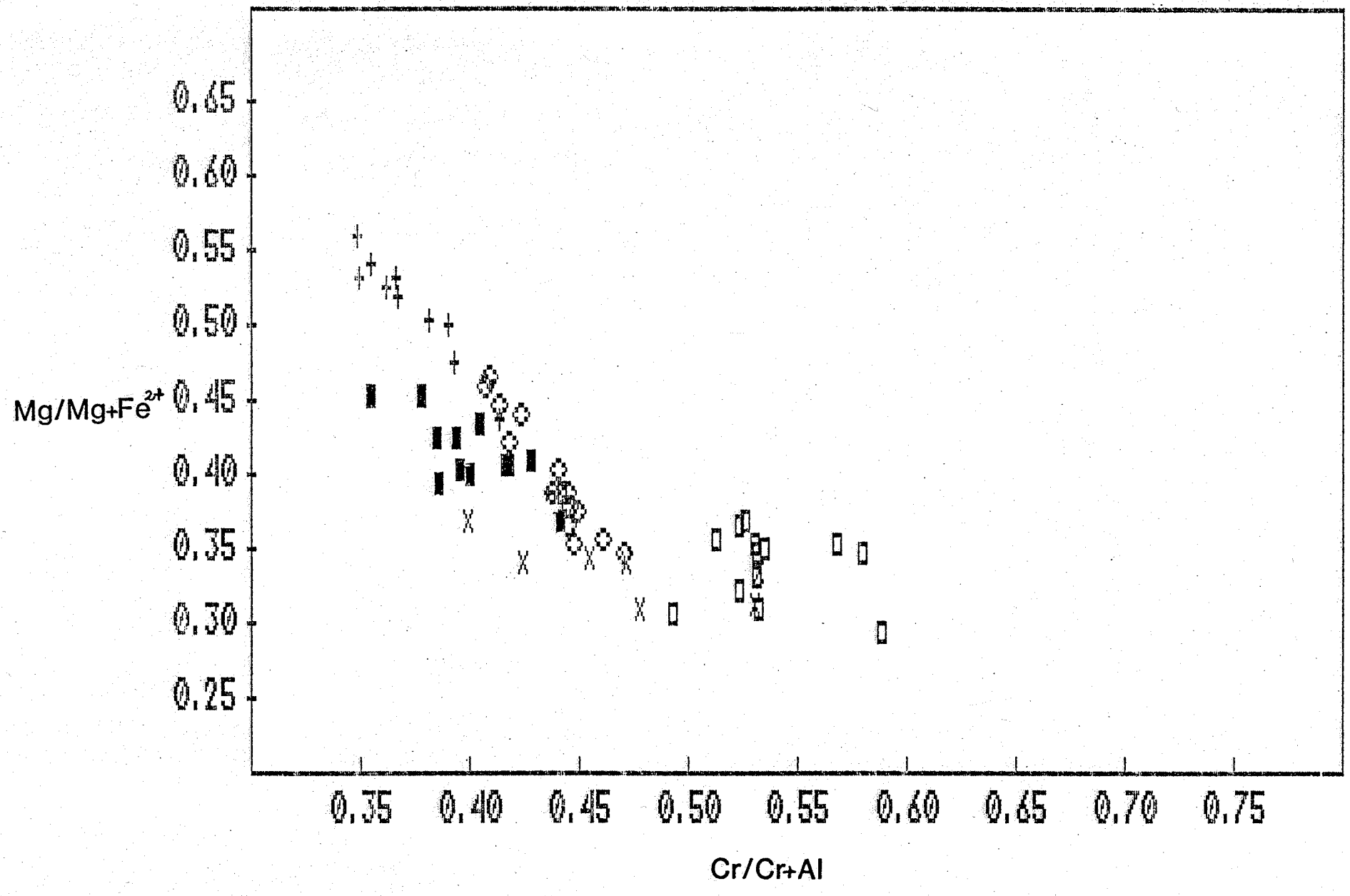
0.65
0.60
0.55
0.50
0.45
0.40
0.35
0.30
0.25
Mg/Mg+Fe2+
0.35
0.40
0.45
0.50
0.55
0.60
0.65
0.70
0.75
Cr/Cr+Al

Fig. 20

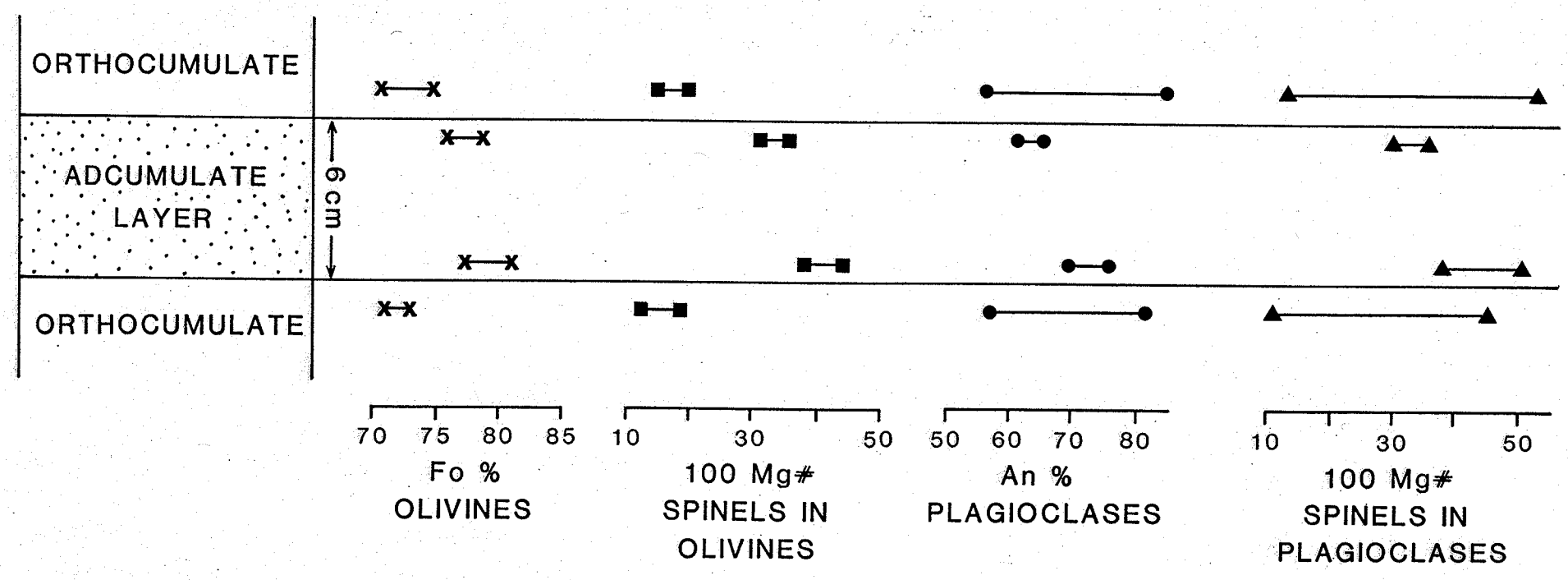
ORTHOCUMULATE
ADCUMULATE LAYER
6 cm
ORTHOCUMULATE
70 75 80 85
Fo %
OLIVINES
10 30 50
100 Mg#
SPINELS IN
OLIVINES
50 60 70 80
An %
PLAGIOCLASES
10 30 50
100 Mg#
SPINELS IN
PLAGIOCLASES

Fig. 21

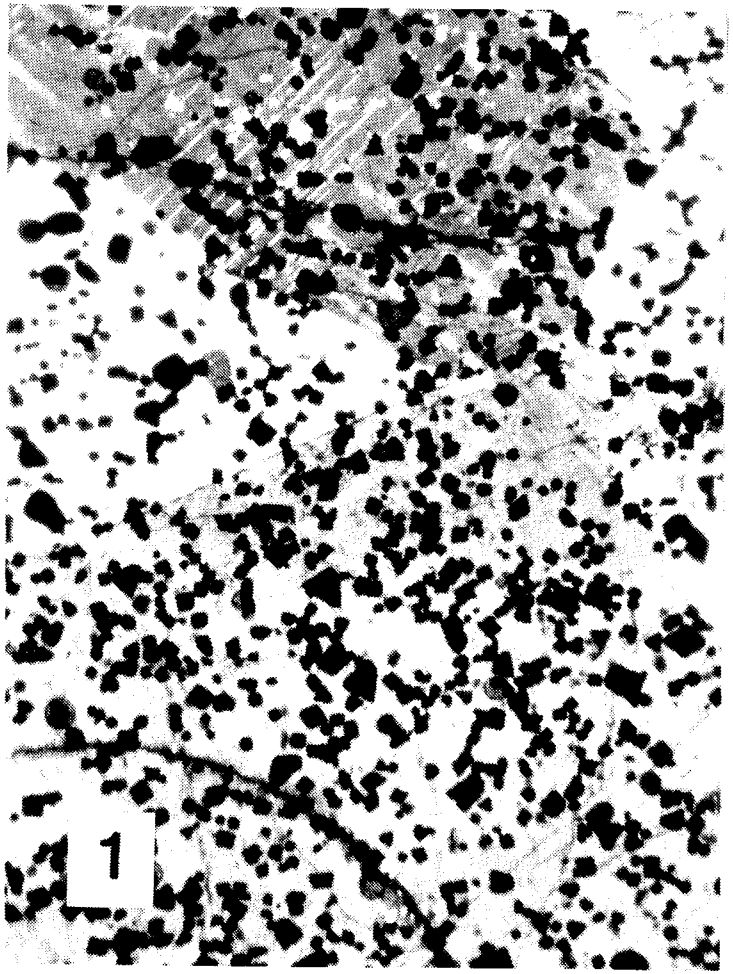
1

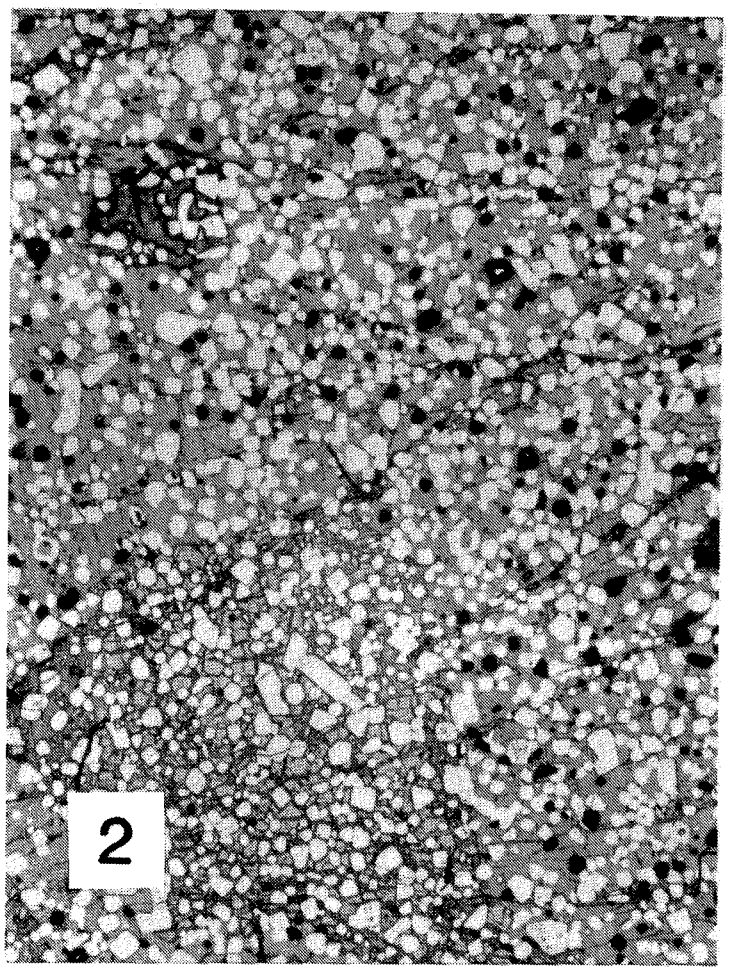
2

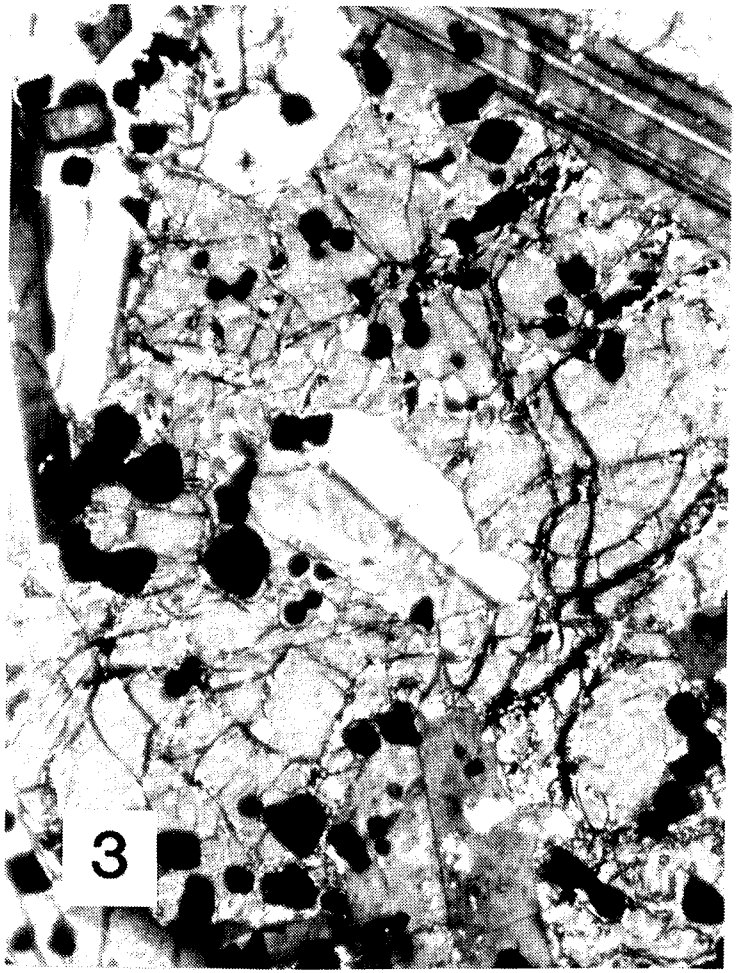
3


4

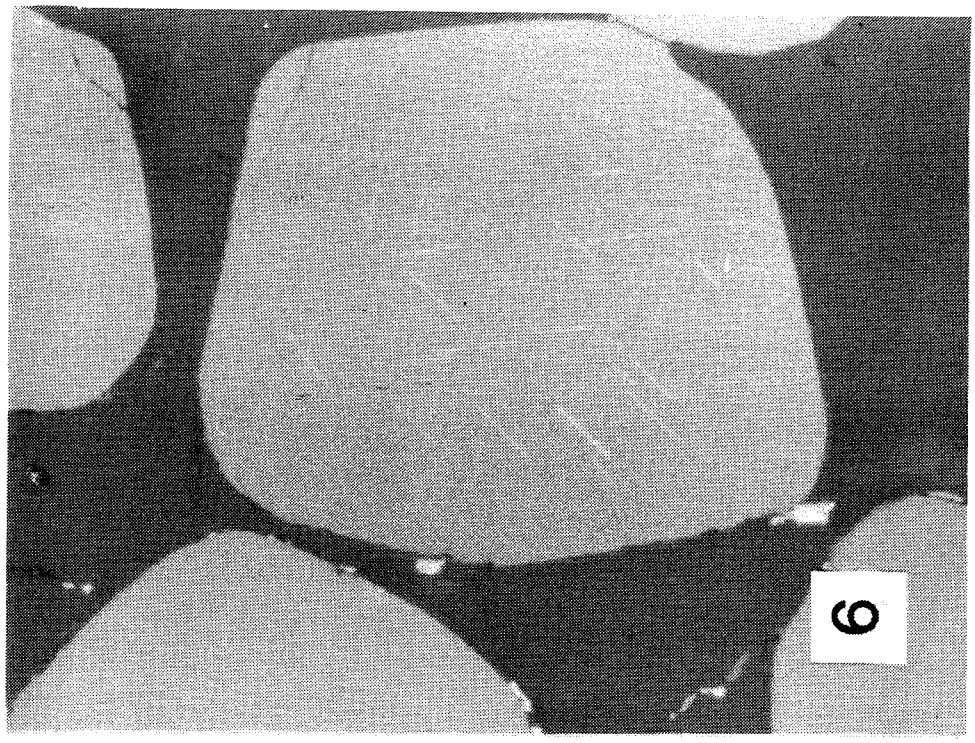
6

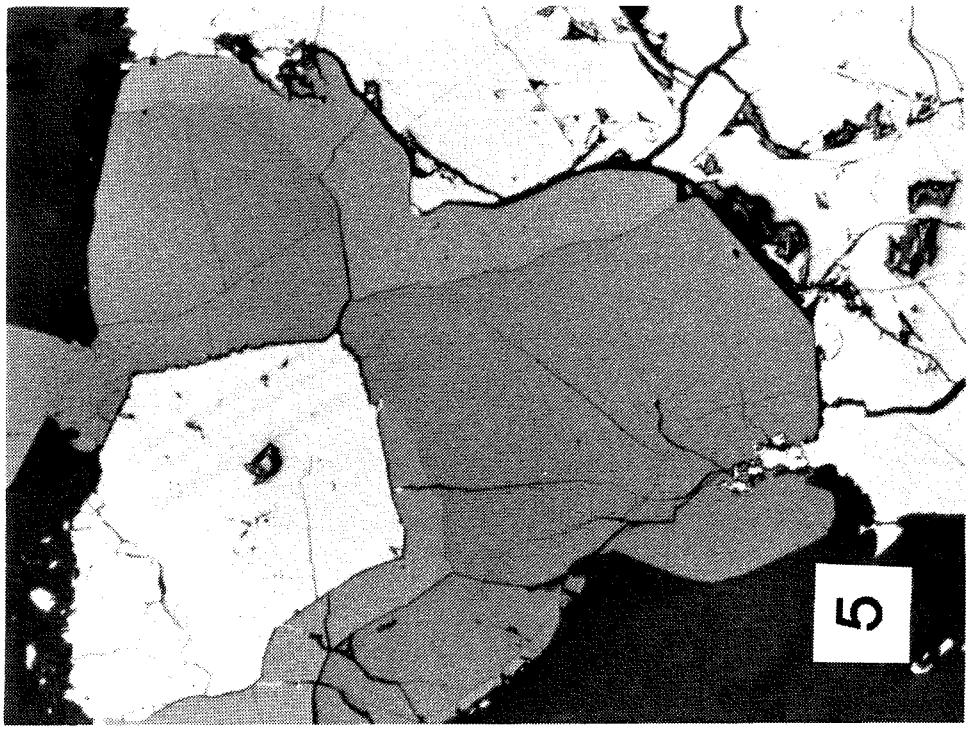
5

TABLE 1. SPINEL GROUPS COMPOSITIONAL RANGES
(ANALYSES ARE GIVEN IN TABLES 3 TO 19)

SPINEL GROUPS	MGO WT %	AL2O3 WT %	CR2O3 WT %	FEO WT %	FE2O3 WT %	TIO2 WT %
GROUP I	12-7	30-17	24-27	21-27	10-13	2-4
GROUP II	7-3	17-8	27-30	27-35	13-18	4-8
GROUP III	7-5	19-18	24-29	27-32	16-18	3-4
GROUP IV	5-3	8-5	27-18	32-37	18-22	8-11
GROUP V	3-2	5-4	18-13	37-41	22-27	11-13
GROUP VI	3-1	4-3	28-21	36-41	17-22	8-11

TABLE 2. CHROME SPINEL BEARING GABBROS IN THE CYCLIC ZONE

CONVENTIONAL NAMES	CUMULATE TYPES
TROCTOLITES	CHROME-SPINEL POIKILITICAL ADCUMULATE OLIVINE-CHROME SPINEL POIKILITICAL ADCUMULATE
OLIVINE GABBROS	PLAGIOCLASE-OLIVINE-CHROME SPINEL POIKILITICAL ORTHOCUMULATE OLIVINE-CHROME SPINEL POIKILITICAL ORTHOCUMULATE

TABLE 3. CHROME-SPINELS IN PLAGIOCLASE AT THE BASE OF AN ADCUMULATE LAYER
CHROME-SPINEL GROUP 1

	1	2	3	4	5	6	7	8	9	MEAN
MGO	8.16	8.56	8.93	9.95	10.71	11.47	10.15	10.40	10.68	9.89
FEO	27.00	26.18	25.32	23.71	22.17	20.39	23.25	21.59	21.76	23.49
MNO	0.30	0.20	0.10	nd	0.10	0.10	nd	0.10	0.46	0.19
CR2O3	26.86	26.86	16.99	26.73	26.20	24.93	27.06	26.51	27.26	25.49
FE2O3	14.64	14.26	13.41	12.19	12.33	11.53	13.22	12.29	13.96	13.09
AL2O3	17.51	18.69	20.21	23.34	25.29	28.52	22.31	25.80	21.63	22.59
TIO2	5.61	5.10	4.52	3.72	3.05	2.08	3.71	3.13	3.70	3.85
V2O3	0.31	0.39	0.31	0.39	0.24	0.32	0.47	0.24	nd	0.33
TOTAL	100.39	100.24	99.79	100.03	100.09	99.34	100.17	101.06	99.75	100.10
				CATIONS PER 32 OXYGENS						
MG	3.16	3.29	3.41	3.72	3.95	4.18	3.80	4.15	4.01	3.74
FE2	5.86	5.65	5.43	4.97	4.59	4.17	4.89	4.40	4.58	4.95
MN	.06000	.04000	.02000	nd	.02000	.02000	nd	.02000	.09000	.03857
CR	5.51	5.48	5.47	5.30	5.13	4.82	5.38	5.11	5.43	5.29
FE3	2.86	2.77	2.59	2.30	2.29	2.12	2.50	2.25	2.64	2.48
AL	5.36	5.68	6.11	6.90	7.38	8.22	6.61	7.42	6.51	6.69
TI	1.09	.99000	.87000	.70000	.56000	.38000	.70000	.57000	.70000	.72889
V	.06000	.08000	.06000	.07000	.04000	.06000	.09000	.04000	nd	.06250
MG/MG+FE	.35033	.36801	.38575	.42808	.46253	.50060	.43728	.48538	.46682	.43164
CR/CR+AL	.50690	.49104	.47237	.43443	.41007	.36963	.44871	.40782	.45477	.44397
CR+AL	10.87	11.16	11.58	12.20	12.51	13.04	11.99	12.53	11.94	11.98
FE/FE+CR	.20830	.19885	.18278	.15862	.15473	.13984	.17253	.15223	.18107	.17211
TI/TI+CR	.09114	.08148	.06988	.05426	.04285	.02832	.05516	.04351	.05538	.05800

1 - TROCTOLITE 14-7-3 CYCLE 4
2 - TROCTOLITE 14-7-4 CYCLE 4
3 - TROCTOLITE 14-7-5 CYCLE 4
4 - TROCTOLITE 14-7-6 CYCLE 4
5 - TROCTOLITE 14-7-7 CYCLE 4
6 - TROCTOLITE 14-7-9 CYCLE 4
7 - TROCTOLITE 14-7-12 CYCLE 4
8 - TROCTOLITE 14-7-13 CYCLE 4
9 - TROCTOLITE 14-7-15 CYCLE 4
MEAN - MEAN OF ALL SPINELS

TABLE 4. CHROME-SPINELS IN PLAGIOCLASE AT THE UPPER ZONE OF AN ADCUMULATE LAYER. CHROME-SPINEL GROUP 1.

	1	2	3	4	5	6	7	8	MEAN
MGO	7.96	8.30	8.31	7.85	8.01	7.86	8.13	7.25	7.96
FEO	25.94	26.01	25.83	26.75	26.49	26.53	27.83	27.66	26.63
MNO	0.20	nd	0.20	0.20	0.10	nd	0.20	0.20	0.18
CR2O3	28.16	28.56	28.72	28.74	28.46	27.65	30.27	28.15	28.59
FE2O3	13.90	14.34	14.65	13.50	14.06	14.44	13.91	14.31	14.14
AL2O3	17.97	17.47	17.40	16.97	16.89	16.12	14.74	17.19	16.84
TIO2	4.42	4.63	4.55	5.08	5.00	5.24	6.29	4.84	5.01
V2O3	0.31	0.39	0.46	0.39	0.39	0.39	0.61	0.46	0.43
TOTAL	98.86	99.70	100.12	99.48	99.40	98.23	101.98	100.06	99.73
			CATIONS PER 32 OXYGENS						
MG	3.12	3.23	3.22	3.07	3.13	3.12	3.14	2.83	3.11
FE2	5.70	5.68	5.62	5.88	5.82	5.92	6.03	6.07	5.84
MN	.04000	nd	.04000	.04000	.02000	nd	.04000	.04000	.03667
CR	5.85	5.89	5.91	5.97	5.91	5.83	6.20	5.84	5.93
FE3	2.75	2.81	2.87	2.67	2.78	2.90	2.71	2.82	2.79
AL	5.57	5.37	5.33	5.26	5.23	5.07	4.50	5.32	5.21
TI	.87000	.91000	.89000	1.00	.99000	1.05	1.22	.95000	.98500
V	.06000	.08000	.09000	.08000	.08000	.08000	.12000	.09000	.08500
MG/MG+FE	.35374	.36251	.36425	.34302	.34972	.34513	.34242	.31798	.34735
CR/CR+AL	.51226	.52309	.52580	.53161	.53052	.53486	.57944	.52330	.53261
CR+AL	11.42	11.26	11.24	11.23	11.14	10.90	10.70	11.16	11.13
FE/FE+CR	.19407	.19972	.20340	.19209	.19971	.21015	.20209	.20172	.20037
TI/TI+CR	.07079	.07477	.07337	.08177	.08162	.08787	.10235	.07845	.08137

1 - TROCTOLITE 141-1-2 CYCLE 4
2 - TROCTOLITE 141-1-3 CYCLE 4
3 - TROCTOLITE 141-1-4 CYCLE 4
4 - TROCTOLITE 141-1-7 CYCLE 4
5 - TROCTOLITE 141-1-8 CYCLE 4
6 - TROCTOLITE 141-1-9 CYCLE 4
7 - TROCTOLITE 141-1-10 CYCLE 4
8 - TROCTOLITE 141-1-13 CYCLE 4
MEAN - MEAN OF ALL SPINELS

TABLE 5. CHROME-SPINELS IN OLIVINE AT THE BASE OF AN ADCUMULATE LAYER
CHROME-SPINEL GROUP 1

	1	2	3	4	5	6	7	MEAN
MGO	9.23	8.88	9.52	8.69	9.22	10.17	10.24	9.42
FEO	24.54	25.54	23.54	24.41	24.34	22.50	22.48	23.91
MNO	0.20	0.10	0.20	0.20	0.20	0.10	nd	0.17
CR2O3	25.85	26.42	24.56	24.21	25.28	23.88	23.22	24.77
FE2O3	13.48	13.41	12.39	12.75	13.29	13.06	12.59	13.00
AL2O3	24.39	22.33	26.37	25.81	22.67	26.43	28.41	25.20
TIO2	3.10	3.92	2.67	2.51	3.86	2.68	2.20	2.99
V2O3	0.31	0.31	0.31	0.39	0.31	0.24	0.24	0.30
TOTAL	101.10	100.91	99.56	98.97	99.17	99.06	99.38	99.74
			CATIONS PER 32 OXYGENS					
MG	3.42	3.33	3.54	3.27	3.50	3.78	3.76	3.51
FE2	5.11	5.38	4.91	5.16	5.19	4.69	4.64	5.01
MN	.04000	.02000	.04000	.04000	.04000	.02000	nd	.03333
CR	5.09	5.26	4.84	4.84	5.09	4.71	4.53	4.91
FE3	2.52	2.54	2.32	2.42	2.55	2.45	2.33	2.45
AL	7.15	6.63	7.75	7.69	6.81	7.77	8.26	7.44
TI	.58000	.74000	.50000	.47000	.74000	.50000	.40000	.56143
V	.06000	.06000	.06000	.07000	.06000	.04000	.04000	.05571
MG/MG+FE	.40094	.38232	.41893	.38790	.40276	.44628	.44762	.41239
CR/CR+AL	.41585	.44239	.38443	.38627	.42773	.37740	.35418	.39832
CR+AL	12.24	11.89	12.59	12.53	11.90	12.48	12.79	12.35
FE/FE+CR	.17073	.17602	.15560	.16187	.17647	.16410	.15410	.16556
TI/TI+CR	.04524	.05859	.03820	.03615	.05854	.03852	.03033	.04365

1 - TROCTOLITE 14-10-1 CYCLE 4
2 - TROCTOLITE 14-10-2 CYCLE 4
3 - TROCTOLITE 14-10-3 CYCLE 4
4 - TROCTOLITE 14-10-6 CYCLE 4
5 - TROCTOLITE 14-10-7 CYCLE 4
6 - TROCTOLITE 14-10-58 CYCLE 4
7 - TROCTOLITE 14-10-59 CYCLE 4
MEAN - MEAN OF ALL SPINELS

TABLE 6. CHROME-SPINELS IN OLIVINE AT THE UPPER ZONE OF AN ADCUMULATE LAYER

CHROME-SPINEL GROUP 1

	1	2	3	4	5	6	MEAN
MGO	7.57	7.13	7.59	7.72	7.63	8.17	7.64
FEO	27.27	28.19	26.59	26.53	26.82	25.47	26.81
MNO	0.20	nd	0.10	0.10	0.10	0.20	0.14
CR2O3	28.63	28.26	27.22	26.31	26.12	24.99	26.92
FE2O3	14.21	14.88	13.70	14.03	12.40	13.26	13.75
AL2O3	16.92	16.76	20.45	21.20	23.75	25.18	20.71
TIO2	4.91	4.91	3.68	3.61	3.17	2.50	3.80
V2O3	0.61	0.38	0.31	0.46	0.31	0.39	0.41
TOTAL	100.32	100.51	99.64	99.96	100.30	100.16	100.15
			CATIONS PER 32 OXYGENS				
MG	2.95	2.78	2.93	2.96	2.88	3.06	2.93
FE2	5.96	6.18	5.76	5.71	5.69	5.36	5.78
MN	.04000	nd	.02000	.02000	.02000	.04000	.02800
CR	5.92	5.86	5.57	5.35	5.24	4.97	5.49
FE3	2.79	2.93	2.67	2.71	2.37	2.51	2.66
AL	5.21	5.18	6.24	6.43	7.11	7.47	6.27
TI	.96000	.96000	.71000	.69000	.60000	.47000	.73167
V	.12000	.08000	.06000	.09000	.06000	.07000	.08000
MG/MG+FE	.33109	.31027	.33717	.34141	.33606	.36342	.33627
CR/CR+AL	.53190	.53080	.47163	.45416	.42429	.39952	.46648
CR+AL	11.13	11.04	11.81	11.78	12.35	12.44	11.76
FE/FE+CR	.20043	.20974	.18439	.18703	.16101	.16789	.18468
TI/TI+CR	.07940	.08000	.05671	.05533	.04633	.03641	.05858

1 - TROCTOLITE 141-1-14 CYCLE 4
2 - TROCTOLITE 141-1-15 CYCLE 4
3 - TROCTOLITE 141-1-16 CYCLE 4
4 - TROCTOLITE 141-1-17 CYCLE 4
5 - TROCTOLITE 141-1-18 CYCLE 4
6 - TROCTOLITE 141-1-19 CYCLE 4
MEAN - MEAN OF ALL SPINELS

TABLE 7. CHROME-SPINELS IN ADCUMULATE BIOTITE
CHROME-SPINEL GROUP 1

	1	2	3	4	5	6	7	8	MEAN
MGO	7.96	8.50	7.99	9.96	9.63	10.58	10.06	10.35	9.38
FEO	26.57	25.24	26.15	23.24	24.18	22.32	22.85	22.27	24.10
MNO	0.10	0.10	0.20	nd	nd	0.10	nd	0.10	0.12
CR2O3	26.82	27.93	26.63	25.70	25.66	25.78	26.94	26.81	26.53
FE2O3	11.76	11.27	12.49	12.10	11.56	12.85	11.50	11.49	11.88
AL2O3	22.20	23.26	20.93	23.45	24.01	25.03	25.60	26.24	23.84
TIO2	3.92	3.17	4.15	3.72	3.87	3.07	2.58	2.43	3.36
V2O3	0.39	0.31	0.39	0.39	0.31	0.31	0.39	0.24	0.34
TOTAL	99.72	99.78	98.93	98.57	99.22	100.04	99.92	99.93	99.51
				CATIONS PER 32 OXYGENS					
MG	3.04	3.21	3.09	3.77	3.62	3.91	3.73	3.81	3.52
FE	5.69	5.36	5.67	4.93	5.10	4.63	4.75	4.61	5.09
MN	.02000	.02000	.04000	nd	nd	.02000	nd	.02000	.02400
CR	5.43	5.60	5.46	5.16	5.12	5.06	5.29	5.25	5.30
FE3	2.26	2.15	2.43	2.31	2.19	2.40	2.15	2.14	2.25
AL	6.70	6.96	6.40	7.02	7.14	7.32	7.50	7.65	7.09
TI	.75000	.60000	.80000	.71000	.73000	.57000	.48000	.45000	.63625
V	.08000	.06000	.08000	.08000	.06000	.06000	.07000	.04000	.06625
MG/MG+FE	.34822	.37456	.35274	.43333	.41514	.45785	.43986	.45249	.40927
CR/CR+AL	.44765	.44586	.46037	.42365	.41762	.40872	.41360	.40698	.42806
CR+AL	12.13	12.56	11.86	12.18	12.26	12.38	12.79	12.90	12.38
FE/FE+CR	.15705	.14616	.17005	.15942	.15156	.16238	.14391	.14229	.15410
TI/TI+CR	.05823	.04559	.06319	.05508	.05620	.04402	.03617	.03371	.04902

1 - TROCTOLITE 14-11-1 CYCLE 4
2 - TROCTOLITE 14-11-2 CYCLE 4
3 - TROCTOLITE 14-11-5 CYCLE 4
4 - TROCTOLITE 14-6-4R CYCLE 4
5 - TROCTOLITE 14-6-5E CYCLE 4
6 - TROCTOLITE 14-6-6E CYCLE 4
7 - TROCTOLITE 14-6-7 CYCLE 4
8 - TROCTOLITE 14-6-8R CYCLE 4
MEAN - MEAN OF ALL SPINELS

TABLE 8. CHROME-SPINELS IN ORTHOCUMULATE PLAGIOCLASE. PAGE 1. CHROME-SPINEL GROUP 1, 2 AND 3.

	1	2	3	4	5	6	7	8	9	10	11	12
MGO	9.70	10.05	10.21	10.51	9.66	8.65	8.16	7.88	7.32	6.19	4.92	4.45
FEO	22.04	21.69	21.93	21.00	22.39	24.81	25.58	26.54	27.11	28.59	33.46	33.85
MN	0.10	nd	nd	0.20	0.20	0.20	0.10	0.20	0.20	0.20	0.29	0.19
CR2O3	25.45	26.35	27.57	25.63	26.88	29.51	29.37	30.20	30.06	29.31	26.38	27.67
FE2O3	11.58	12.10	11.15	11.26	11.43	13.16	11.93	13.96	14.40	14.30	16.04	15.87
AL2O3	27.63	26.30	26.23	28.18	25.49	20.21	20.96	16.93	14.65	16.61	9.42	8.04
TIO2	1.46	1.68	1.91	1.54	2.13	3.37	3.30	4.46	5.04	4.22	8.89	8.78
V2O3	0.24	0.32	0.32	0.32	0.32	0.54	0.54	0.61	0.54	0.46	0.45	0.60
TOTAL	98.20	98.49	99.32	98.64	98.50	100.45	99.94	100.78	99.32	99.88	99.85	99.45
					CATIONS	PER 32	OXYGENS					
MG	3.62	3.76	3.79	3.88	3.63	3.29	3.12	3.05	2.91	2.45	2.03	1.86
FE2	4.62	4.55	4.56	4.35	4.72	5.30	5.49	5.77	6.05	6.35	7.75	7.94
MN	.02000	nd	nd	.04000	.04000	.04000	.02000	.04000	.04000	.04000	.06000	.04000
CR	5.04	5.23	5.42	5.02	5.36	5.96	5.96	6.20	6.34	6.15	5.77	6.14
FE3	2.18	2.28	2.08	2.10	2.17	2.53	2.30	2.73	2.89	2.85	3.34	3.35
AL	8.17	7.78	7.70	8.23	7.58	6.09	6.34	5.19	4.61	5.19	3.07	2.66
TI	.27000	.31000	.35000	.28000	.40000	.64000	.63000	.87000	1.01	.84000	1.85	1.85
V	.04000	.06000	.06000	.06000	.06000	.11000	.11000	.12000	.11000	.09000	.10000	.13000
MG/MG+FE	.43932	.45247	.45389	.47145	.43473	.38300	.36237	.34581	.32478	.27841	.20757	.18980
CR/CR+AL	.38153	.40200	.41311	.37887	.41422	.49461	.48455	.54434	.57900	.54233	.65272	.69773
CR+AL	13.21	13.01	13.12	13.25	12.94	12.05	12.30	11.39	10.95	11.34	8.84	8.80
FE/FE+CR	.14165	.14912	.13684	.13681	.14361	.17353	.15753	.19334	.20881	.20085	.27422	.27572
TI/TI+CR	.02003	.02327	.02598	.02069	.02999	.05043	.04872	.07096	.08445	.06897	.17306	.17371

1 - DIS.OLIVINE GABBRO 2522-8-1 CYCLE 2
2 - DIS.OLIVINE GABBRO 2522-8-2 CYCLE 2
3 - DIS.OLIVINE GABBRO 2522-8-4 CYCLE 2
4 - DIS.OLIVINE GABBRO 2522-8-24 CYCLE 2
5 - DIS.OLIVINE GABBRO 2522-8-25 CYCLE 2
6 - DIS.OLIVINE GABBRO 2522-8-7 CYCLE 2
7 - DIS.OLIV.GABBRO 2522-8-8 CYCLE 2
8 - DIS.OLIV.GABBRO 2522-8-9 CYCLE 2
9 - DIS.OLIV.GABBRO 2522-8-10 CYCLE 2
10 - DIS.OLIV.GABBRO 2522-8-21 CYCLE 2
11 - DIS.OLIV.GABBRO 2522-8-13 CYCLE 2
12 - DIS.OLIV.GABBRO 2522-8-15 CYCLE 2

TABLE 8. CHROME-SPINELS IN ORTHOCUMULATE PLAGIOCLASE. PAGE 2. CHROME-SPINEL GROUP 1, 2 AND 3.

	13	14	15	16	17	18	19	20
MGO	4.81	3.48	3.32	4.17	3.83	10.03	7.64	4.14
FEO	35.57	36.09	37.49	37.19	37.31	21.81	26.53	35.85
MN	0.10	0.39	0.29	0.19	0.29	0.17	0.18	0.25
CR2O3	25.86	26.31	23.42	23.48	23.97	26.38	29.69	25.30
FE2O3	16.20	17.62	18.48	17.78	18.03	11.50	13.55	17.15
AL2O3	7.29	6.59	6.00	6.81	6.51	26.77	17.87	7.24
TIO2	10.75	9.67	11.01	11.46	11.22	1.74	4.08	10.25
V2O3	0.60	0.67	0.59	0.59	0.44	0.30	0.54	0.56
TOTAL	101.18	100.82	100.60	101.67	101.60	98.63	100.07	100.74
			CATIONS PER 32 OXYGENS					
MG	1.98	1.46	1.40	1.72	1.59	3.74	2.96	1.72
FE2	8.22	8.48	8.87	8.62	8.69	4.56	5.79	8.37
MN	.02000	.09000	.07000	.04000	.06000	.03000	.04000	.05000
CR	5.65	5.85	5.24	5.14	5.28	5.21	6.12	5.58
FE3	3.37	3.72	3.93	3.71	3.77	2.16	2.66	3.60
AL	2.37	2.18	2.00	2.22	2.13	7.89	5.48	2.38
TI	2.33	2.04	2.34	2.39	2.35	.32000	.80000	2.16
V	.13000	.15000	.13000	.12000	.09000	.06000	.11000	.12000
MG/MG+FE	.19412	.14688	.13632	.16634	.15467	.45000	.34000	.17000
CR/CR+AL	.70449	.72852	.72376	.69837	.71255	.40000	.53000	.70000
CR+AL	8.02	8.03	7.24	7.36	7.41	13.11	11.61	7.96
FE/FE+CR	.29587	.31660	.35184	.33514	.33721	.14000	.19000	.31000
TI/TI+CR	.22512	.20258	.24426	.24513	.24078	.02000	.06000	.21000

13 - DIS.OLIV.GABBRO 2522-8-22 CYCLE 2
14 - DIS.OLIV.GABBRO 2522-8-11 CYCLE 2
15 - DIS.OLIV.GABBRO 2522-8-12 CYCLE 2
16 - DIS.OLIV.GABBRO 2522-8-23 CYCLE 2
17 - DIS.OLIV.GABBRO 2522-8-34 CYCLE 2
18 - MEAN OF CHR.SPINELS IN PLAGIOCLASE CORE
19 - MEAN OF CHR.SPINELS IN PLAGIOCLASE INNER OVERGROWTH
20 - MEAN OF CHR.SPINELS IN PLAGIOCLASE MARGINAL ZONE

TABLE 9. CHROME-SPINELS IN PLAGIOCLASE OF DISRUPTED ADCUMULATE CHROME-SPINEL GROUP 2

	1	2	3	4	5	6	7	8	9	10	11	12
MGO	7.85	8.54	10.52	10.47	9.14	6.68	6.23	7.52	11.96	12.92	11.41	7.66
FEO	25.92	24.57	21.43	22.12	24.06	29.50	31.39	27.78	19.28	18.51	20.34	27.20
MN	nd	0.20	nd	nd	nd	0.20	0.20	0.10	nd	nd	nd	0.18
CR2O3	29.37	27.58	27.80	27.93	29.22	30.65	28.24	27.87	26.14	25.07	26.73	28.82
FE2O3	13.43	12.03	11.04	12.11	13.65	14.56	14.19	14.13	12.14	11.95	11.81	13.67
AL2O3	15.51	21.52	25.16	24.31	17.89	9.69	9.68	13.35	27.32	29.65	26.61	14.41
TIO2	4.93	3.40	2.29	2.66	4.20	7.50	8.83	6.72	1.87	1.80	2.16	5.93
V2O3	0.39	0.55	0.47	0.47	0.47	0.53	0.53	0.54	0.32	0.40	0.42	0.50
TOTAL	97.40	98.39	98.71	100.07	98.62	99.31	99.29	98.01	99.03	100.30	99.53	98.50
					CATIONS	PER 32	OXYGENS					
MG	3.15	3.29	3.93	3.88	3.56	2.73	2.55	3.04	4.38	4.61	4.20	3.05
FE	5.84	5.32	4.49	4.60	5.26	6.76	7.22	6.30	3.96	3.70	4.19	6.12
MN	nd	.04000	nd	nd	nd	.04000	.04000	.02000	nd	nd	nd	.04000
CR	6.26	5.64	5.51	5.50	6.04	6.64	6.14	5.98	5.08	4.74	5.21	6.12
FE3	2.72	2.34	2.08	2.27	2.68	3.00	2.93	2.88	2.24	2.15	2.19	2.76
AL	4.92	6.57	7.44	7.13	5.51	3.13	3.14	4.27	7.91	8.37	7.71	4.59
TI	1.00	.66000	.43000	.49000	.82000	1.54	1.82	1.37	.34000	.32000	.39000	1.20
V	.08000	.11000	.09000	.09000	.09000	.11000	.11000	.11000	.06000	.07000	.08000	.10000
MG/MG+FE	.35039	.38211	.46675	.45755	.40363	.28767	.26100	.32548	.52518	.55475	.50000	.34000
CR/CR+AL	.55993	.46192	.42548	.43547	.52294	.67963	.66164	.58341	.39107	.36156	.40000	.58000
CR+AL	11.18	12.21	12.95	12.63	11.55	9.77	9.28	10.25	12.99	13.11	12.92	10.71
FE/FE+CR	.19568	.16082	.13839	.15235	.18833	.23493	.23997	.21935	.14708	.14089	.14000	.21000
TI/TI+CR	.08210	.05128	.03214	.03735	.06629	.13616	.16396	.11790	.02551	.02383	.03000	.10000

1 - DISRUPT. TROCTOLITE 244A-6-30 CYCLE 1
2 - DISRUPT. TROCT.244A-6-31 CYCLE 1
3 - DISRUP. TROCT.244A-6-33 CYCLE 1
4 - DISRUP. TROCT.244A-6-34 CYCLE 1
5 - DISRUPT. TROCT 244A-6-36 CYCLE 1
6 - DISRUPT. TROCT 244A-6-37 CYCLE 1
7 - DISRUPT. TROCT.244A-2-27 CYCLE 1
8 - DISRUP. TROCT.244A-2-28R CYCLE 1
9 - DISRUP. TROCT.244A-2-29E CYCLE 1
10 - DISRUPT. TROCT.244A-2-30R CYCLE 1
11 - MEAN OF CHR. SPINELS IN PLAGIOCLASE CORE
12 -MEAN OF CHR.SPINELS IN PLAGIOCLASE OVERGROWTH

TABLE 10. CHROME-SPINELS IN OLIVINE OF DISRUPTED ADCUMULATE

CHROME-SPINEL GROUP 2

	1	2	3	4	5	6	7	8	9	10	MEAN
MGO	4.73	5.24	4.78	5.26	4.93	4.93	4.29	3.97	4.13	3.95	4.62
FEO	32.38	31.82	33.37	32.16	33.17	32.88	33.48	34.61	33.48	33.49	33.08
MNO	nd	nd	nd	nd	nd	0.29	0.29	0.10	0.19	0.39	0.25
CR2O3	30.27	29.63	29.78	30.69	29.04	27.94	27.72	28.70	27.95	27.67	28.94
FE2O3	14.94	16.08	15.73	15.55	15.46	15.54	16.44	16.49	16.81	17.16	16.02
AL2O3	10.86	10.70	9.15	9.43	9.62	8.42	9.01	8.84	8.61	8.51	9.32
TIO2	6.58	6.73	7.80	7.30	7.90	8.65	7.94	7.90	7.71	7.70	7.62
V2O3	0.60	0.53	0.52	0.60	0.60	0.53	0.60	0.75	0.67	0.60	0.60
TOTAL	100.36	100.73	101.13	100.98	100.72	99.18	99.77	101.36	99.55	99.47	100.33
				CATIONS PER 32 OXYGENS							
MG	1.93	2.12	1.95	2.14	2.01	2.05	1.78	1.63	1.72	1.65	1.90
FE2	7.42	7.25	7.65	7.35	7.61	7.69	7.81	7.98	7.85	7.87	7.65
MN	nd	nd	nd	nd	nd	.06000	.06000	.02000	.04000	.09000	.05400
CR	6.56	6.38	6.46	6.63	6.30	6.18	6.11	6.26	6.20	6.15	6.32
FE3	3.08	3.29	3.24	3.20	3.19	3.27	3.45	3.42	3.54	3.63	3.33
AL	3.50	3.43	2.95	3.04	3.11	2.77	2.96	2.87	2.84	2.82	3.03
TI	1.35	1.38	1.60	1.50	1.63	1.82	1.66	1.63	1.62	1.63	1.58
V	.13000	.11000	.11000	.13000	.13000	.11000	.13000	.16000	.15000	.13000	.12900
MG/MG+FE	.20642	.22625	.20313	.22550	.20894	.21047	.18561	.16962	.17973	.17332	.19890
CR/CR+AL	.65209	.65036	.68650	.68563	.66950	.69050	.67365	.68565	.68584	.68562	.67653
CR+AL	10.06	9.81	9.41	9.67	9.41	8.95	9.07	9.13	9.04	8.97	9.35
FE/FE+CR	.23440	.25115	.25613	.24864	.25317	.26759	.27556	.27251	.28140	.28810	.26286
TI/TI+CR	.11832	.12332	.14532	.13429	.14764	.16899	.15471	.15149	.15197	.15377	.14498

1 - DISRUPTED TROCTOLITE 244A-6-22
2 - DISRUP.TROCT.244A-6-24 CYCLE 1
3 - DISRUP.TROCT.244A-6-26 CYCLE 1
4 - DISRUP.TROCT.244A-6-27 CYCLE 1
5 - DISRUP.TROCT.244A-6-28 CYCLE 1
6 - DISRUP.TROCT.244A-6-29 CYCLE 1
7 - DISRUP.TROCT.243-1-6 CYCLE 1
8 - DISRUP.TROCT.243-1-7 CYCLE 1
9 - DISRUP.TROCT.243-1-8 CYCLE 1
10 - DISRUP.TROCT.243-1-9 CYCLE 1
MEAN - MEAN OF ALL SAMPLES

TABLE 11. CHROME-SPINELS IN SUBHEDRAL OLIVINE OF ORTHOCUMULATE
CHROME-SPINEL GROUP 2

	1	2	3	4	MEAN
MGO	3.79	3.63	3.64	3.28	3.59
FEO	33.49	34.26	35.38	32.88	34.00
MNO	0.10	nd	0.10	nd	0.10
CR2O3	28.60	29.05	27.45	31.38	29.12
FE2O3	17.67	17.55	17.06	17.84	17.53
AL2O3	8.15	8.36	7.27	8.74	8.13
TIO2	7.14	7.19	8.80	5.21	7.09
V2O3	0.67	0.60	0.74	0.67	0.67
TOTAL	99.61	100.64	100.44	100.00	100.17
	CATIONS PER 32 OXYGENS				
MG	1.59	1.50	1.52	1.37	1.50
FE2	7.89	7.99	8.31	7.72	7.98
MN	.02000	nd	.02000	nd	.02000
CR	6.37	6.41	6.09	6.97	6.46
FE3	3.74	3.68	3.60	3.77	3.70
AL	2.70	2.75	2.40	2.89	2.69
TI	1.51	1.50	1.86	1.10	1.49
V	.15000	.13000	.16000	.15000	.14750
MG/MG+FE	.16772	.15806	.15463	.15072	.15778
CR/CR+AL	.70232	.69978	.71731	.70690	.70658
CR+AL	9.07	9.16	8.49	9.86	9.14
FE/FE+CR	.29196	.28660	.29777	.27660	.28823
TI/TI+CR	.14272	.14071	.17971	.10037	.14088

1 - DISRUPTED OLIVINE GABBRO 2521-1-7 CYCLE 2
2 - DISRUPTED OLIVINE GABBRO 2521-1-8 CYCLE 2
3 - DISRUPTED OLIVINE GABBRO 2521-1-9 CYCLE 2
4 - DISRUPTED OLIVINE GABBRO 2521-1-10 CYCLE 2
MEAN - MEAN OF ALL SPINELS

TABLE 12. CHROME-SPINELS IN POIKILITICAL OLIVINE OF ORTHOCUMULATE. PAGE 1.
CHROME-SPINEL GROUP 3

	1	2	3	4	5	6	7	8	9	10	11	12
MGO	4.19	5.50	5.14	5.93	6.80	6.78	7.07	5.87	3.87	3.74	3.15	3.31
FEO	30.68	28.87	28.53	28.48	26.72	27.34	26.45	27.87	31.57	32.80	36.36	36.15
MNO	0.19	0.29	0.20	0.33	0.25	0.26	0.18	0.16	nd	0.10	0.39	nd
CR2O3	25.23	24.10	24.00	23.92	23.52	23.14	23.75	24.07	27.80	28.47	24.32	24.12
FE2O3	21.35	19.15	17.42	17.78	15.24	16.06	16.17	17.09	19.57	18.55	20.11	19.77
AL2O3	15.64	21.66	21.65	21.40	26.47	26.57	25.30	22.53	15.54	13.15	6.91	6.70
TIO2	3.07	1.97	1.83	2.78	1.38	1.54	1.62	1.98	2.98	4.61	9.26	9.29
V2O3	0.53	0.38	0.31	nd	nd	nd	nd	nd	0.45	0.45	0.59	0.67
TOTAL	100.88	101.92	99.08	100.62	100.38	101.69	100.54	99.57	101.78	101.87	101.09	100.01
					CATIONS	PER 32	OXYGENS					
MG	1.68	2.10	2.02	2.29	2.56	2.52	2.66	2.28	1.54	1.50	1.31	1.40
FE2	6.90	6.20	6.29	6.17	5.64	5.71	5.60	6.07	7.05	7.40	8.54	8.58
MN	.04000	.06000	.04000	.07000	.05000	.05000	.03000	.03000	nd	.02000	.09000	nd
CR	5.36	4.89	5.00	4.90	4.69	4.57	4.75	4.95	5.87	6.07	5.40	5.41
FE3	4.31	3.70	3.46	3.47	2.89	3.02	3.08	3.35	3.93	3.76	4.25	4.22
AL	4.95	6.56	6.73	6.54	7.88	7.82	7.55	6.91	4.89	4.18	2.29	2.24
TI	.62000	.38000	.36000	.54000	.26000	.29000	.30000	.38000	.60000	.93000	1.95	1.98
V	.11000	.07000	.06000	nd	nd	nd	nd	nd	.09000	.09000	.13000	.15000
MG/MG+FE	.19580	.25301	.24308	.27069	.31220	.30620	.32203	.27305	.17928	.16854	.13299	.14028
CR/CR+AL	.51988	.42707	.42626	.42832	.37311	.36885	.38618	.41737	.54554	.59220	.70221	.70719
CR+AL	10.31	11.45	11.73	11.44	12.57	12.39	12.30	11.86	10.76	10.25	7.69	7.65
FE/FE+CR	.29480	.24422	.22778	.23273	.18693	.19598	.20026	.22025	.26753	.26838	.35595	.35552
TI/TI+CR	.05672	.03212	.02978	.04508	.02027	.02287	.02381	.03105	.05282	.08318	.20228	.20561

1 - DISRUPTED OLIVINE GABBRO 2712-6-3R CYCLE 3
2 - DISRUP.OLIV.GABBRO 2712-6-4E CYCLE 3
3 - DISRUP.OLIV GABBRO 2712-6-5S CYCLE 3
4 - DISRUP.OLIV GABBRO 2712-6-6 CYCLE 3
5 - DISRUP.OLIV.GABBRO 2712-6-7 CYCLE 3
6 - DISRUP.OLIV GABBRO 2712-6-8 CYCLE 3
7 - DISRUP.OLIV.GABBRO 2712-6-9 CYCLE 3
8 - DISRUP.OLIV GABBRO 2712-6-10 CYCLE 3
9 - DISRUP.OLIV.GABBRO 2712-6-1 CYCLE 3
10 - DISRUP.OLIV.GABBRO 2712-6-2 CYCLE 3
11 - DISRUPTED OLIVINE GABBRO 2712-7-6E CYCLE 3
12 - DISRUPTED OLIVINE GABBRO 2712-7-7 CYCLE 3

TABLE 12. PAGE 2.

	13	MEAN
MGO	3.28	4.97
FEO	33.53	30.41
MNO	0.29	0.24
CR2O3	29.16	25.05
FE2O3	18.86	18.24
AL2O3	9.45	17.92
TIO2	5.84	3.70
V2O3	0.52	0.49
TOTAL	100.93	100.80
CATIONS PER 32 OXYGENS		
MG	1.36	1.94
FE2	7.79	6.76
MN	.06000	.04909
CR	6.40	5.25
FE3	3.94	3.64
AL	3.09	5.51
TI	1.22	.75462
V	.11000	.10125
MG/MG+FE	.14863	.22660
CR/CR+AL	.67439	.50527
CR+AL	9.49	10.76
FE/FE+CR	.29337	.25721
TI/TI+CR	.11391	.07073

13 - DISRUPTED OLIVINE GABBRO 272-7-8 CYCLE 3
MEAN - MEAN OF ALL SPINELS

TABLE 13. CHROME-SPINELS IN POIKILITICAL OLIVINE OF ORTHOCUMULATE. CHROME-SPINEL GROUP 3

	1	2	3	4	5	6	7	8	9	MEAN
MGO	6.03	6.41	6.50	6.80	5.82	5.00	6.26	6.31	5.69	6.09
FEO	28.28	27.78	27.62	26.92	28.31	30.87	28.05	27.95	28.68	28.27
MNO	nd	nd	nd	0.20	nd	nd	nd	0.20	nd	0.20
CR2O3	29.10	26.52	25.53	25.64	27.03	29.10	26.68	26.97	27.51	27.12
FE2O3	16.20	15.88	15.18	15.42	15.96	16.01	15.97	16.70	16.05	15.93
AL2O3	17.88	20.70	22.47	22.57	18.73	13.64	20.43	19.19	18.29	19.32
TIO2	2.89	2.61	2.40	2.25	2.98	5.00	2.68	2.97	3.05	2.98
V2O3	0.38	0.54	0.31	0.46	0.38	0.45	0.38	0.54	0.46	0.43
TOTAL	100.76	100.44	100.01	100.26	99.21	100.07	100.45	100.83	99.73	100.20
				CATIONS	PER 32	OXYGENS				
MG	2.36	2.47	2.50	2.60	2.30	2.02	2.42	2.44	2.24	2.37
FE2	6.21	6.02	5.96	5.78	6.28	6.99	6.09	6.09	6.36	6.20
MN	nd	nd	nd	.04000	nd	nd	nd	.04000	nd	.04000
CR	6.04	5.44	5.21	5.21	5.67	6.23	5.48	5.55	5.76	5.62
FE3	3.20	3.10	2.95	2.98	3.19	3.26	3.12	3.27	3.20	3.14
AL	5.53	6.33	6.83	6.84	5.86	4.35	6.26	5.89	5.71	5.96
TI	.57000	.51000	.46000	.43000	.59000	1.01	.52000	.58000	.60000	.58556
V	.08000	.11000	.06000	.09000	.08000	.09000	.08000	.11000	.09000	.08778
MG/MG+FE	.27538	.29093	.29551	.31026	.26807	.22420	.28437	.28605	.26047	.27725
CR/CR+AL	.52204	.46219	.43272	.43237	.49176	.58885	.46678	.48514	.50218	.48711
CR+AL	11.57	11.77	12.04	12.05	11.53	10.58	11.74	11.44	11.47	11.58
FE/FE+CR	.21666	.20847	.19680	.19827	.21671	.23555	.20996	.22230	.21813	.21365
TI/TI+CR	.04695	.04153	.03680	.03446	.04868	.08714	.04241	.04825	.04971	.04844

1 - DISRUPTED OLIVINE GABBRO 2671-3-1 CYCLE 3
2 - DISRUPTED OLIVINE GABBRO 2671-3-2 CYCLE 3
3 - DISRUPTED OLIVINE GABBRO 2671-3-4 CYCLE 3
4 - DISRUPTED OLIVINE GABBRO 2671-3-5 CYCLE 3
5 - DISRUPTED OLIVINE GABBRO 2671-3-6 CYCLE 3
6 - DISRUPTED OLIVINE GABBRO 2671-3-7 CYCLE 3
7 - DISRUPTED OLIVINE GABBRO 2671-3-9 CYCLE 3
8 - DISRUPTED OLIVINE GABBRO 2671-3-8 CYCLE 3
9 - DISRUPTED OLIVINE GABBRO 2671-3-10 CYCLE 3
MEAN - MEAN OF ALL SPINELS

TABLE 14. CHROME-SPINELS IN POIKILITICAL TO INTERSTITIAL OLIVINE OF ORTHOCUMULATE. CHROME-SPINEL GROUP 4

	1	2	3	4	5	6	7	8	9	10	MEAN
MGO	2.99	3.34	3.31	2.80	3.31	2.82	2.49	2.49	2.82	2.66	2.90
FEO	37.57	37.48	36.88	37.13	35.88	37.20	37.76	37.70	36.49	37.83	37.19
MNO	nd	0.10	0.10	0.19	0.10	0.10	0.29	0.19	0.19	0.19	0.16
CR2O3	23.38	22.59	23.36	24.18	24.10	21.10	17.77	19.20	23.41	19.72	21.88
FE2O3	20.42	20.75	18.84	19.04	19.21	23.10	25.97	24.80	22.37	24.37	21.89
AL2O3	5.92	5.63	5.99	5.89	6.48	5.94	4.94	4.83	5.63	4.94	5.62
TIO2	10.10	10.69	10.44	9.90	9.42	9.68	10.35	10.19	9.07	10.40	10.02
V2O3	0.66	0.66	0.74	0.74	0.67	0.73	0.66	0.73	0.66	0.66	0.69
TOTAL	101.04	101.24	99.66	99.87	99.17	100.67	100.23	100.13	100.64	100.77	100.34
				CATIONS PER 32 OXYGENS							
MG	1.26	1.40	1.41	1.19	1.41	1.19	1.06	1.06	1.19	1.13	1.23
FE2	8.88	8.84	8.81	8.89	8.59	8.85	9.10	9.09	8.69	9.05	8.88
MN	nd	.02000	.02000	.04000	.02000	.02000	.07000	.04000	.04000	.04000	.03444
CR	5.22	5.03	5.27	5.47	5.45	4.74	4.05	4.37	5.27	4.46	4.93
FE3	4.34	4.40	4.04	4.10	4.14	4.94	5.63	5.38	4.79	5.24	4.70
AL	1.97	1.87	2.01	1.98	2.18	1.99	1.67	1.64	1.89	1.66	1.89
TI	2.14	2.26	2.24	2.13	2.02	2.07	2.24	2.21	1.94	2.23	2.15
V	.15000	.15000	.17000	.17000	.15000	.16000	.15000	.16000	.15000	.15000	.15600
MG/MG+FE	.12426	.13672	.13796	.11806	.14100	.11853	.10433	.10443	.12045	.11100	.12167
CR/CR+AL	.72601	.72899	.72390	.73423	.71429	.70431	.70804	.72712	.73603	.72876	.72317
CR+AL	7.19	6.90	7.28	7.45	7.63	6.73	5.72	6.01	7.16	6.12	6.82
FE/FE+CR	.37641	.38938	.35689	.35498	.35174	.42331	.49604	.47234	.40084	.46127	.40832
TI/TI+CR	.22937	.24672	.23529	.22234	.20933	.23523	.28141	.26886	.21319	.26707	.24088

1 - DISRUPTED OLIVINE GABBRO 2521-2-4 CYCLE 2
2 - DISRUPTED OLIVINE GABBRO 2521-2-4A CYCLE 2
3 - DISRUPTED OLIVINE GABBRO 2521-2-5A CYCLE 2
4 - DISRUPTED OLIVINE GABBRO 2521-2-6 CYCLE 2
5 - DISRUPTED OLIVINE GABBRO 2521-2-7 CYCLE 2
6 - DISRUPTED OLIVINE GABBRO 2521-3-1A CYCLE 2
7 - DISRUPTED OLIVINE GABBRO 2521-3-3 CYCLE 3
8 - DISRUPTED OLIVINE GABBRO 2521-3-6 CYCLE 2
9 - DISRUPTED OLIVINE GABBRO 2521-3-7 CYCLE 2
10 - DISRUPTED OLIVINE GABBRO 2521-3-7A CYCLE 2
MEAN - MEAN OF ALL SPINELS

TABLE 15. CHROME-SPINELS IN INTERSTITIAL AUGITE OF ORTHOCUMULATE. CHROME-SPINEL GROUP 4

	1	2	3	4	5	6	7	8	9	10	11	12
MGO	3.83	3.32	3.67	3.83	4.01	3.49	6.43	6.10	6.25	6.06	3.69	6.21
FEO	37.54	37.76	37.71	37.47	36.99	37.61	31.71	32.51	31.61	32.38	37.51	32.05
MNO	0.19	0.19	0.29	0.39	0.10	0.29	0.20	0.39	nd	nd	0.24	0.29
CR2O3	21.42	20.70	21.52	21.25	21.92	21.87	26.31	26.46	25.87	26.06	21.45	26.18
FE2O3	18.83	19.37	19.74	18.88	19.81	18.49	15.73	16.01	16.37	15.38	19.19	15.87
AL2O3	5.70	5.59	5.72	5.81	6.22	5.80	9.66	8.95	9.34	9.22	5.81	9.29
TIO2	12.00	11.72	11.75	12.08	11.26	11.70	9.22	9.66	9.03	9.55	11.75	9.37
V2O3	0.74	0.67	0.66	0.74	0.67	0.74	0.68	0.83	0.68	0.53	0.70	0.68
TOTAL	100.25	99.32	101.06	100.45	100.98	99.99	100.04	100.91	99.15	99.18	100.34	99.82
					CATIONS PER 32 OXYGENS							
MG	1.61	1.42	1.54	1.61	1.67	1.47	2.61	2.48	2.57	2.50	1.55	2.54
FE2	8.89	9.06	8.87	8.85	8.67	8.95	7.24	7.41	7.30	7.49	8.88	7.36
MN	.04000	.04000	.06000	.09000	.02000	.07000	.04000	.09000	nd	nd	.05000	.07000
CR	4.79	4.70	4.79	4.74	4.86	4.92	5.68	5.70	5.65	5.69	4.80	5.68
FE3	4.01	4.18	4.18	4.01	4.18	3.96	3.23	3.28	3.40	3.20	4.09	3.28
AL	1.90	1.89	1.89	1.93	2.05	1.94	3.10	2.87	3.04	3.00	1.93	3.00
TI	2.55	2.53	2.48	2.56	2.37	2.50	1.91	1.97	1.87	1.98	2.50	1.93
V	.16000	.15000	.15000	.16000	.15000	.16000	.14000	.18000	.15000	.11000	.15000	.15000
MG/MG+FE	.15333	.13550	.14793	.15392	.16151	.14107	.26497	.25076	.26039	.25025	.15000	.26000
CR/CR+AL	.71599	.71320	.71707	.71064	.70333	.71720	.64693	.66511	.65017	.65478	.71000	.65000
CR+AL	6.69	6.59	6.68	6.67	6.91	6.86	8.78	8.57	8.69	8.69	6.73	8.68
FE/FE+CR	.37477	.38812	.38490	.37547	.37692	.36599	.26894	.27679	.28122	.26913	.38000	.27000
TI/TI+CR	.27597	.27741	.27074	.27736	.25539	.26709	.17867	.18691	.17708	.18557	.27000	.18000

1 - DISRUPTED OLIVINE GABBRO 2522-8-48 CYCLE 2
2 - DISRUPTED OLIVINE GABBRO 2522-8-49 CYCLE 2
3 - DISRUPTED OLIVINE GABBRO 2522-8-50 CYCLE 2
4 - DISRUPTED OLIVINE GABBRO 2522-8-51 CYCLE 2
5 - DISRUPTED OLIVINE GABBRO 2522-8-52 CYCLE 2
6 - DISRUPTED OLIVINE GABBRO 2522-8-53 CYCLE 2
7 - DISRUPTED OLIVINE GABBRO 2522-1-28 CYCLE 2
8 - DISRUPTED OLIVINE GABBRO 2522-1-29 CYCLE 2
9 - DISRUPTED OLIVINE GABBRO 2522-1-30 CYCLE 2
10 DISRUPTED OLIVINE GABBRO 2522-1-31 CYCLE 2
11 - MEAN OF ALL SPINELS IN AUGITE 8
12 - MEAN OF ALL SPINELS IN AUGITE 1

TABLE 16. CHROME-SPINELS ASSOCIATED WITH MINERAL ASSEMBLAGE POLARITY (MAP) TEXTURED SULPHIDES. CHROME-SPINEL GROUP 5. PAGE 1.

	1	2	3	4	5	6	7	8	9	10	11	12
MGO	2.32	1.97	2.13	3.01	1.96	1.43	1.79	2.65	3.33	3.16	2.14	2.05
FEO	40.67	42.11	41.16	38.93	40.80	41.48	40.29	39.88	40.10	37.26	41.31	40.38
MNO	0.67	0.29	0.29	0.39	0.58	0.58	0.38	0.29	0.39	0.29	0.42	0.48
CR2O3	15.39	12.86	16.16	15.77	12.57	12.38	11.59	15.98	16.67	19.16	14.80	13.08
FE2O3	24.72	25.61	22.32	24.15	25.76	25.49	28.11	22.24	19.96	22.92	24.22	25.88
AL2O3	4.44	4.45	4.62	4.73	4.74	4.43	4.03	5.02	5.01	5.63	4.50	4.48
TIO2	13.19	13.88	13.37	12.59	13.19	13.25	12.61	13.05	14.32	10.90	13.48	12.91
V2O3	0.51	0.44	0.51	0.81	0.66	0.73	0.44	0.66	0.59	0.59	0.49	0.66
TOTAL	101.91	101.61	100.62	100.38	100.26	99.77	99.24	99.77	100.37	99.91	101.38	99.91
					CATIONS PER 32 OXYGENS							
MG	0.98	0.84	0.91	1.28	0.84	0.62	0.78	1.13	1.41	1.35	0.91	0.88
FE2	9.67	10.07	9.90	9.33	9.88	10.14	9.91	9.62	9.56	8.92	9.88	9.81
MN	.16000	.07000	.07000	.09000	.14000	.14000	.09000	.07000	.09000	.07000	.10000	.12000
CR	3.46	2.91	3.67	3.57	2.87	2.86	2.69	3.64	3.75	4.33	3.35	3.00
FE3	5.29	5.51	4.84	5.21	5.61	5.61	6.22	4.83	4.28	4.93	5.21	5.66
AL	1.49	1.50	1.56	1.60	1.61	1.52	1.39	1.70	1.68	1.89	1.52	1.53
TI	2.82	2.98	2.89	2.71	2.87	2.91	2.78	2.88	3.06	2.34	2.90	2.82
V	.11000	.10000	.11000	.08000	.15000	.17000	.10000	.15000	.13000	.13000	.11000	.13000
MG/MG+FE	.09202	.07699	.08418	.12064	.07836	.05762	.07297	.10512	.12853	.13145	.08000	.08000
CR/CR+AL	.69899	.65986	.70172	.69052	.64063	.65297	.65931	.68165	.69061	.69614	.69000	.66000
CR+AL	4.95	4.41	5.23	5.17	4.48	4.38	4.08	5.34	5.43	6.22	4.86	4.53
FE/FE+CR	.51660	.55544	.48064	.50193	.55600	.56156	.60388	.47493	.44078	.44215	.52000	.56000
TI/TI+CR	.36293	.40325	.35591	.34391	.39048	.39918	.40525	.35037	.36042	.27336	.37000	.38000

1 - IN INTERSTITIAL OLIVINE 268-14-35 CYCLE 3
2 - IN INTERSTITIAL OLIVINE 268-14-36 CYCLE 3
3 - IN INTERSTITIAL OLIVINE 268-14-40 CYCLE 3
4 - IN PLAGIOCLASE OVERGROWTH 268-6-20 CYCLE 3
5 - IN PLAGIOCLASE OVERGROWTH 268-15-20 CYCLE 3
6 - IN PLAGIOCLASE OVERGROWTH 268-15-22 CYCLE 3
7 - IN PLAGIOCLASE OVERGROWTH 268-15-26 CYCLE 3
8 - IN AUGITE 268-7-1 CYCLE 3
9 - IN AUGITE 268-7-3 CYCLE 3
10 - IN AUGITE 268-6-5 CYCLE 3
11 - MEAN OF ALL SPINELS IN INTERSTITIAL OLIVINE
12 - MEAN OF ALL SPINELS IN PLAGIOCLASE OVERGROWTH

TABLE 16. PAGE 2

	13
MGO	3.05
FEO	39.08
MNO	0.32
CR2O3	17.27
FE2O3	21.71
AL2O3	5.22
TIO2	12.76
V2O3	0.61
TOTAL	100.02
MG	1.30
FE2	9.37
MN	.08000
CR	3.91
FE3	4.68
AL	1.76
TI	2.76
V	.14000
MG/MG+FE	.12000
CR/CR+AL	.69000
CR+AL	5.66
FE/FE+CR	.45000
TI/TI+CR	.33000

13 - MEAN OF ALL SPINELS IN AUGITE

TABLE 17. CHROME-SPINEL INTERGRAINS.
CHROME-SPINEL GROUP 5

	1	2	3	4	5	6	7	MEAN
MGO	2.60	2.42	2.94	2.76	3.33	3.49	2.98	2.93
FEO	36.35	37.52	37.81	37.83	38.57	36.73	37.25	37.44
MNO	0.19	0.19	0.29	nd	0.48	0.10	0.19	0.24
CR2O3	15.43	14.59	15.16	18.07	13.91	16.84	13.29	15.33
FE2O3	29.11	28.29	24.49	23.82	25.58	25.06	30.46	26.69
AL2O3	6.20	5.47	5.53	7.19	4.95	6.38	4.98	5.81
TIO2	8.87	10.02	11.60	10.01	12.72	10.50	10.47	10.60
V2O3	0.95	1.10	0.88	0.88	1.17	0.88	0.87	0.96
TOTAL	99.70	99.60	98.70	100.56	100.71	99.98	100.49	99.96
			CATIONS	PER 32	OXYGENS			
MG	1.11	1.04	1.27	1.16	1.41	1.48	1.27	1.25
FE2	8.76	9.09	9.18	8.96	9.19	8.74	8.94	8.98
MN	.04000	.04000	.07000	nd	.11000	.02000	.04000	.05333
CR	3.51	3.34	3.48	4.04	3.13	3.79	3.01	3.47
FE3	6.31	6.16	5.35	5.08	5.48	5.37	6.57	5.76
AL	2.10	1.86	1.89	2.40	1.66	2.14	1.68	1.96
TI	1.92	2.18	2.53	2.13	2.72	2.24	2.26	2.28
V	.22000	.25000	.20000	.20000	.26000	.20000	.20000	.21857
MG/MG+FE	.11246	.10267	.12153	.11462	.13302	.14481	.12439	.12193
CR/CR+AL	.62567	.64231	.64804	.62733	.65344	.63912	.64179	.63967
CR+AL	5.61	5.20	5.37	6.44	4.79	5.93	4.69	5.43
FE/FE+CR	.52936	.54225	.49907	.44097	.53359	.47522	.58348	.51485
TI/TI+CR	.25498	.29539	.32025	.24854	.36218	.27417	.32518	.29724

1 - DISRUPTED OLIVINE GABBRO 243-1-16 CYCLE 1
2 - DISRUPTED OLIVINE GABBRO 243-1-17 CYCLE 1
3 - DISRUPTED OLIVINE GABBRO 243-1-19 CYCLE 1
4 - DISRUPTED OLIVINE GABBRO 243-2-38 CYCLE 1
5 - DISRUPTED OLIVINE GABBRO 243-2-39 CYCLE 1
6 - DISRUPTED OLIVINE GABBRO 243-2-40 CYCLE 1
7 - DISRUPTED OLIVINE GABBRO 243-2-41 CYCLE 1
MEAN - MEAN OF ALL SPINELS

TABLE 18. CHROME-SPINELS IN BIOTITES OF DISRUPTED ADCUMULATES. PAGE 1.
CHROME-SPINEL GROUP 6

	1	2	3	4	5	6	7	8	9	10	MEAN	12
MGO	3.17	2.65	2.81	2.48	2.47	2.63	2.64	1.80	1.80	1.60	2.41	2.69
FEO	35.94	36.44	34.98	37.64	37.10	35.71	35.54	37.83	38.52	39.88	36.96	36.19
MNO	0.19	0.39	0.48	0.29	0.39	0.10	nd	0.10	0.29	0.39	0.29	0.31
CR2O3	27.45	28.45	29.47	26.18	26.56	27.35	28.06	27.12	26.78	25.14	27.26	27.65
FE2O3	18.95	17.63	17.99	18.20	18.17	19.50	19.44	17.68	16.75	15.61	17.99	18.55
AL2O3	4.89	4.27	5.48	3.57	4.07	6.03	5.39	4.40	4.08	3.01	4.52	4.81
TIO2	9.19	9.39	7.95	10.57	9.99	7.97	7.88	9.43	10.31	12.12	9.48	8.99
V2O3	0.59	0.52	0.59	0.52	0.66	0.37	0.52	0.59	0.88	0.66	0.59	0.54
TOTAL	100.37	99.74	99.75	99.45	99.41	99.72	99.47	98.95	99.41	98.41	99.47	99.70
					CATIONS	PER 32	OXYGENS					
MG	1.34	1.14	1.20	1.07	1.07	1.12	1.13	0.78	0.78	0.70	1.03	1.15
FE2	8.58	8.81	8.40	9.16	9.02	8.57	8.57	9.27	9.40	9.89	8.97	8.73
MN	.04000	.09000	.11000	.07000	.09000	.02000	nd	.02000	.07000	.09000	.06667	.07000
CR	6.19	6.50	6.68	6.03	6.10	6.20	6.40	6.28	6.18	5.89	6.25	6.30
FE3	4.07	3.83	3.88	3.99	3.97	4.21	4.22	3.89	3.68	3.48	3.92	4.02
AL	1.64	1.45	1.85	1.22	1.39	2.05	1.83	1.52	1.40	1.05	1.54	1.63
TI	1.97	2.04	1.71	2.31	2.18	1.72	1.71	2.07	2.26	2.70	2.07	1.95
V	.13000	.12000	.13000	.12000	.15000	.08000	.12000	.13000	.20000	.15000	.13300	.12000
MG/MG+FE	.13508	.11457	.12500	.10459	.10605	.11558	.11649	.07761	.07662	.06610	.10377	.12000
CR/CR+AL	.79055	.81761	.78312	.83172	.81442	.75152	.77764	.80513	.81530	.84870	.80357	.80000
CR+AL	7.83	7.95	8.53	7.25	7.49	8.25	8.23	7.80	7.58	6.94	7.79	7.93
FE/FE+CR	.34202	.32513	.31265	.35498	.34642	.33788	.33896	.33276	.32682	.33397	.33516	.34000
TI/TI+CR	.20102	.20420	.16699	.24163	.22544	.17252	.17203	.20973	.22967	.28008	.21033	.20000

1 - DISRUP. TROCTOLITE 254B-6-1 CYCLE 2
2 - DISRUP. TROCTOLITE 254B-6-3 CYCLE 2
3 - DISRUP. TROCTOLITE 254B-6-5 CYCLE 2
4 - DISRUP .TROCTOLITE 254C-8-11 CYCLE 2
5 - DISRUP. TROCTOLITE 254C-8-12 CYCLE 2
6 - DISRUP. TROCTOLITE 254C-8-13 CYCLE 2
7 - DISRUP. TROCTOLITE 254C-8-14 CYCLE 2
8 - DISRUP. TROCTOLITE 246-1-19 CYCLE 1
9 - DISRUP. TROCTOLITE 246-1-20 CYCLE 1
10 -DISRUP. TROCTOLITE 246-1-21 CYCLE 1
MEAN - MEAN OF ALL CHROME-SPINELS
12 -MEAN OF CHROME-SPINELS IN SAMPLE 254B-C CYCLE 2

TABLE 18. CHROME-SPINELS.
PAGE 2.

	13
MGO	1.73
FEO	38.74
MNO	0.26
CR2O3	26.35
FE2O3	16.68
AL2O3	3.83
TIO2	10.62
V2O3	0.71
TOTAL	98.92
MG	0.75
FE2	9.52
MN	.06000
CR	6.12
FE3	3.68
AL	1.32
TI	2.34
V	.16000
MG/MG+FE	.07000
CR/CR+AL	.82000
CR+AL	7.44
FE/FE+CR	.33000
TI/TI+CR	.24000

13 - MEAN OF CHR SPINELS IN SAMPLE 246 CYCLE 1

TABLE 19. CHROME-SPINELS IN BIOTITES OF ORTHOCUMULATES. CHROME-SPINEL GROUP 6

	1	2	3	4	5	6	7	8	9	MEAN
MGO	1.81	1.81	1.61	1.02	1.43	2.12	2.48	1.41	1.41	1.68
FEO	40.54	41.16	39.46	42.62	40.41	38.19	38.46	39.83	40.83	40.17
MN	0.19	0.29	0.39	0.19	0.19	0.39	0.39	0.38	0.19	0.29
CR2O3	24.51	23.99	24.78	16.34	17.50	21.20	20.80	23.85	21.82	21.64
FE2O3	16.96	16.60	17.72	23.32	26.26	20.64	21.18	18.83	19.27	20.09
AL2O3	3.89	3.89	3.66	3.12	3.56	4.58	4.70	3.67	3.57	3.85
TIO2	12.09	12.68	11.21	13.25	11.21	10.86	11.29	11.12	12.04	11.75
V2O3	0.51	0.66	0.66	0.80	0.80	0.59	0.66	0.81	0.80	0.70
TOTAL	100.50	101.08	99.49	100.66	101.36	98.57	99.96	99.90	99.93	100.16
				CATIONS PER 32 OXYGENS						
MG	0.77	0.77	0.70	0.44	0.61	0.92	1.06	0.61	0.61	0.72
FE2	9.80	9.89	9.66	10.42	9.77	9.37	9.28	9.73	9.98	9.77
MN	.04000	.07000	.09000	.04000	.04000	.09000	.09000	.09000	.04000	.06556
CR	5.60	5.45	5.73	3.77	4.00	4.91	4.74	5.51	5.04	4.97
FE3	3.69	3.59	3.90	5.13	5.71	4.56	4.60	4.14	4.24	4.40
AL	1.32	1.31	1.26	1.07	1.21	1.58	1.60	1.26	1.23	1.32
TI	2.63	2.74	2.46	2.91	2.43	2.39	2.45	2.44	2.64	2.57
V	.11000	.15000	.15000	.18000	.18000	.13000	.15000	.18000	.18000	.15667
MG/MG+FE	.07285	.07223	.06757	.04052	.05877	.08941	.10251	.05899	.05760	.06894
CR/CR+AL	.80925	.80621	.81974	.77893	.76775	.75655	.74763	.81388	.80383	.78931
CR+AL	6.92	6.76	6.99	4.84	5.21	6.49	6.34	6.77	6.27	6.29
FE/FE+CR	.34779	.34686	.35813	.51454	.52289	.41267	.42048	.37947	.40343	.41181
TI/TI+CR	.27539	.28842	.26032	.37548	.31806	.26914	.27873	.26493	.29630	.29186

1 - DISRUPTED OLIVINE GABBRO 2711-2-80 CYCLE 3
2 - DISRUPTED OLIVINE GABBRO 2711-2-81 CYCLE 3
3 - DISRUPTED OLIVINE GABBRO 2711-2-82 CYCLE 3
4 - DISRUPTED OLIVINE GABBRO 2712-2-24 CYCLE 3
5 - DISRUPTED OLIVINE GABBRO 2712-2-25 CYCLE 3
6 - DISRUPTED OLIVINE GABBRO 268-10-10 CYCLE 3
7 - DISRUPTED OLIVINE GABBRO 268-10-11 CYCLE 3
8 - DISRUPTED OLIVINE GABBRO 252-2-40 CYCLE 2
9 - DISRUPTED OLIVINE GABBRO 252-2-41 CYCLE 2
MEAN - MEAN OF ALL CHROME-SPINELS